

**Flavoproteins:
Studies on flavodoxins and phenol hydroxylase**

CENTRALE LANDBOUWCATALOGUS



0000 0714 5838

Promotor: : dr. C. Veeger
hoogleraar in de Biochemie

Co-promotor : dr. ir. J. Vervoort
universitair docent
vakgroep Biochemie

NN08201, 2103

**Flavoproteins:
Studies on flavodoxins and phenol hydroxylase**

J.C.J. Peelen

Proefschrift
ter verkrijging van de graad van doctor
in de landbouw- en milieuwetenschappen
op gezag van de rector magnificus,
dr. C.M. Karssen,
in het openbaar te verdedigen
op woensdag 12 juni 1996
des voormiddags te elf uur in de Aula
van de Landbouwuniversiteit te Wageningen.

ISBN 927465

LIBRARY
SCHOOL OF AGRICULTURE
WAGeningen

The logo for the Netherlands Organization for Scientific Research (NWO). It features the letters 'NWO' in a bold, sans-serif font. A stylized, curved line arches over the 'W', resembling a swoosh or a partial circle.

The research described in this thesis was carried out at the Department of Biochemistry, Agricultural University, Wageningen, The Netherlands, under direction of Prof. dr. C. Veeger. The investigations were supported by the Netherlands Foundation for Chemical Research (SON) with financial aid from the Netherlands Organization for Scientific Research (NWO).

Stellingen

1. Deprotonering van de fenolische hydroxylgroep leidt tot verhoogde omzetting van het substraat door fenol hydroxylase.

Hoofdstuk 4 van dit proefschrift.

2. De residuen asparagine-11, serine-68 en asparagine-72 van het *Azotobacter chroococcum* flavodoxine zijn betrokken bij de interactie met het Fe-eiwit van het nitrogenase complex.

Hoofdstuk 3 van dit proefschrift.

3. De regioselectieve hydroxylering van 3-fluorofenol door fenol hydroxylase is pH afhankelijk.

Hoofdstuk 4 van dit proefschrift.

4. Het feit dat de eiwitmatrix van sulfiet reductase uit *D. vulgaris* niet bijdraagt tot een efficiënte katalyse, rechtvaardigt niet de conclusie van Soriano en Cowan dat hetzelfde geldt voor andere enzymen met een anorganische cofactor.

A. Soriano & J.A. Cowan (1995) J. Am. Chem. Soc. 117, 4724-4725.

5. Prionen (PrP^{Sc}) kunnen "pathogene chaperones" genoemd worden omdat ze het normale eiwit PrP^C kunnen omzetten in prionen.

F.E. Cohen, K.-M. Pan, Z. Huang, M. Baldwin, R.J. Fletterick & S.B. Prusiner (1996) Science 264, 530-531.

6. Het mag geen verrassing genoemd worden dat na verwijdering van het FMN molecuul uit flavodoxine, de vrijgekomen plaats opgevuld wordt door "active-site" aminozuren.

C.G. Genzor, A. Perales-Alcón, J. Sancho & A. Romero (1996) Nature Structural Biology 3, 329-332.

7. Eiwitten waarbij de N-terminus van α -helices voornamelijk waterstofbruggen vormt met positief geladen aminozuren zullen niet stabiel zijn.

D. Gandini, L. Gogioso, M. Bolognesi & D. Bordo (1996) Proteins: Structure, Function and Genetics 24, 439-449.

8. Het gebrek aan communicatie tussen wetenschappers en beleidsmakers, en niet de kwaliteit van het onderzoek, is de reden dat onderzoeksresultaten geen weerklank vinden in beleid.
9. De toename van de capaciteit van het Internet zal uiteindelijk niet leiden tot een snellere overdracht van gegevens.
10. De minst belangrijke stellingen genieten vaak de meeste belangstelling.

Stellingen behorende bij het proefschrift "**Flavoproteins: Studies on flavodoxins and phenol hydroxylase**" van J.C.J. Peelen, Landbouwniversiteit Wageningen, 12 juni 1996.

Woord vooraf

Sinds mijn aanvang aan het promotie onderzoek dat tot dit proefschrift heeft geleid is er heel wat water door de Rijn gestroomd. Iedereen die mij in deze periode, direct of indirect, heeft geholpen met het tot stand komen van dit proefschrift, wil ik op deze plaats van harte bedanken. Zonder deze mensen zou dit proefschrift nog heel wat liters verwijderd zijn van zijn voltooiing.

Allereerst wil ik Cees Veeger bedanken voor de gelegenheid die hij mij geboden heeft om te promoveren. Jacques jou wil ik bedanken voor je dagelijkse steun en begeleiding. En ondanks dat het promotieonderzoek anders verlopen is dan we in eerste instantie gepland hadden, zijn we er toch in geslaagd het tot een goed einde te brengen. Dit voornamelijk ook door de enorme hulp die ik van Ivonne en Marelle gekregen heb bij het phenol hydroxylase onderzoek. Zonder deze hulp was dit proefschrift nu niet klaar geweest. Ook wil ik Willem bedanken voor de nuttige discussies die we over phenol hydroxylase hadden.

Twee andere personen die hebben gezorgd dat ik verder kon met mijn onderzoek zijn Robert Eady en Neville Henderson. Bob and Neville, many thanks for the labelled *A. chroococcum* flavodoxin and for the nice time I had in Brighton. I also want to thank Robert Robson for the cloning and sequencing of the flavodoxin gene. Paul en Stefan wil ik bedanken voor hun bijdrage aan mijn onderzoek. Jullie waren beiden niet te beroerd om tot diep in de nacht met mij door te werken. Wat betreft het laser onderzoek dat ik samen met Paul heb verricht wil ik Ton en Arie bedanken. Helaas heb ik dit werk niet in dit proefschrift kunnen verwerken.

Het vele NMR werk heb ik natuurlijk niet alleen verricht. Sybren en Jacques bedankt voor het op tijd klaar hebben van de triple-resonance experimenten. Deze hebben heel wat (late) uurtjes achter de console in Nijmegen gekost. In dit kader wil ik ook Carlo bedanken voor zijn hulp en advies. Voor technische ondersteuning kon ik altijd terecht bij Adrie de Jager en Jos Joordens. De 600 MHz NMR metingen heb ik mogen verrichten op de SON/NWO Nationale HF-NMR faciliteit in Nijmegen. Ook wil ik Elles bedanken voor haar hulp bij het aanpassen van de Felix macro's. Ik hoop trouwens dat het NMR discussie groepje goed blijft lopen. Frank Vergeldt wil ik bedanken omdat hij altijd bereid was te helpen als ik problemen had met een of ander workstation. Bedankt ook voor het schrijven van de nawk scripts, die erg handig waren bij het verwerken van de phenol hydroxylase data.

Hans Peters wil ik bedanken voor het maken van het "geraytraced" FMN molecuul dat voorop dit proefschrift staat.

Voor de gezellige koffie/thee pauzes op lab 9 wil ik Nicole, Sjef, Marelle, Ans, Janneke, Jillert en Marjon bedanken. De leden van de vakgroep Biochemie wil ik bedanken voor de leuke periode die ik in Wageningen gehad heb.

Mijn ouders van harte bedankt voor jullie steun. En Petra bedankt voor je steun en het vele geduld dat je hebt moeten hebben.

aan mijn ouders

Abbreviations

1D, 2D, 3D	one-, two-, three-dimensional
ADP	adenosine diphosphate
ATP	adenosine triphosphate
β	resonance integral
B_0	external magnetic field
B_1	magnetic field from radio frequency pulse
c_i	coefficient of orbital i
CBCA(CO)NH	3D triple-resonance $^{13}\text{C}\beta^{13}\text{C}\alpha(^{13}\text{CO})\text{-}^{15}\text{N}\text{-}^1\text{HN}$ correlation spectroscopy
CBCANH	3D triple-resonance $^{13}\text{C}\beta^{13}\text{C}\alpha\text{-}^{15}\text{N}\text{-}^1\text{HN}$ correlation spectroscopy
τ	constant time
DNA	deoxyribose nucleic-acid
DQ-COSY	double quantum filtered correlated spectroscopy
DSS	2,2-dimethyl-2-silapentane-5-sulfonate
E_a	activation energy
EDTA	ethylene-diamine-tetra-acetate
E(HOMO)	energy of the highest occupied molecular orbital
E(LUMO)	energy of the lowest unoccupied molecular orbital
FAD	flavin adenosine diphosphate
FID	free induction decay
FMN	riboflavin 5'-monophosphate
GTP	guanosine triphosphate
HBHA(CO)NH	3D triple-resonance $^1\text{H}\beta^1\text{H}\alpha(^{13}\text{C}\beta^{13}\text{C}\alpha^{13}\text{CO})\text{-}^{15}\text{N}\text{-}^1\text{HN}$ correlation spectroscopy
HOMO	highest occupied molecular orbital
HMQC	heteronuclear multiple quantum coherence spectroscopy
HNCA	3D triple-resonance $^1\text{HN}\text{-}^{15}\text{N}\text{-}^{13}\text{C}\alpha$ correlation spectroscopy
HNCO	3D triple-resonance $^1\text{HN}\text{-}^{15}\text{N}\text{-}^{13}\text{CO}$ correlation spectroscopy
HNHA	3D triple resonance $^1\text{HN}\text{-}^{15}\text{N}\text{-}^1\text{H}\alpha$ correlation spectroscopy
HSQC	heteronuclear single quantum correlation spectroscopy
LUMO	lowest unoccupied molecular orbital
μ	magnetic dipole moment
MO-QSAR	molecular-orbital-based quantitative structure-activity relationship
M_x, M_y, M_z	magnetization along the x-, y-, z-axis
NADPH	nicotinamide adenine dinucleotide phosphate (reduced)
NADP ⁺	nicotinamide adenine dinucleotide phosphate (oxidized)
<i>nif</i>	nitrogen-fixation

NMR	nuclear magnetic resonance
NOE	nuclear Overhauser effect
NOESY	nuclear Overhauser spectroscopy
P	probability or steric factor
SDS/PAGE	sodium dodecyl sulfate polyacrylamide gel electrophoresis
SQ	semiquinone
ppm	parts per million
rf	radio frequency
TOCSY	total correlation spectroscopy
TPPI	time proportional phase incrementation
TSP	3-(trimethylsilyl)-propionate
ω_0	Larmor precession frequency
Z	collision number

Amino acids

Ala	A	alanine
Arg	R	arginine
Asn	N	asparagine
Asp	D	aspartic acid
Cys	C	cysteine
Gln	Q	glutamine
Glu	E	glutamic acid
Gly	G	glycine
His	H	histidine
Ile	I	isoleucine
Leu	L	leucine
Lys	K	lysine
Met	M	methionine
Phe	F	phenylalanine
Pro	P	proline
Ser	S	serine
Thr	T	threonine
Trp	W	tryptophan
Tyr	Y	tyrosine
Val	V	valine

Contents

1	<i>General introduction</i>	
1.1	Flavin and flavoproteins	1
1.1.1	Flavodoxins	2
1.1.2	Phenol hydroxylase	4
1.2	NMR and structure determination	6
1.2.1	Introduction to NMR	6
1.2.2	Sequential assignments	9
1.2.3	Sensitivity and pulse field gradients	12
1.2.4	Structure determination	14
1.3	Transition state and Frontier orbital theory	14
1.4	Outline of this thesis	18
1.5	References	19
2	<i>Two-dimensional NMR studies of the flavin binding site of <i>Desulfovibrio vulgaris</i> flavodoxin in its three redox-states</i>	
2.1	Introduction	24
2.2	Materials and methods	25
2.3	Results and discussion	26
2.3.1	Phosphate binding region	29
2.3.2	Isoalloxazine binding region	36
2.4	Conclusions	39
2.5	References	39
3	<i>Short extra loop of the long-chain flavodoxin from <i>Azotobacter chroococcum</i> may be important for electron transfer to nitrogenase. Complete ^1H, ^{15}N and ^{13}C backbone assignments and secondary solution structure of the flavodoxin</i>	
3.1	Introduction	42
3.2	Materials and methods	43

3.3	Results	53
3.3.1	Sequential assignments	55
3.3.2	Secondary structure	62
3.3.3	Titration of flavodoxin with Fe-protein	65
3.4	Discussion	66
3.5	References	72
4	<i>¹⁹F-NMR study on the pH-dependent regioselectivity and rate of the ortho-hydroxylation of 3-fluorophenol by phenol hydroxylase from Trichosporon cutaneum: Implications for the reaction mechanism</i>	
4.1	Introduction	78
4.2	Materials and methods	79
4.3	Results	81
4.3.1	Regioselectivity of hydroxylation	81
4.3.2	NMR binding studies	86
4.3.3	Molecular orbital calculations	91
4.4	Discussion	93
4.5	References	95
5	<i>Conversion of phenol derivatives to hydroxylated products by phenol hydroxylase from Trichosporon cutaneum. A comparison of regioselectivity and rate of conversion with calculated molecular orbital substrate characteristics</i>	
5.1	Introduction	98
5.2	Materials and methods	99
5.3	Results	103
5.3.1	Determination of k_{cat} values	103
5.3.2	Characterisation of the reaction products	105
5.3.3	Metabolite patterns	107
5.3.4	Molecular orbital characteristics of the substituted phenols	107

5.3.5	Comparison of calculated molecular orbital characteristics of phenolic substrates and the regioselectivity of their conversion by phenol hydroxylase	110
5.4	Discussion	112
5.5	References	116
6	<i>Summarizing discussion</i>	
6.1	Flavodoxins	119
6.2	Phenol hydroxylase	121
6.3	References	124
	<i>Samenvatting</i>	125
	<i>Curriculum vitae</i>	131
	<i>List of publications</i>	132

1

General introduction

1.1 Flavin and flavoproteins

Flavin, which was first observed in whey more than a hundred years ago (Blyth, 1879), is abundantly found in nature. The name of this yellow pigment originates from the Latin word 'flavus'. This means yellow and is nicely demonstrated by egg yolk whose colour mainly is determined by flavins. The most well-known flavin is riboflavin, which is better known as vitamin B₂ (Fig. 1.1). Flavins are produced by lower organisms, whereas mammals can not produce it and, therefore, have to take up flavins via their food. Free flavins are versatile compounds and are capable of performing a whole range of chemical reactions (see Müller, 1991). In order to be specific for a particular reaction, the flavin-cofactor is bound to an apoflavoprotein.

Due to the versatility of the flavin and the many different surrounding apoproteins, flavoproteins provide an important tool to nature to catalyse a variety of reactions. These range from redox catalysis and 'DNA damage repair' to light emission (Ghisla and Massey, 1989). A common feature of flavoproteins is that they catalyse electron transfer reactions in which the flavin is reduced as it accepts one or two electrons from the reducing substrate (reductive half-reaction) and is reoxidized as it transfers one or two electrons to an acceptor (oxidative half-reaction). Considering the reaction that they catalyse, 'simple' flavoproteins, i.e. flavoproteins containing no other prosthetic group than the flavin, can be classified in three major groups (Singer and Edmondson, 1978): (1) oxidases, which accept electrons from

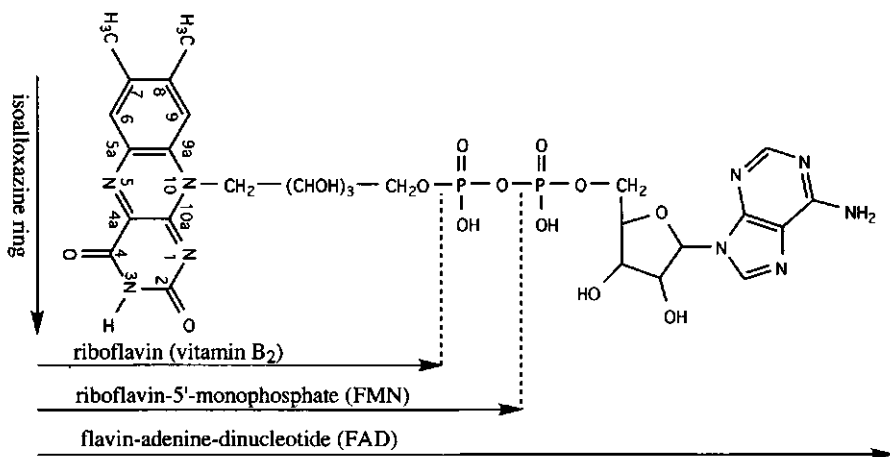


Fig. 1.1. Flavin

substrates and use O₂ as the terminal electron acceptor, forming H₂O₂ and oxidized substrate; (2) monooxygenases, which split the O₂ molecule, inserting one oxygen into the substrate while reducing the other oxygen atom to water; (3) dehydrogenases, which do not reduce molecular oxygen, but transfer electrons to other substrates or to other proteins (Stankovich, 1991). Using this classification the pure electron-transferases are classified in group 3. According to Massey and Hemmerich (1980) these flavoproteins should be classified in a separate group: (4) the pure electron-transferases.

Two flavoproteins, flavodoxin and phenol hydroxylase, were studied in this thesis. These flavoproteins belong to different classes. Flavodoxin belongs to the electron transferring proteins of group 4 and phenol hydroxylase, which uses phenol as a substrate, is a monooxygenase and belongs to group 2. These two flavoproteins are discussed in the next two paragraphs.

1.1.1 Flavodoxins

Flavodoxins are small flavoproteins which contain a single molecule of riboflavin-5'-monophosphate (FMN) (Fig. 1.1). They function as electron-transferring proteins in low potential oxidation-reduction reactions (Mayhew and Tollin, 1992).

Flavodoxins have been isolated from various prokaryotes (see e.g. Cusanovich and Edmondson, 1971; Deistung and Thorneley, 1986; Dubourdieu, et al., 1975; Mayhew, 1971; Mayhew and Massey, 1969) as well as from eukaryotic algae and seaweed (Fitzgerald, et al., 1978; Zumft and Spiller, 1971). Flavodoxins have yet not been found in higher plants and animals. The molecular weights of the monomeric flavodoxins range from 14-23 kDa. According to their weight they are roughly divided into two groups, one in the 14-17 kDa range and the other in the 20-23 kDa range.

Flavodoxins function as electron carriers between other redox proteins in e.g. pyruvate catabolising, sulfate reducing, CO₂- and N₂-fixing systems (Simondson and Tollin, 1980). The non-covalently bound FMN molecule is the redox-active group in flavodoxins and can exist in three redox-states, i.e. oxidized (quinone), one-electron reduced (semiquinone) and two-electron reduced (hydroquinone) (see Fig. 2.1 Chapter 2). At physiological conditions flavodoxins cycle between the one- and the two-electron reduced redox-states. However, it is observed for the activation of methionine synthetase that also the one-electron reduced state can act as the electron donor (Fujii and Huennekens, 1977). The redox potentials of the FMN change strongly upon binding to the apoflavodoxin (Ludwig and Luschinsky, 1992). Due to the different protein environments in the various flavodoxins the FMN redox potentials for the semiquinone/hydroquinone redox couple range from -370 to -520 mV (Mayhew and Tollin, 1992). Due to the variability in this redox-potentials, flavodoxins are uniquely tailored to the potentials of its specific electron acceptor or donor.

Crystal structures have been determined for oxidized flavodoxins from *Clostridium Beijerinckii* MP (Burnett, et al., 1974), *Desulfovibrio vulgaris* (Watenpaugh, et al., 1973), *Anacystis nidulans* (Smith, et al., 1983), *Chondrus crispus* (Fukuyama, et al., 1990) and *Anabaena* 7120 (Rao, et al., 1992). Crystal structures also have been determined for the reduced states of *Clostridium Beijerinckii* MP (Ludwig, et al., 1976; Smith, et al., 1977) and *Desulfovibrio vulgaris* (Watt, et al., 1991) flavodoxins. Solution structures using multi-dimensional NMR have been determined only for *Megaspaera elsdonii* flavodoxin (Mierlo van, et al., 1990a; Mierlo van, et al., 1990b). Secondary solution structure information for the flavodoxins from *Desulfovibrio vulgaris* (Knauf, et al., 1993; Stockman, et al., 1993; Stockman, et al., 1994), *Anacystis nidulans* (Clubb, et al., 1991) and *Anabaena* 7120 (Stockman, et al., 1990) also has been obtained by multi-dimensional NMR

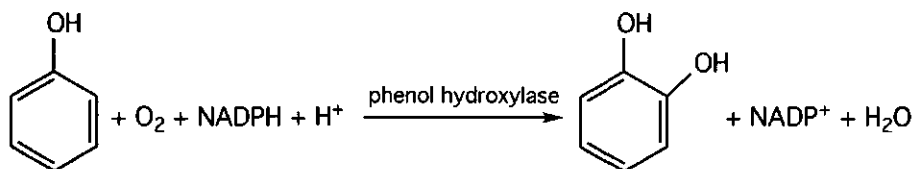
spectroscopy. All the known flavodoxin structures share a common polypeptide fold of a five-stranded parallel central β -sheet surrounded by four or five α -helices. The long-chain flavodoxins, having a molecular weight in the 20-23 kDa range, differ from the short-chain flavodoxins mainly by an insertion of a loop of about 20 residues in the fifth strand of the β -sheet (Mayhew and Tollin, 1992).

Because flavodoxins are small, highly stable proteins and easy to isolate they are very well suited for structure determination by multidimensional NMR.

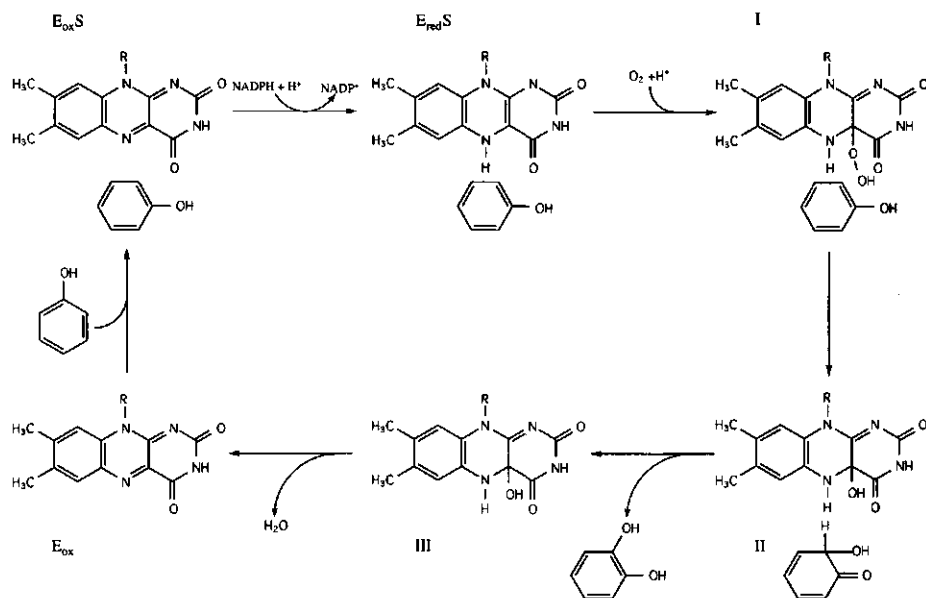
1.1.2 Phenol hydroxylase

One of the most abundant biopolymer, which is responsible for the firmness of plants and trees, is lignin. Lignin is composed of substituted benzene rings, which are linked together. These substituted benzene rings are released after partial degradation of lignin. The degradation of such aromatic compounds into metabolites of the Krebs cycle is essential for the steady state of the natural carbon cycle. The catabolism of aromatic compounds is carried out mainly by micro-organisms (Dagley, 1982). Many of the enzymes capable of converting aromatic compounds are flavoproteins. These aromatic compounds share a common feature in that their rings contain either a hydroxyl or an aminofunction (Berkel van and Müller, 1991). One of these enzymes is phenol hydroxylase, which converts phenol into 1,2-dihydroxybenzene (catechol) (for a review see Neujahr, 1991).

Phenol hydroxylase belongs to group 2 as it is a monooxygenase; in the presence of NADPH the enzyme splits molecular oxygen, inserting one oxygen atom into the substrate, i.e. phenol, while the other oxygen atom is reduced to water. The prosthetic group in phenol hydroxylase responsible for this reaction is flavin adenine dinucleotide (FAD) (Fig. 1.1), which is non-covalently bound to the apoprotein.



Scheme 1.1. Overall reaction for the conversion of phenol to catechol by phenol hydroxylase.



Scheme 1.2. Proposed reaction mechanism for phenol hydroxylase according to Maeda-Yorita and Massey (1993).

The overall reaction for this hydroxylation of phenol to 1,2-dihydroxybenzene is depicted in Scheme 1.1. The reaction cycle consists of various steps starting with the binding of the substrate, followed by NADPH binding, reduction of the flavin, release of $NADP^+$, formation of the C(4a)-hydroperoxyflavin enzyme intermediate (intermediate I), transfer of one oxygen molecule to the substrate, formation of intermediate II, formation of the C(4a)-hydroxyflavin enzyme intermediate (intermediate III), product release and release of a molecule of water with simultaneous reoxidation of the flavin (Scheme 1.2) (Detmer and Massey, 1984; Maeda-Yorita and Massey, 1993). In the absence or at low concentrations of substrate the enzyme acts as a NADPH oxidase, reducing molecular oxygen to H_2O_2 (Neujahr and Kjellén, 1978).

The phenol hydroxylase studied in this thesis is from an eukaryote, the strictly aerobic soil yeast *Trichosporon cutaneum*. The enzyme is a homodimer, containing one FAD molecule per monomer (Neujahr, 1991). The structure of phenol

hydroxylase is still unknown. Recently however, Neujahr and co-workers were able to crystallize phenol hydroxylase (Enroth, et al., 1994). It is therefore expected that the structure will be known within the near future.

1.2 NMR and structure determination

1.2.1 Introduction to NMR

The phenomenon of Nuclear Magnetic Resonance (NMR) first was predicted by Gorter in 1936 (Gorter, 1936). However, it lasted until 1945 before the first NMR signal was detected (Bloch, et al., 1946). Ever since, NMR has developed to a very important tool in biomolecular chemistry, especially since the introduction of *Fourier transform NMR* (Ernst and Anderson, 1966).

Magnetic Resonance originates from the fact that some nuclei (and electrons) behave like 'little magnets' (i.e. magnetic dipoles (μ Fig. 1.2a)). This is because a nucleus is a charged spinning particle. This spinning produces a small circular current. Analogous to an electromagnet this current induces a magnetic field. A NMR sample does not contain just one nucleus but a whole ensemble, typically 10^{17} , of identical nuclei. Because the magnetic moments of all these nuclei are randomly orientated, no net magnetic field is induced. However, if the NMR sample is placed in a strong

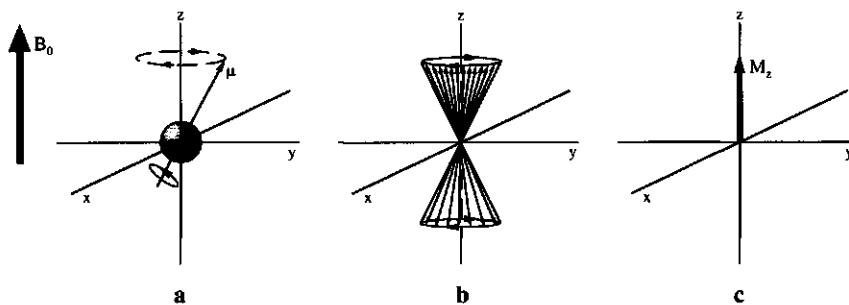


Fig. 1.2. (a) One spinning nucleus in an external magnetic field B_0 , causing the magnetic dipole μ of this nucleus to precess. (b) A whole ensemble of nuclei, with their μ 's precessing either in a parallel or anti-parallel fashion about B_0 . (c) The net magnetization M_z resulting from b.

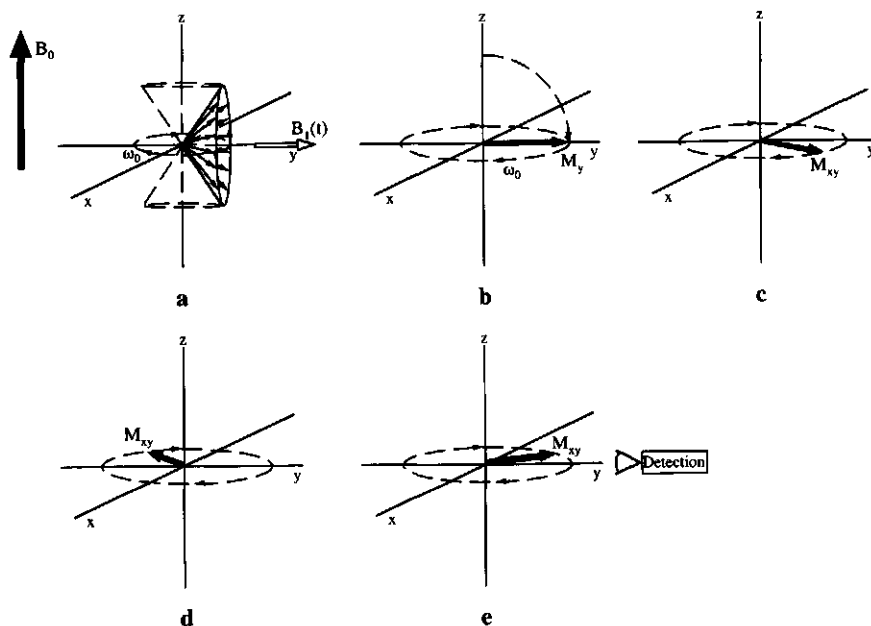


Fig. 1.3. (a) The on-resonance magnetic field B_1 causes a precession of the magnetic moments of the nuclei about this field. (b) After a 90_x° pulse the magnetization vector is along the y-axis and (c-e) starts to precess about B_0 . The projection of the magnetization vector on the y-axis is detected by the detector.

external magnetic field (B_0) the magnetic moments of the nuclei, discussed here, orientate in such a way that they precess about the external magnetic field, either in a 'parallel' or 'anti-parallel' fashion (Fig. 1.2b). The parallel orientation is energetically most favourable. So most nuclei will have their magnetic moments parallel to B_0 . However at room temperature and at 11.7 T the population difference between these two states is very small; for 10^{17} nuclei (~ 0.5 mM) this difference is about 10^{12} (~ 2 nM). It is only this difference which can be observed by NMR spectroscopy. Due to this small difference NMR is an intrinsically insensitive technique. Nevertheless, it is a very powerful tool for e.g. determining molecular structure and dynamics. A vector summation of all the precessing magnetic moments in an external magnetic field along the z-axis (it is customary to define the axis along B_0 as the z-axis) gives a net magnetization vector M_z along the +z-axis (Fig. 1.2c). If a second magnetic field (B_1)

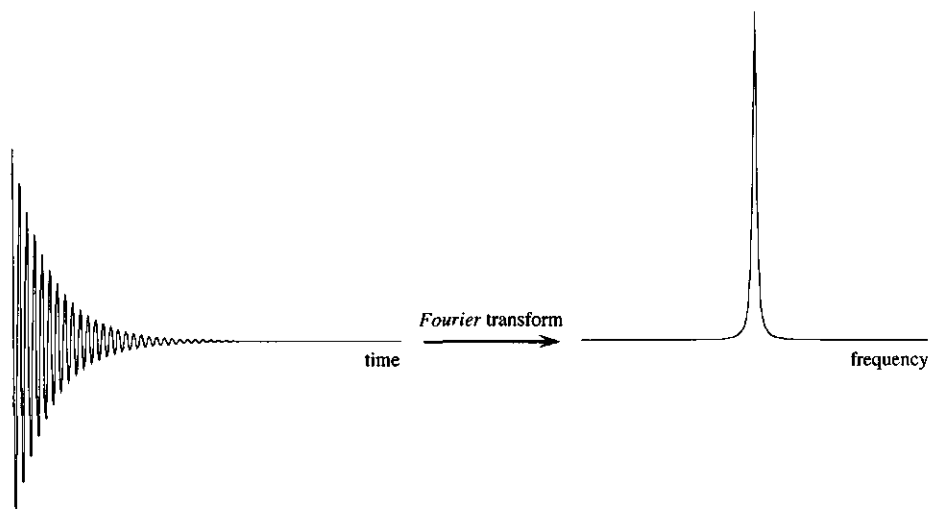


Fig. 1.4. Fourier transformation of the Free Induction Decay (FID) gives a Lorentzian peak.

is applied perpendicular to B_0 then one can imagine that, analogous to the precession of the magnetic moments about B_0 , M_z starts to precess about B_1 (Fig. 1.3a), thus tilting M_z away from the z-axis, inducing now also M_y magnetization (Fig. 1.3b). This however will only happen if this B_1 field, which is induced by generating an electric current in a coil which is wound around the sample, rotates with (almost) the same frequency (Fig. 1.3, ω_0) as the individual magnetic moments. If so, this B_1 is on-resonance with the individual magnetic moments, and hence the name Nuclear Magnetic Resonance. B_1 can be switched on for such a short time that the total magnetization will be along the y-axis (i.e. M_y) and then switched off. In other words a 90_x° pulse is given, because M_z is rotated 90° around the x-axis. Because of B_0 , M_y will start to precess around B_0 (Fig. 1.3b-e). Just like a rotating magnet in the dynamo of a bicycle will cause a current, this precession of M_y will cause an oscillating current in the coil mentioned above. This current is the signal that is detected in NMR spectroscopy. This signal, called Free Induction Decay (FID) (Fig. 1.4), is a damped sine (and is actually the projection of the rotating M_{xy} vector on the y-axis, along which, in our case, the detector is positioned (Fig. 1.3b-e)). This damping of the signal is caused by relaxation processes, which eventually cause M_y to return to its

equilibrium state M_z , and is comparable to the fading of the sound after a gong stroke. *Fourier* transformation of this FID gives a NMR peak (Fig. 1.4).

A protein of course, contains different nuclei, which are located at different positions in the protein, and thus in different environments. They will, therefore, experience slightly different external magnetic fields. This will cause the magnetization vectors of these nuclei to precess at different velocities. *Fourier* transformation of these differently rotating magnetization vectors will result in different peak positions, i.e. chemical shifts, for the different nuclei in a NMR spectrum. For a whole protein this means that peaks of all the different nuclei, e.g. protons, will be observed in a NMR spectrum (Fig. 1.5).

The above paragraph only gives a brief and somewhat simplified introduction to NMR. For a more detailed treatment of NMR theory, the reader is referred to the many text books, which are available on this subject (e.g. Bovey, 1969; Derome, 1987; Jardetzky and Roberts, 1981).

1.2.2 Sequential assignments

A proton NMR spectrum of a protein contains information of all the individual protons of the protein. This information, for example, can be used to obtain the protein structure. However, before the structure can be obtained all these peaks of a NMR spectrum have to be assigned to their corresponding protons. Due to overlap of many of the large number of NMR peaks in such a one-dimensional (1D) NMR spectrum this is not possible for proteins. The solution is to resort to multi-dimensional NMR spectra. In such spectra the chemical shift of a nucleus which has an interaction (see below) with another nucleus, can be correlated to the chemical shift of the latter in a multi-dimensional way (see e.g. Fig. 2.2 and Figs. 3.3 and 3.4). In this way overlapping chemical shifts can be resolved in a two-, three- or even higher dimensional spectrum. The chemical shift resolution of protons in a protein is not very high (Fig. 1.5), so that even resorting to multiple dimensions can not prevent overlap in a multi-dimensional proton NMR spectrum of a protein (> 10 kDa). Their good chemical shift resolution, makes ^{13}C and ^{15}N very suited for overcoming overlap problems in NMR spectra. The natural abundant nuclei ^{12}C and ^{14}N , however, are not suited for structure determination by NMR. If all carbon and nitrogen atoms in the protein are respectively, ^{13}C and ^{15}N , then these nuclei, just like protons, are very well

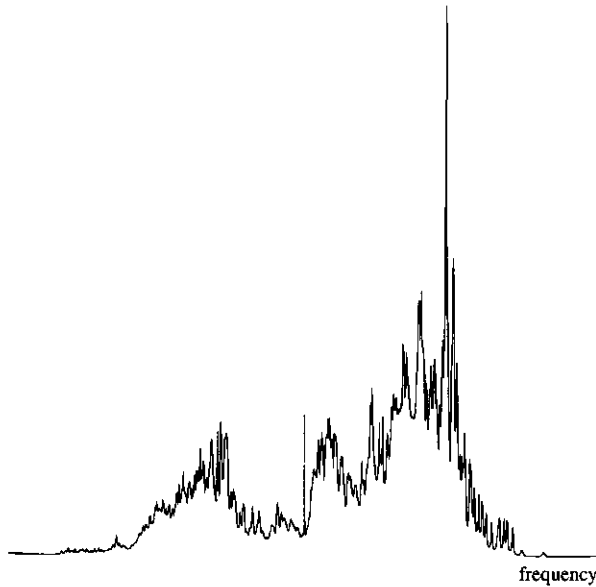


*Fig. 1.5. 1D-NMR ^1H spectrum of the oxidized flavodoxin from *A. chroococcum*. All the NMR peaks observed arise from the different protons of the flavodoxin.*

suiting for structure determination by high resolution NMR. The protein then is called to be uniformly $^{13}\text{C}/^{15}\text{N}$ labelled. Two cases can be distinguished now: the homonuclear NMR experiments and the heteronuclear NMR experiments. In the former experiments only interactions between protons are involved and in the latter experiments interactions between protons (^1H) and ^{15}N and/or ^{13}C are involved.

To assign all the NMR peaks (resonances) in principle two sorts of interactions are used. The through bond interaction and the through space interaction (theoretical description see Ernst, et al., 1967). The former is determined by measuring the so-called J-coupling, which is an interaction between two NMR sensitive nuclei which are not further than three chemical bonds apart. The latter is determined by measuring the so-called nuclear Overhauser effect (NOE). The smaller the through space distance between two NMR sensitive nuclei is, the larger is their NOE. However no NOE is observed when two nuclei are further than approximately 0.5 nm apart.

First, assignments based on homonuclear experiments will be discussed. Fig. 1.6 shows part of a polypeptide chain. From this figure it is clear that within one amino acid (boxed region Fig. 1.6) protons can be 'linked together' via the three-bond

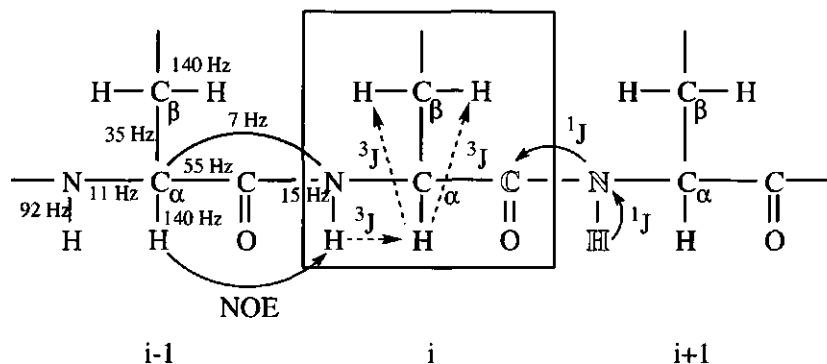


Fig. 1.6. A tripeptide segment of a protein backbone. The boxed region contains a single amino acid (spin system i). The dashed arrows indicate the homonuclear three-bond 3J -couplings observed within a spin system. Correlations to neighbouring amino acids ($i-1$ and $i+1$) can be made via the NOE (through space) or via heteronuclear one-bond 1J -couplings (through bond). Heteronuclear J -coupling constants are indicated in amino acid residue $i-1$. The open atoms indicate the correlations observed in a HNC(O) experiment.

3J -coupling (Fig. 1.6, dashed arrows), thus forming a so-called *spin system*. This is not possible for two protons from different amino acids, because they are at least four chemical bonds apart. The different proton resonances can now be assigned as part of a (J -coupled) spin system, i.e. amino acid. This is done mainly by two very important 2D-NMR experiments: DQF-COSY (Piantini, et al., 1982; Rance, et al., 1983; Shaka and Freeman, 1983) and TOCSY (Braunschweiler and Ernst, 1983). Without going into any detail, the spectra of these experiments correlate protons to protons to which they are J -coupled, and thus show if protons belong to the same spin system (amino acid). Now we need to assign these spin systems to the corresponding amino acids in the polypeptide chain. Via the NOE interaction the different spin systems can be correlated. For example, when a H_α proton has a strong NOE interaction with a backbone amide proton of another spin system this means that they are close in space, which in this case often means that their spin systems are sequential neighbours (NOE arrow Fig. 1.6). This procedure can be repeated for many protons, and in this way it is possible to sequentially walk from one spin system to the next, thus assigning the spin systems to a specific amino acid in the polypeptide chain

(Wüthrich, 1986). The 2D-NMR experiment used for these assignments is called NOESY (Jeener, et al., 1979).

Due to the three-dimensional fold of the polypeptide chain forming a protein, and due to the through space nature of the NOE interaction, it is very well possible that two protons which are coupled by a strong NOE are no sequential neighbours. Thus, the assignment of sequential neighbours via NOE's is not unambiguous. On the other hand neighbours can unambiguously be assigned if they are correlated via the J-coupling. For protons this is not possible, because inter-residual protons are separated by more than three chemical bonds. However, if the protein is $^{13}\text{C}/^{15}\text{N}$ labelled, two neighbouring amino acids can be correlated via the heteronuclear J-coupling, because now the NMR sensitive nuclei are only one bond apart. A whole set of heteronuclear NMR experiments is available to correlate NMR peaks of an amino acid to peaks of a neighbouring amino acid and thus unambiguously assign the NMR peaks to the corresponding atom (Bax and Grzesiek, 1993; Clore and Gronenborn, 1991). The correlations detected by these so-called triple resonance experiments can easily be derived from their names. For example, the so-called HNCO (Grzesiek and Bax, 1992c; Ikura, et al., 1990) correlates the amide proton (H) and nitrogen (N) of an amino acid to the carbonyl carbon (CO) of the preceding amino acid (Fig. 1.6; open atoms), whereas the CBCA(CO)NH (Grzesiek and Bax, 1992a) gives the correlation between the beta (CB) and alpha (CA) carbon atoms of an amino acid with the amide nitrogen (N) and proton (H) of the following amino acid, via the carbonyl carbon ((CO)) of the former amino acid. Analogous to the homonuclear case it is possible to sequentially walk from one spin system to the next, thus assigning the spin systems to a specific amino acid in the polypeptide chain. Especially the combination of the CBCA(CO)NH and the CBCANH (Grzesiek and Bax, 1992b) experiments is very powerful for this sequential assignments (see Fig. 3.4a). Due to the through bond correlation used in these experiments, the neighbouring spin systems can unambiguously be assigned.

1.2.3 Sensitivity and pulse field gradients

The sensitivity of a triple resonance experiment depends strongly on the size of the heteronuclear coupling constants used to correlate the nuclei in that particular experiment (Fig. 1.6). Large J-couplings improve the sensitivity of the triple

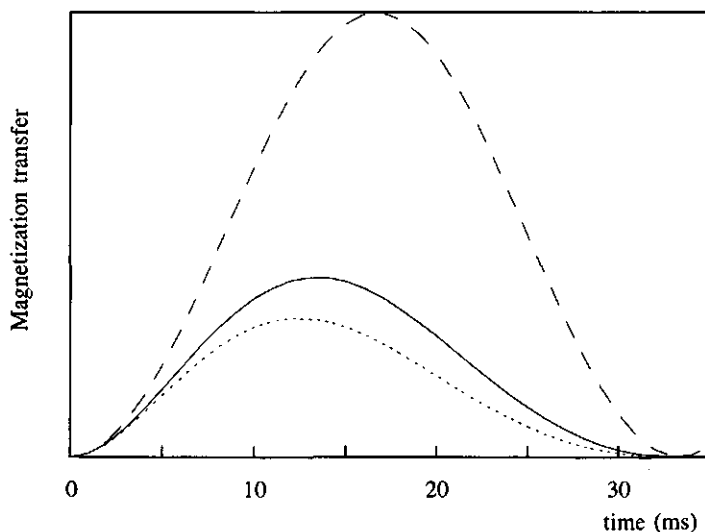


Fig. 1.7. Theoretical magnetization transfer from N to CO in a HNC0 experiment without T_2 relaxation (dashed line) and with a T_2 relaxation time of 65 ms (solid line) and 50 ms (dotted line).

resonance experiment, because the transfer of the magnetization from one nucleus to another will be faster than for a small coupling. The faster this transfer the less magnetization will be lost due to relaxation (in fact T_2 relaxation). The theoretical optimum for the magnetization transfer time from N to CO in the HNC0 experiment (T_N Fig. 3.2c) is $(4\pi J_{NCO})^{-1}$, i.e. 16.7 ms $(4\pi 15 \text{ Hz})^{-1}$ if no relaxation is taken into account. When relaxation is taken into account the optimum for a 20 kDa protein will be about 13.7 ms. This is nicely illustrated in Fig. 1.7. All the magnetization transfer delays in the triple resonance experiments used in this thesis are optimized to have a maximum magnetization transfer and thus sensitivity. It is clear from Fig. 1.7 that a shorter T_2 relaxation time also will decrease the sensitivity. This T_2 relaxation time will decrease with increasing molecular weight. This means that structure determination by high resolution NMR will be impossible for large proteins (> 40 kDa).

To select the desired magnetization transfer pathway two methods are available, phase cycling (Bodenhausen, et al., 1984) and pulse field gradients (Hurd, 1990). The latter is more advantageous in that unwanted signals are better suppressed. Furthermore, no presaturation of the water is needed, which means that protons of

the protein which exchange with water protons will be observed better in a NMR spectrum. The disadvantage of the use of pulse field gradients in combination with multi-dimensional NMR is a decrease in sensitivity of $\sqrt{2}$. This can be prevented by using sensitivity enhancement (Cavanagh, et al., 1991; Cavanagh and Rance, 1990; Palmer III, et al., 1991) in combination with pulse field gradients (Kay, et al., 1992). In this thesis the original triple resonance NMR experiments are adjusted to incorporate pulse field gradients. To prevent loss in sensitivity, the pulse field gradients are incorporated in a sensitivity enhanced way (chapter 3; Fig. 3.2).

1.2.4 Structure determination

When all (or most) NMR sensitive nuclei are assigned to their corresponding atoms in the protein, we still do not have the three-dimensional protein structure. In order to determine this structure we resort to our through space interaction: the NOE. By using (variants of) the NOESY experiment (see Clore and Gronenborn, 1991), it is determined which protons are close to a certain other proton. Furthermore, from the NOE intensity the approximate distance between two protons can be determined. This distance information of many proton pairs in the protein is used in Distance Geometry calculations and Restrained Molecular Dynamics calculations to determine the three-dimensional solution structure of the protein.

1.3 Transition state and Frontier orbital theory

For any chemical reaction holds that the step in which the intermediate with the highest relative free-energy occurs determines the overall rate of the reaction. This high-energy intermediate is known as the *transition state* (Fig. 1.8). The theory which accounts for chemical catalysis is called the transition state theory (Evans and Polanyi, 1935; Eyring, 1935; Fersht, 1985; Pelzer, 1932). The only physical entities considered in this theory are the reagents, or ground state, and the most unstable species on the reaction pathway, the above mentioned transition state. In the transition state chemical bonds are in the process of being made and broken. The rate by which the transition state is formed is given by the following (first-order) rate constant:

$$k_f = PZ \exp\left(\frac{-E_a}{RT}\right) \quad (1.1)$$

P	Probability or steric factor
Z	Collision number
R	Gas constant
T	Absolute temperature
E_a	Activation energy

It is clear from Eqn. 1.1 that a decrease of the activation energy of the transition state (E_a) will result in an increase of reaction rate (k_f). A catalyst can increase the reaction rate by stabilizing the transition state. Enzymes are proteins which act as catalysts of the chemical reactions undergone by their substrates, without self being altered.

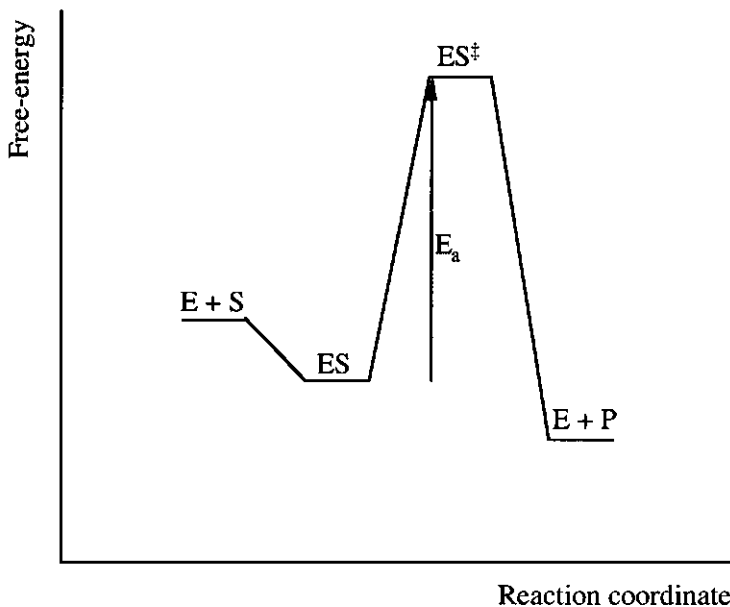


Fig. 1.8. Free-energy profile of an enzymatic reaction. The relative free-energy of the enzyme E + substrate S (free), ES (bound), the transition state ES^\ddagger and the enzyme + product P are given in the energy profile. The height of the activation energy barrier E_a determines the reaction rate k_{cat} (Eqn. 1.1).

They thus can increase the rate of a reaction by stabilizing the transition state, i.e. by lowering its activation energy (E_a). For an enzyme forming a so-called 'Michaelis-Menten' complex (Michaelis and Menten, 1913) with its substrate, k_{cat} is the first-order rate constant for the chemical conversion of the substrate by its enzyme. When the enzyme is saturated with substrate molecules, this k_{cat} readily follows from Eqn. 1.1 by replacing k_f by k_{cat} . Analogously, a lower energy for the transition state in an enzyme-substrate complex (ES^\ddagger) will result in a higher rate of conversion (k_{cat}) of the corresponding substrate by the enzyme.

When the substrate is in the active-site, the orbitals of the substrate and the catalytic residue(s) of the enzyme will interact and form new orbitals (Fig. 1.9). The new orbitals will then be an approximation of the orbitals of the transition state. For the description of *differential* chemical reactivity mainly the so-called *frontier orbitals* (Fukui, et al., 1952), i.e. HOMO (highest occupied molecular orbital) and LUMO (lowest unoccupied molecular orbital) of the reactants, are of importance (Fleming, 1976). When the HOMO of one molecule (in this thesis the substrate) interacts with the LUMO of another molecule (in this thesis the catalytic residue of the enzyme) new orbitals are formed (Fig. 1.9). The energy of the HOMO of these new orbitals will be lower than the energy of the old HOMO. Thus, as these new orbitals are an approximation of the orbitals of the transition state, the energy of the transition state will be lowered ($-\Delta E_f$). Klopman and Salem have used perturbation theory to derive an expression for this ΔE_f (Klopman, 1968; Salem, 1968a; Salem, 1968b). A simplified version of their expression, valid for two non-charged reactants, is given by Eqn. 1.2 (Fleming, 1976).

$$\Delta E_f = \frac{2(c_{nuc} \cdot c_{el} \cdot \beta)^2}{E(\text{HOMO})_{(nuc.)} - E(\text{LUMO})_{(el.)}} \quad (1.2)$$

c_{nuc} .	Coefficient of the HOMO for the nucleophile
c_{el} .	Coefficient of the LUMO for the electrofile
β	Resonance integral
$E(\text{HOMO})_{(nuc.)}$	Energy of the HOMO of the nucleophile
$E(\text{LUMO})_{(el.)}$	Energy of the LUMO of the electrofile

From Eqn. 1.2 in combination with Eqn. 1.1 it follows that a (negative) increase in ΔE_f must result in a decrease of E_a and thus in an increase of the reaction rate k_{cat} .

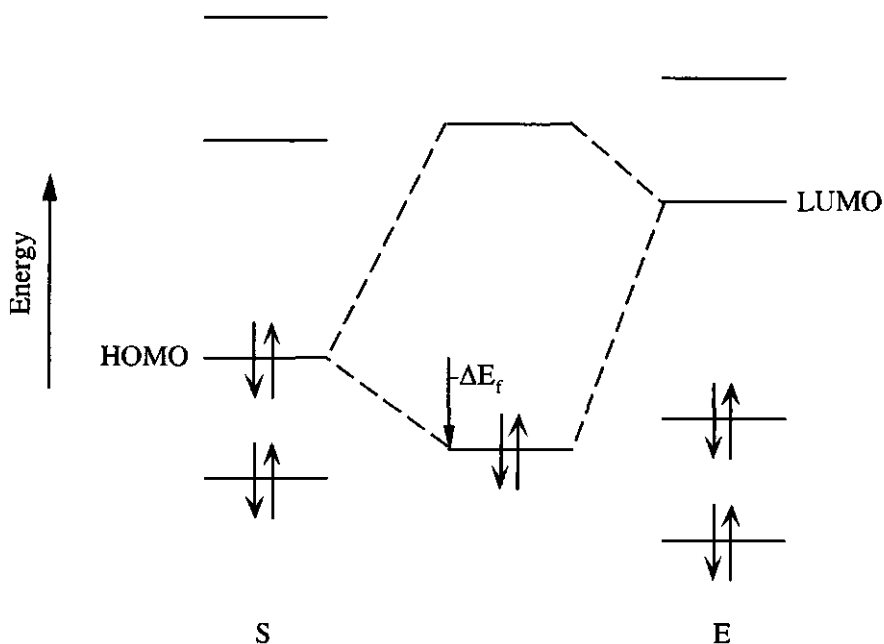


Fig. 1.9. Energy diagram of the interaction of the HOMO of one molecule (S) (in this thesis the substrate) with the LUMO of another (E) (in this thesis the flavin of the enzyme). This interaction results in the formation of a new orbital. The formation of this new orbital results in an energy gain of ΔE_f .

Hence it can be expected that frontier orbital characteristics are of importance for the rate of an enzymatic reaction.

The enzymatic reaction considered in this thesis is the nucleophilic attack of the HOMO electrons of a phenolic substrate on the LUMO of the C(4a)-hydroperoxyflavin of phenol hydroxylase (Scheme 1.2). A series of closely related fluorinated phenols is expected not to bind differently to the active site of phenol hydroxylase. These comparable substrates probably will not have a different effect on the energy of the LUMO of the C(4a)-hydroperoxyflavin. Different energies of the HOMO electrons of the phenolic substrates however, must result in differences in ΔE_f , and thus in differences in E_a . Due to the relationship between E_a and k_{cat} (Eqn. 1.1) a correlation is expected between the energy of the HOMO electrons of the substrates and k_{cat} of the enzyme reaction, assuming the nucleophilic attack of the HOMO

electrons of the substrate on the LUMO of the C(4a)-hydroperoxyflavin is rate-limiting in the enzyme reaction. For another flavin monooxygenase, *p*-hydroxybenzoate hydroxylase, indeed a linear correlation between the E(HOMO) of a series of substrates and the natural logarithm of their rate of conversion (Husain, et al., 1980) has been observed (Vervoort, et al., 1992).

1.4 Outline of this thesis

In this thesis flavoproteins from two different classes have been studied, i.e. flavodoxins and phenol hydroxylase. Flavodoxins are small and stable proteins, and are therefore very well suited for structure determination by multi-dimensional NMR. Although the overall fold of all flavodoxins is the same, their redox-potentials are not. This must be caused by the different apoproteins. To understand the effect of the apoprotein on the redox-potential of FMN in flavodoxin it is necessary to have insight in the interactions between the apoflavodoxin and the FMN. For the flavodoxin from *Desulfovibrio vulgaris* (Hildenborough) differences in these interactions between the three redox-states have been studied by 2D-NMR (chapter 2). The results are discussed in relation with the existing X-ray structures. The flavodoxin from *Azotobacter chroococcum* has completely different redox-potentials as compared to the one from *D. vulgaris*. In order to gain insight in this difference, the solution structure of the *A. chroococcum* flavodoxin is needed. In order to determine this structure by NMR, the resonances have to be assigned first. For the structure determination by NMR, latter flavodoxin had to be uniformly labelled with ^{13}C and ^{15}N . The assignments of the ^1H , ^{13}C and ^{15}N resonances of the backbone atoms of the *A. chroococcum* flavodoxin are given in chapter 3. For the assignment the original triple resonance NMR experiments are adjusted to incorporate pulse field gradients in a sensitivity enhanced way. In this chapter also the topology of the secondary structure elements of this flavodoxin, as determined by heteronuclear multi-dimensional NMR spectroscopy, are given. Furthermore residues which interact with the nitrogenase enzyme complex from *A. chroococcum* are determined.

Phenol hydroxylase from the yeast *Trichosporon cutaneum* catalyses the hydroxylation of various substituted phenols. The regioselectivity and rate of the *ortho*-hydroxylation of 3-fluorophenol by phenol hydroxylase is investigated by ^{19}F -NMR (chapter 4). Based on the ^{19}F -NMR results in combination with molecular

orbital calculations, a hypothesis is put forward explaining the pH effect on hydroxylation observed. In chapter 5 the regioselectivity of the *ortho*-hydroxylation of a series of substituted phenols is studied using ^{19}F -NMR. Also, the conversion rates for all the different substituted phenols are determined. These reaction rates are correlated to the calculated energy of the reactive electrons in the highest occupied molecular orbitals of the substrates.

1.5 References

- Bax, A. and Grzesiek, S. (1993) *Accounts Chem. Res.* **26**, 131-138.
- Berkel van, W.J.H. and Müller, F. (1991) in *Chemistry and biochemistry of flavoenzymes* (Müller, F., Ed.) Vol. 2, pp. 1-29, CRC Press, Boca Raton.
- Bloch, F., Hansen, W.W. and Packard, M.E. (1946) *Phys. Rev.* **69**, 127.
- Blyth, A.W. (1879) *J. Chem. Soc.* **35**, 530-539.
- Bodenhausen, G., Kogler, H. and Ernst, R.R. (1984) *J. Magn. Reson.* **58**, 370.
- Bovey, F.A. (1969) *Nuclear magnetic resonance spectroscopy*, Academic Press inc., New York.
- Braunschweiler, L. and Ernst, R.R. (1983) *J. Magn. Res.* **53**, 521-528.
- Burnett, R.M., Darling, G.D., Kendall, D.S., LeQuesne, M.E., Mayhew, S.G., Smith, W.W. and Ludwig, M.L. (1974) *J. Biol. Chem.* **249**, 4383-4392.
- Cavanagh, J., Palmer III, A.G., Wright, P.E. and Rance, M. (1991) *J. Magn. reson.* **91**, 429-436.
- Cavanagh, J. and Rance, M. (1990) *J. Magn. Reson.* **88**, 72-85.
- Clore, G.M. and Gronenborn, A.M. (1991) *Prog. NMR Spectr.* **23**, 43-92.
- Clubb, R.T., Thanabal, V., Osborne, C. and Wagner, G. (1991) *Biochemistry* **30**, 7718-7730.
- Cusanovich, M.A. and Edmondson, D.E. (1971) *Biochim Biophys. Res. Commun.* **45**, 327-336.
- Dagley, S. (1982) in *Flavins and flavoproteins* (Massey, V. and Williams, C.H., Eds.) pp. 311-317, Elsevier, New York.
- Deistung, J. and Thomeley, R.N.F. (1986) *Biochem. J.* **239**, 69-75.
- Derome, A.E. (1987) *Modern NMR techniques for chemistry research*, Pergamon Press, Oxford.
- Detmer, K. and Massey, V. (1984) *J. Biol. Chem.* **259**, 11265-11272.

- Dubourdieu, M., LeGall, J. and Favaudon, V. (1975) *Biochim. Biophys. Acta* **376**, 519-532.
- Enroth, C., Huang, W., Waters, S., Neujahr, H., Lindqvist, Y. and Schneider, G. (1994) *J. Mol. Biol.* **238**, 128-130.
- Ernst, R.R. and Anderson, W.A. (1966) *Rev. Sci. Instrumen.* **37**, 93-102.
- Evans, D.J., Jones, R., Woodley, P.R., Wilborn, J.R. and Robson, R.L. (1991) *J. Bacteriol.* **173**, 5457-5469.
- Evans, M.G. and Polanyi, M. (1935) *Trans. Faraday Soc.* **31**, 875.
- Eyring, H. (1935) *Chem. Rev.* **17**, 65.
- Fersht, A. (1985) *Enzyme structure and mechanism*, W.H. Freeman and company,
- Fitzgerald, M.P., Husain, A. and Rogers, L.J. (1978) *Biochem Biophys. Res. Commun.* **81**, 630-635.
- Fleming, I. (1976) *Frontier orbitals and organic chemical reactions*, John Wiley & Sons, Chichester.
- Fujii, K., Galivan, J. H. and Huennekens, F.M. (1977) *Arch. Biochem. Biophys.* **178**, 662-670.
- Fukui, K., Yonezawa, T. and Shingu, H. (1952) *J. Chem. Phys.* **20**, 722-725.
- Fukuyama, K., Wakabayashi, S., Matsubara, H. and Rogers, L.J. (1990) *J. Biol. Chem.* **265**, 15804-15812.
- Ghisla, S. and Massey, V. (1989) *Eur. J. Biochem.* **181**, 1-17.
- Gorter, C.J. (1936) *Physica* **3**, 995-998.
- Grzesiek, S. and Bax, A. (1992a) *J. Am. Chem. Soc.* **114**, 6291-6293.
- Grzesiek, S. and Bax, A. (1992b) *J. Magn. Reson.* **99**, 201-207.
- Grzesiek, S. and Bax, A. (1992c) *J. Magn. Reson.* **96**, 432-440.
- Hurd, R.E. (1990) *J. Magn. Reson.* **87**, 422-428.
- Husain, M., Entsch, B., Ballou, D.P., Massey, V. and Chapman, P.J. (1980) *J. Biol. Chem.* **255**, 4189-4197.
- Ikura, M., Kay, L.E. and Bax, A. (1990) *Biochemistry* **29**, 4659-4667.
- Jardetzky, O. and Roberts, G.C.K. (1981) *NMR in molecular biology*, Academic Press inc., New York.
- Jeener, J., Meier, B.H., Bachmann, P. and Ernst, R.R. (1979) *J. Chem. Phys.* **71**, 4546-4553.
- Kay, L.E., Keifer, P. and Saarinen, T. (1992) *J. Am. Chem. Soc.* **114**, 10663-10665.
- Klopman, G. (1968) *J. Am. Chem. Soc.* **90**, 223-234.
- Knauf, M.A., Löhr, F., Curley, G.P., O'Farrell, P., Mayhew, S.G. and Müller, F. (1993) *Eur. J. Biochem.* **213**, 167-184.

- Ludwig, M.L., Burnett, R.M., Darling, G.D., Jordan, S.R., Kendall, D.S. and Smith, W.W. (1976) in *Flavins and Flavoproteins* (Singer, T.P., Ed.) pp. 393-404, Elsevier, Amsterdam.
- Ludwig, M.L. and Luschinsky, C.L. (1992) in *Chemistry and Biochemistry of Flavoenzymes* (Müller, F., Ed.) Vol. 3, pp. 427-466, CRC Press, Boca Raton.
- Maeda-Yorita, K. and Massey, V. (1993) *J. Biol. Chem.* **268**, 4134-4144.
- Massey, V. and Hemmerich, P. (1980) *Biochem. Soc. Trans* **8**, 246-257.
- Mayhew, S.G. (1971) *Biochem. Biophys. Acta* **235**, 276-288.
- Mayhew, S.G. and Massey, V. (1969) *Eur. J. Biochem.* **244**, 794-802.
- Mayhew, S.G. and Tollin, G. (1992) in *Chemistry and Biochemistry of Flavoenzymes* (Müller, F., Ed.) pp. 389-426, CRC Press, Boca Raton.
- Michaelis, L. and Menten, M.L. (1913) *Biochem. Z.* **49**, 333-369.
- Mierlo van, C.P.M., Lijnzaad, P., Vervoort, J., Müller, F., Berendsen, H.J.C. and Vlieg de, J. (1990a) *Eur. J. Biochem.* **194**, 185-188.
- Mierlo van, C.P.M., Müller, F. and Vervoort, J. (1990b) *Eur. J. Biochem.* **189**, 589-600.
- Müller, F. (1991) in *Chemistry and Biochemistry of Flavoenzymes* (Müller, F., Ed.) Vol. 1, pp. 1-71, CRC Press, Boca Raton.
- Neujahr, H.Y. (1991) in *Chemistry and biochemistry of flavoenzymes* (Müller, F., Ed.) Vol. 2, pp. 65-85, CRC Press, Boca Raton.
- Neujahr, H.Y. and Kjellén, K.G. (1978) *J. Biol. Chem.* **253**, 8835-8841.
- Palmer III, A.G., Cavanagh, J., Wright, P.E. and Rance, M. (1991) *J. Magn. Reson.* **93**, 151-170.
- Pelzer, H. (1932) *Z. Phys. Chem.* **B15**, 445-471.
- Piantini, U., Sørensen, O.W. and Ernst, R.R. (1982) *J. Am. Chem. Soc.* **104**, 6800-6801.
- Rance, M., Sørensen, O.W., Bodenhausen, G., Wagner, G., Ernst, R.R. and Wüthrich, K. (1983) *Biochem. Biophys. Res. Commun.* **117**, 479-485.
- Rao, S.T., Shaffie, F., Yu, C., Sathysur, K.A., Stockman, B.J., Markley, J.L. and Sundaralingam, M. (1992) *Protein Science* **1**, 1413-1427.
- Salem, L. (1968a) *J. Am. Chem. Soc.* **90**, 543-552.
- Salem, L. (1968b) *J. Am. Chem. Soc.* **90**, 553-566.
- Shaka, A.J. and Freeman, R. (1983) *J. Magn. Res.* **51**, 169-173.
- Simondson, R.P. and Tollin, G. (1980) *Mol. Cell. Biochem.* **33**, 13-24.
- Singer, T.P. and Edmondson, D.E. (1978) in *Methods in Enzymology* (Fleischer, S. and Packer, L., Eds.) Vol. 53, pp. 397-418, Academic Press inc., New York.
- Smith, W.W., Burnett, R.M., Darling, G.D. and Ludwig, M.L. (1977) *J. Mol. Biol.* **117**, 195-225.

- Smith, W.W., Pattridge, K.A., Ludwig, M.L., Petsko, G.A., Tsernoglou, D., Tanaka, M. and Yasanobu, K.T. (1983) *J. Mol. Biol.* **165**, 737-755.
- Stankovich, M.T. (1991) in *Chemistry and biochemistry of flavoproteins* (Müller, F., Ed.) Vol. 1, pp. 401-425, CRC Press, Boca Raton.
- Stockman, B.J., Euvrard, A., Kloosterman, D.A., Scahill, T.A. and Swenson, R.P. (1993) *J. Biomol. NMR* **3**, 133-149.
- Stockman, B.J., Krezel, A.M., Markley, J.L., Leonhardt, K.G. and Strauss, N.A. (1990) *Biochemistry* **29**, 9600-9609.
- Stockman, B.J., Richardson, T.E. and Swenson, R.P. (1994) **33**, 15298-15308.
- Vervoort, J., Rietjens, I.M.C.M., Berkel van, W.J.H. and Veeger, C. (1992) *Eur. J. Biochem.* **206**, 479-484.
- Watenpugh, K.D., Sieker, L.C. and Jensen, L. (1973) *Proc. Natl. Acad. Sci. USA* **70**, 3857-3860.
- Watt, W., Tulinsky, A., Swenson, R.P. and Watenpugh, K.D. (1991) *J. Mol. Biol.* **218**, 195-208.
- Wüthrich, K. (1986) *NMR of proteins and nucleic acids*, Wiley & Sons Inc., New York.
- Zumft, W.G. and Spiller, H. (1971) *Biochem. Biophys. Res. Commun.* **45**, 112-118.

2

Two-dimensional NMR studies of the flavin binding site of *Desulfovibrio vulgaris* flavodoxin in its three redox-states

Sjaak Peelen and Jacques Vervoort

Published in *Archives of Biochemistry and Biophysics* **314** (1994), 291-300.

The FMN binding site of Desulfovibrio vulgaris flavodoxin in the diamagnetic oxidized and two-electron reduced form was investigated using two-dimensional proton NMR. The NMR results are compared to existing X-ray crystallographic data. In the paramagnetic one-electron reduced redox-state resonances of protons which are close to the FMN ring are strongly broadened due to the paramagnetic properties of the flavin-ring. From comparison of the NMR spectra of the three redox-states it could be concluded that outside the FMN binding site no structural changes occur upon reduction. Strong hydrogen bonds are observed between the N(1) and C(2) carbonyl of the isoalloxazine ring and the amide protons of Asp⁹⁵ and Cys¹⁰² respectively. The amide resonances of Asp⁹⁵ and Cys¹⁰² are strongly downfield shifted upon two-electron reduction, caused by the negative charge in the N(1)-C(2) carbonyl region in the two-electron reduced FMN. It is suggested that the ring current of the central pyrazine ring of the FMN molecule in the two-electron reduced flavodoxin is decreased as compared to the oxidized flavodoxin. The decrease in ring current is apparently caused by the loss of aromaticity of this pyrazine moiety due to protonation of N(5). Strong hydrogen bonds between the

flavin phosphate group and amide and hydroxyl protons of the apoprotein are observed. Resonances of protons involved in this hydrogen bonding network are up to 3.5 ppm downfield shifted. It is suggested that the negative charges of the dianionic FMN phosphate group are stabilized by local peptide dipoles. On reduction of the protein from the oxidized to the one-electron reduced form, a conformational change occurs in the FMN binding region. No conformational change can be observed between the one-electron and the two-electron reduced state.

2.1 Introduction

Flavodoxins are small redox-proteins which are found in several microorganisms. They function as electron-transfer proteins and contain a non-covalently bound FMN molecule (Fig. 2.1), which acts as a prosthetic group. This prosthetic group can exist in three redox-states, oxidized, one-electron reduced (or semiquinone) and two-electron reduced (or hydroquinone). The redox-potentials of the FMN molecule change strongly upon binding to the protein, especially the semiquinone-hydroquinone couple which changes from -124 mV (free FMN) to -440 mV for *Desulfovibrio vulgaris* flavodoxin (Curley, et al., 1991). The low redox-potential of this couple enables *D. vulgaris* flavodoxin to deliver electrons to the sulfite reducing system. It has long been recognized that the regulation of redox-potentials is due to specific interactions between the apoprotein and the prosthetic group (Vervoort, 1991). It is therefore essential to obtain detailed information about the interaction between the amino acid residues of the apoprotein and the FMN moiety. Recent advances in NMR technology make it feasible to study these interactions in such detail.

The flavodoxin studied here is from the sulphate reducing bacteria *Desulfovibrio vulgaris* (strain Hildenborough). This flavodoxin contains 148 amino acid residues and has a molecular weight of 15.7 kDa (Curley, et al., 1991). The X-ray structures of *Desulfovibrio vulgaris* flavodoxin in its three redox-states have been determined by the group of Watenpaugh (Watt, et al., 1991). From these studies it could be concluded that a conformational change occurs on reduction at the peptide bond of Gly⁶¹-Asp⁶² (Watt, et al., 1991). The carbonyl oxygen of Gly⁶¹ points away from the N(5) group of the isoalloxazine ring of the FMN in the oxidized state whereas it

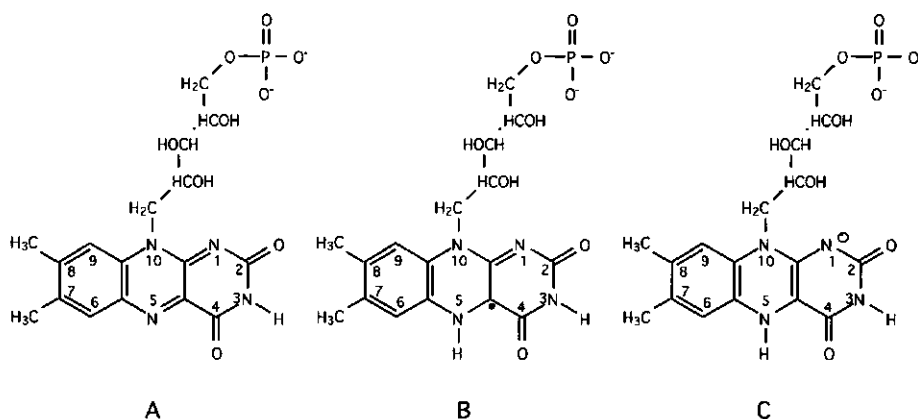


Fig. 2.1 The FMN molecule in its three redox-states: A) oxidized, B) one-electron reduced (semiquinone) and C) two-electron reduced (hydroquinone).

points towards the N(5)H in the two-electron reduced state forming a hydrogen bond with the N(5) proton.

The flavodoxin in its three redox-states has been studied by 2D proton NMR. The proton resonances of the amino acid residues in the immediate neighbourhood of the isoalloxazine ring of the FMN become broadened in the one-electron reduced protein as a result of the paramagnetic character of the isoalloxazine ring in this redox-state (Vervoort, et al., 1991). Comparison of the NMR spectrum of the one-electron reduced flavodoxin to the spectrum of the two-electron reduced flavodoxin was of great help in assigning proton resonances of amino acids in the immediate neighbourhood of the isoalloxazine ring. Proton chemical shifts of these amino acids in the oxidized and the two-electron reduced flavodoxin are compared and related to the X-ray structures of oxidized and two-electron reduced flavodoxin (Watt, et al., 1991).

2.2 Materials and methods

Flavodoxin from *Desulfovibrio vulgaris* (strain Hildenborough) was purified as described elsewhere (Dubourdieu and LeGall, 1970). Protein concentrations of the

oxidized flavodoxin were determined by measuring the absorption at 457 nm, using an extinction coefficient of $10,700 \text{ M}^{-1} \cdot \text{cm}^{-1}$ (Curley, et al., 1991).

All NMR samples contained 2.5-5.5 mM flavodoxin in a 180 mM KCl, 18 mM potassium pyrophosphate and 140 mM potassium phosphate buffer, pH 7.5-8.3. All samples contained 10% (v/v) $^2\text{H}_2\text{O}$ for locking the magnetic field. Wilmad 5 mm precision NMR tubes were used, containing a sample volume of 450 μl . Reduction was done by the addition of a desired amount of an anaerobic sodium dithionite solution to the anaerobic flavodoxin. The flavodoxin was made anaerobic by flushing the sample several times with argon.

The 2D-NMR spectra were recorded at 303 K on a Bruker AM 600 or a Bruker AMX 500 NMR spectrometer. Phase sensitive spectra were obtained by using the time-proportional phase incrementation method (Marion and Wüthrich, 1983). NOESY (Jeener, et al., 1979), DQF-COSY (Piantini, et al., 1982; Rance, et al., 1983; Shaka and Freeman, 1983) and TOCSY (Braunschweiler and Ernst, 1983) spectra using a DIPSI-2 spin-lock sequence (Shaka, 1988) were recorded with 512 t_1 increments each with 2 K data points. The SCUBA technique (Brown, et al., 1988) was used in the NOESY and DQF-COSY experiments, recorded on the AMX 500, to recover saturated proton resonances under the water line. Presaturation during the relaxation delay was employed to suppress the water signal. This relaxation delay was set to 1.5 s. The NOESY spectra were recorded using a mixing-time of 150 ms. The TOCSY spectra were recorded using mixing-times of 54 ms and 65 ms. The experimental data were zero filled to give a 4 K x 1 K data matrix. The data were processed with appropriately matched sine bell functions prior to Fourier transformation.

The X-ray structures of *Desulfovibrio vulgaris* flavodoxin in its three redox-states, as submitted by Watt et al. (1991) in the Brookhaven protein databank, were analysed on Silicon Graphics workstations using Quanta/Charmm software (Molecular Simulations, UK) and Insight/Discover (Biosym, USA).

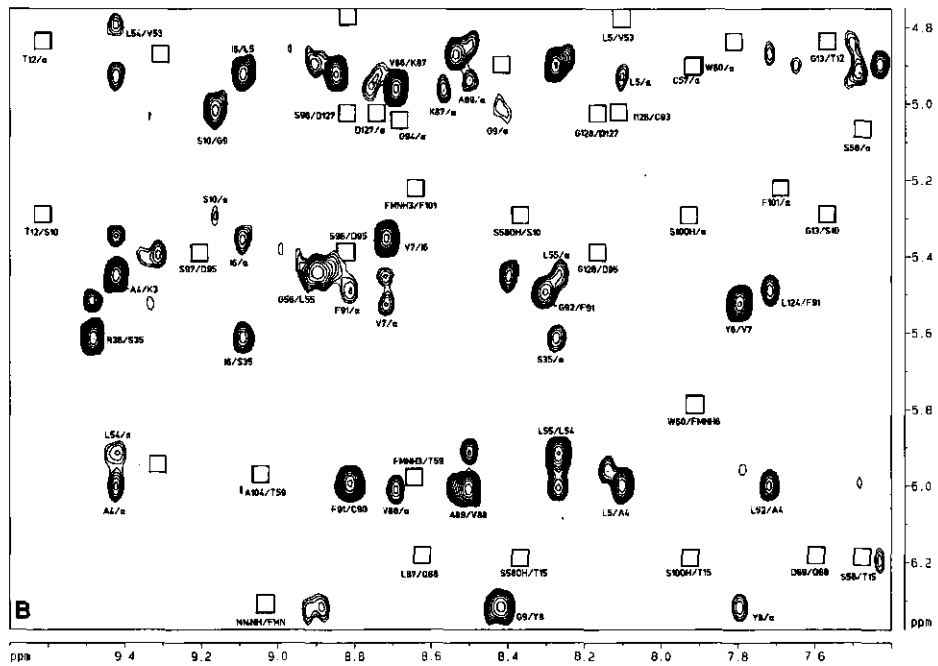
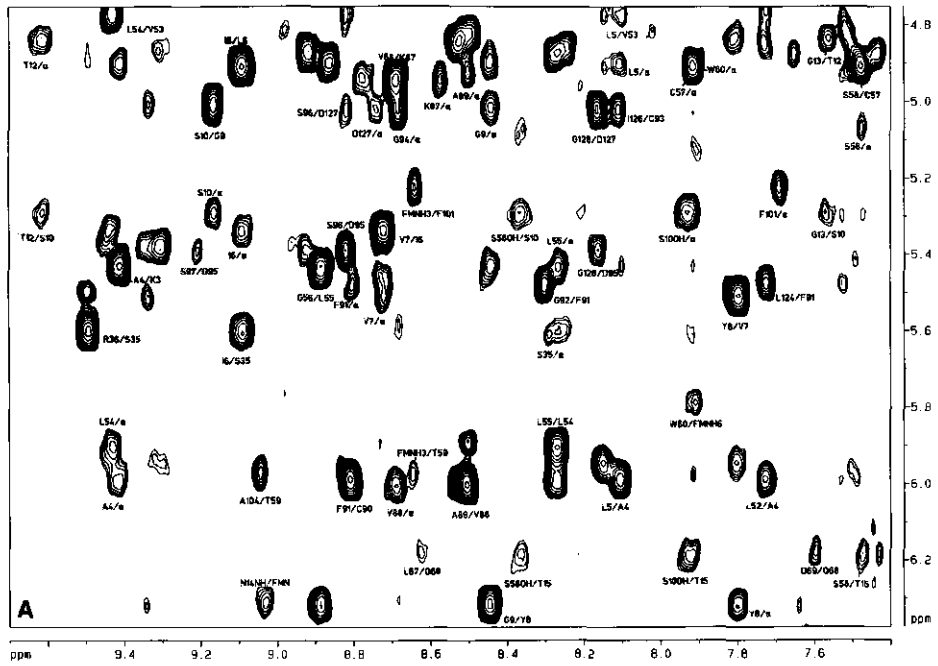
2.3 Results and discussion

Assignments of proton resonances of a protein the size of *D. vulgaris* flavodoxin (148 amino acids) is a formidable problem. Using 2D DQF-COSY (Piantini, et al., 1982; Rance, et al., 1983; Shaka and Freeman, 1983) and TOCSY (Braunschweiler

and Ernst, 1983) experiments about 60% of the non-proline spin-systems were identified. They were assigned to four groups: 1) cysteine, serine, aspartate, asparagine and histidine; 2) phenylalanine, tyrosine and tryptophan; 3) isoleucine, leucine, threonine and valine; 4) glutamate, glutamine, lysine and arginine. Alanine and glycine spin-systems could uniquely be identified. In combination with 2D NOESY (Jeener, et al., 1979) spectra about 80% of the spin-systems were sequentially assigned (Wüthrich, 1986), both for the oxidized and reduced forms of the enzyme. The assignment process was facilitated by several properties of the protein. Firstly, the paramagnetic properties of the isoalloxazine ring in the one-electron reduced flavodoxin give rise to extensive line broadening of all resonances in the immediate neighbourhood of the ring system, yielding spectra with a decreased number of resonances (Vervoort, et al., 1991). Secondly, the fast electron shuttle between the one-electron reduced and two-electron reduced flavodoxin makes it feasible, by changing the ratio of hydroquinone to semiquinone species, to create a varying sphere of amino acid residues which are under the influence of the paramagnetic center (Vervoort, et al., 1991). Thus resonances of protons immediately surrounding the flavin-cofactor could be assigned almost completely.

Comparison of a NOESY spectrum of *Desulfovibrio vulgaris* flavodoxin in its hydroquinone (Fig. 2.2A) and in its semiquinone form (Fig. 2.2B) clearly shows the large amount of resonances that have identical chemical shift values and that do not disappear in the semiquinone spectrum (Fig. 2.2B). These protons are therefore not in the direct neighbourhood of the isoalloxazine ring. The identical chemical shift values of these protons in both redox-states (one-electron and two-electron reduced) indicate that there is virtual no structural difference, outside the FMN binding region, between the two redox-states.

Fig. 2.2C shows part of a NOESY spectrum of oxidized flavodoxin. The differences in chemical shifts between the proton resonances of the oxidized flavodoxin (Fig. 2.2C) and the resonances of the two-electron reduced flavodoxin (Fig. 2.2A) are smaller than 0.04 ppm for almost all resonances observed except for some resonances at the N-terminus and some resonances in the direct environment of the FMN group. No difference in intensities of NOE crosspeaks of comparable resonances of the oxidized and two-electron reduced flavodoxin are observed outside the FMN binding region (Fig. 2.2A, C). This indicates that the tertiary structure outside the FMN binding region of the flavodoxin is identical in all three redox-states.



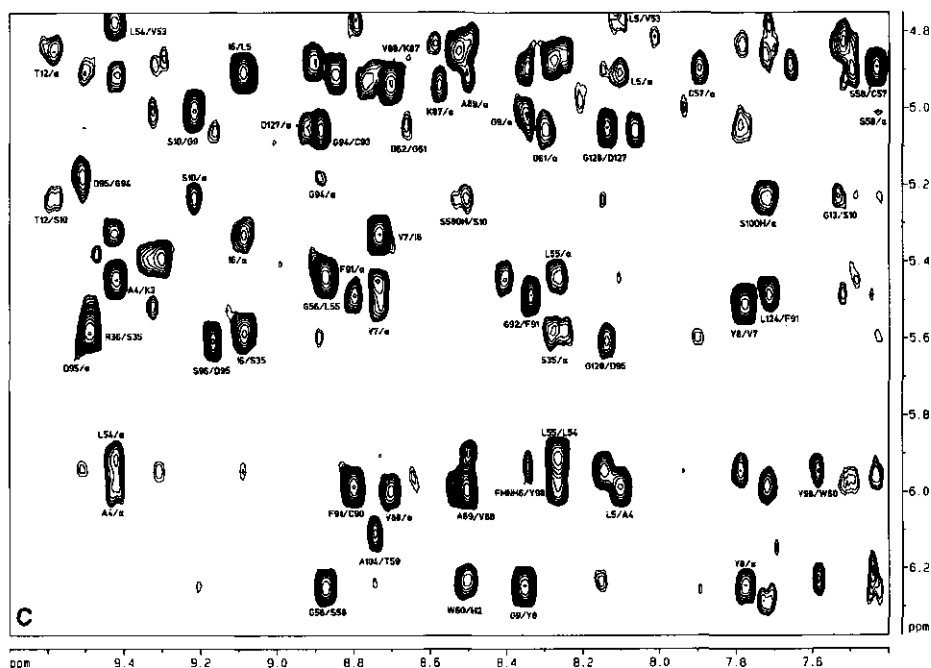


Fig. 2.2 A) Part of a 500 MHz NOESY spectrum of two-electron reduced *Desulfovibrio vulgaris* flavodoxin (3.3 mM) at pH 8.3. B) Same part as A of a 600 MHz NOESY spectrum of one-electron reduced *Desulfovibrio vulgaris* flavodoxin (5.3 mM). The boxes indicate the cross-peaks broadened due to the paramagnetic FMN ring. C) Same part as A of a 500 MHz NOESY spectrum of oxidized *Desulfovibrio vulgaris* flavodoxin (3.5 mM) at pH 7.9. All at 303 K.

2.3.1 Phosphate binding region

A remarkable feature of the ^1H NMR spectrum of *Desulfovibrio vulgaris* flavodoxin is that some amide resonances are shifted to low field as compared to the rest of the amide resonances (Fig. 2.3). Especially the amide resonances of Thr¹¹ and Thr¹⁵ show a large downfield shift (Fig. 2.3A) and resonate at respectively 11.61 and 11.95 ppm for the oxidized protein (Table 2.1). The amide protons of Ser¹⁰, Thr¹² and Asn¹⁴, which are involved in the phosphate hydrogen bonding network as well, resonate at 9.21, 9.56 and 9.75 ppm respectively. Besides amide protons, some hydroxyl protons are involved in hydrogen bonding interactions with the dianionic phosphate. These hydroxyl protons belong to Ser¹⁰, Thr¹², Thr¹⁵ and Ser⁵⁸, and

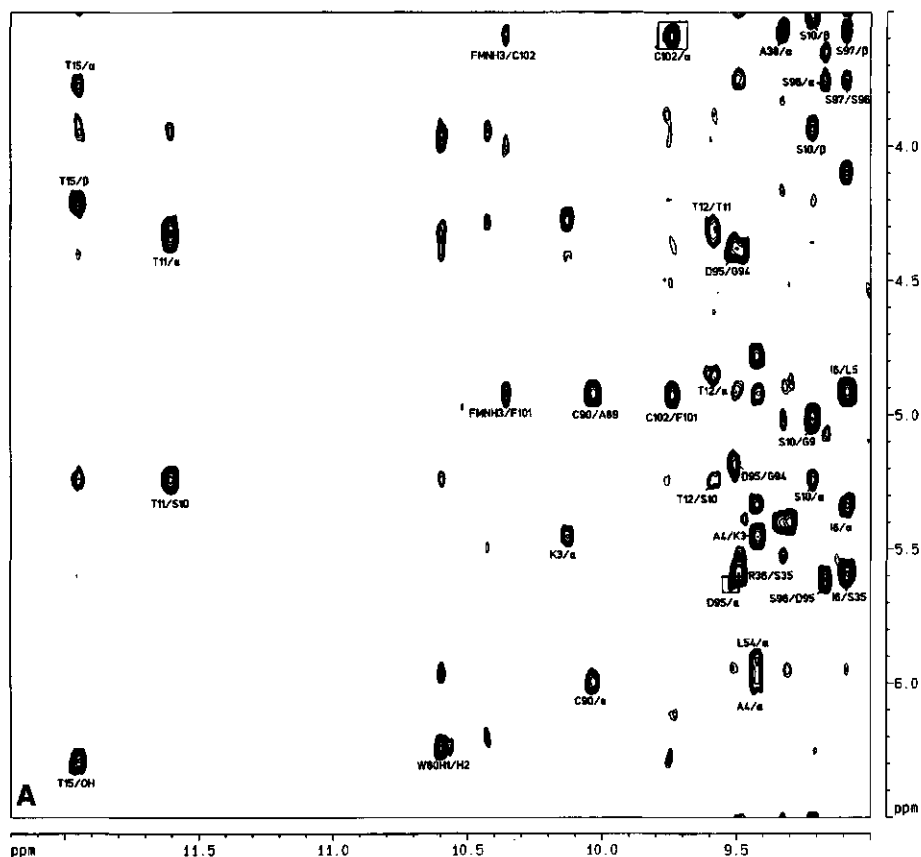


Fig. 2.3A Low field region of a 500 MHz NOESY spectrum of oxidized *Desulfovibrio vulgaris* flavodoxin (3.5 mM) pH 7.9 at 303 K.

resonate respectively at 7.71, 8.32, 6.27 and 8.51 ppm, for the oxidized protein (Table 2.1). Resonances of hydroxyl protons are usually not observed in NMR spectra, especially not at pH 8.3. However, for the flavodoxin of *Megasphaera elsdenii* also resonances of hydroxyl protons close to the phosphate group were observed in the NMR spectra (Mierlo van, et al., 1990). Moreover, these hydroxyl protons are close to or on the surface of the protein as can be observed in the X-ray structure. The hydroxyl protons must therefore form strong hydrogen bonds with the phosphate group of the FMN in order for these protons to be not in fast exchange

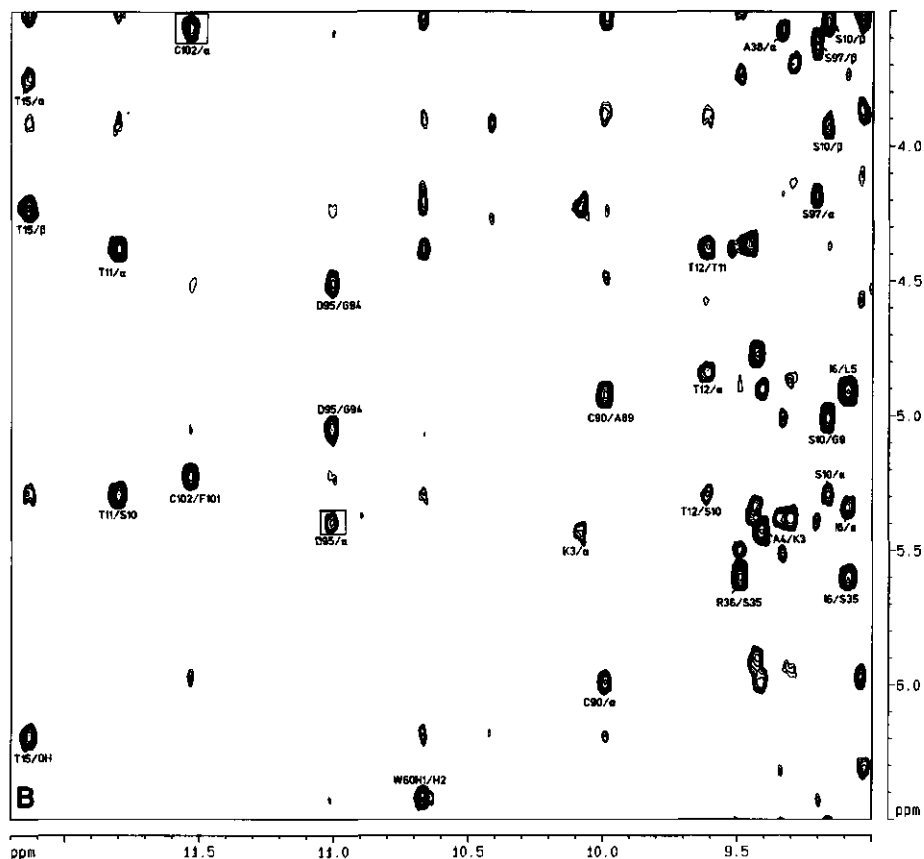


Fig. 2.3B Low field region of a 500 MHz NOESY spectrum of two-electron reduced *Desulfovibrio vulgaris* flavodoxin (3.3 mM) pH 8.3 at 303 K.

with the protons of the bulk water. When all exchangeable protons are replaced by deuterons by preparation of the apoprotein in deuterium oxide as described by Wassink and Mayhew (1975), the above mentioned hydroxyl protons disappear in the 2D NOESY spectrum (data not shown). After freeze-drying and redissolving this deuterated protein in water, the hydroxyl protons again are observed in the NOESY spectrum within two hours after redissolving (data not shown). This result indicates that the hydroxyl protons which form a hydrogen bond with the phosphate group do exchange with the protons of the bulk water, but on a time scale slow as

Table 2.1 Proton chemical shifts of oxidized (Ox.) and two-electron reduced (Red.) flavodoxin from *Desulfovibrio vulgaris* at 303 K.

Residue	Chemical shift (ppm)			Residue	Chemical shift (ppm)		
	Ox. pH 7.9	Ox. pH 8.3	Red. pH 8.3		Ox. pH 7.9	Ox. pH 8.3	Red. pH 8.3
Ser ¹⁰				Thr ⁵⁹			
NH	9.21	9.21	9.16	NH	5.96	5.96	6.28
α	5.24	5.24	5.30	α	4.33	4.33	4.58
β	3.93	3.93	3.93	β	3.19	3.19	3.25
β'	3.47	3.47	3.50	γCH ₃	1.22	1.22	1.36
γOH	7.72	7.71	7.92	γOH	6.12	6.12	5.98
Thr ¹¹				Trp ⁶⁰			
NH	11.61	11.61	11.80	NH	8.51	8.52	7.92
α	4.33	4.33	4.38	α	2.89	2.88	4.91
β	n.d. ^a	n.d.	n.d.	β	3.17	3.17	3.56
γCH ₃	0.88	0.88	0.88	β'	1.99	1.99	3.16
γOH	ex. ^b	ex.	ex.	CH(2)	6.24	6.24	6.43
Thr ¹²				NH(1)	10.60	10.60	10.67
NH	9.56	9.56	9.62	CH(4)	7.00	7.00	7.00
α	4.85	4.85	4.84	CH(7)	8.16	8.16	8.21
β	4.62	4.62	4.58	CH(5)	7.11	7.11	6.72
γCH ₃	1.41	1.41	1.39	CH(6)	7.19	7.19	7.09
γOH	8.32	8.32	8.44	Gly ⁶¹			
Gly ¹³				NH	8.30	8.31	8.61 ^c
NH	7.53	7.53	7.57	α	5.06	5.05	5.01 ^c
α	4.50	4.50	4.50	α'	3.70	3.69	2.88 ^c
α'	3.90	3.90	3.93	Asp ⁶²			
Asn ¹⁴				NH	8.62	8.67	ex.
NH	9.75	9.75	10.01	α	4.90	4.90	n.d.
α	3.46 ^c	3.46 ^c	3.48	β	2.99	2.99	n.d.
β	2.94	2.94	2.94	β'	2.75	2.75	n.d.
β'	n.d.	n.d.	n.d.	Gly ⁹⁴			
δNH	8.82	8.82	9.03	NH	8.89	8.89	8.68
δ'NH	6.81	6.81	6.77	α	5.20	5.20	5.06
Thr ¹⁵				α'	4.37	4.37	4.51
NH	11.95	11.95	12.13	Asp ⁹⁵			
α	3.77	3.77	3.75	NH	9.51	9.51	11.01
β	4.20	4.20	4.23	α	5.62	5.62	5.40
γCH ₃	1.07	1.07	1.07	β	2.97	2.97	3.12
γOH	6.27	6.27	6.20	β'	2.97	2.97	2.71
Ser ⁵⁸				Ser ⁹⁶			
NH	7.43	7.43	7.48	NH	9.17	9.17	8.82
α	5.01	5.01	5.07	α	3.76	3.76	3.63
β	3.96	3.96	4.40	β	2.93 ^c	2.93 ^c	2.83
β'	3.56 ^c	3.56 ^c	4.22	β'	n.d.	n.d.	2.71
γOH	8.51	8.51	8.36	γOH	ex.	ex.	ex.

^a Not determined

^b Exchanges with water

^c Tentative assignment

Table 2.1 Continued

Residue	Chemical shift (ppm)			Residue	Chemical shift (ppm)		
	Ox. pH 7.9	Ox. pH 8.3	Red. pH 8.3		Ox. pH 7.9	Ox. pH 8.3	Red. pH 8.3
Ser ⁹⁷				Phe ¹⁰¹			
NH	9.09	9.09	9.21	NH	8.34	8.34 ^c	7.69
α	4.10	4.10	4.19	α	4.93	4.93	5.23
β	3.57	3.57	3.65	β	3.25	3.25	3.17
β'	3.47	3.47	3.60	β'	2.91	2.91	2.75
γ OH	ex.	ex.	ex.	δ	7.12	7.12	7.08
Tyr ⁹⁸				ϵ	7.16	7.16	7.10
NH	7.60	7.60	7.92	ζ	6.87	6.87	6.81
α	4.00	4.00	4.15	Cys ¹⁰²			
β	3.09	3.09	3.26	NH	9.74	9.73	11.53
β'	2.56	2.56	2.86	α	3.59	3.59	3.57
δ	6.96	6.96	7.19	β	2.53	2.53	2.49
ϵ	5.94	5.94	6.44	β'	1.72	1.72	1.49
Glu ⁹⁹				Gly ¹⁰³			
NH	8.42	8.42	8.48	NH	7.19	7.20	7.69
α	3.73	n.d.	3.70	α	3.99	3.99	3.86
β	n.d.	n.d.	1.64	α'	3.31	3.31	3.35
β'	1.51	n.d.	1.57				
γ	1.81 ^c	n.d.	1.91 ^c	FMN			
γ'	n.d.	n.d.	1.91 ^c	NH(3)	10.36	10.37	8.64
Tyr ¹⁰⁰				NH(5)	-	-	5.13
NH	8.59	8.58	9.29	CH(6)	8.35	8.34	5.80
α	4.84	4.84	4.64	CH ₃ (7)	2.70	2.70	2.11
β	3.14	3.13	3.10	CH ₃ (8)	2.67	2.67	2.02
β'	2.85	2.84	2.65	CH(9)	7.10	7.09	5.43
δ	7.19	7.19	7.05				
ϵ	6.78	6.78	6.62				

compared to the NMR time scale. Apparently the phosphate binding site is a very rigid region with strong hydrogen bonds. No chemical shift changes for the protons in the phosphate binding region are observed in the pH range from 7.0 to 8.3 (data not shown).

The 2D NOESY spectrum of *Desulfovibrio vulgaris* flavodoxin shows that one of the protons of the side-chain amino group of Asn¹⁴ is shifted downfield to 8.82 ppm (Fig. 2.2C), whereas the other amino proton resonates at a normal frequency of 6.81 ppm. This shift can be explained by the presence of a hydrogen bond between this amino proton at 8.82 ppm and the FMN phosphate group.

It is evident from our NMR results that the phosphate group forms a large number of hydrogen bonds with the apoprotein. The H-bonding scheme as

determined from NMR is schematically drawn in Fig. 2.4. This scheme resembles very much the H-bonding scheme determined from the X-ray structure (Watt, et al., 1991), except that the amide proton of Gly¹³ does not seem to form a hydrogen bond to the phosphate as determined by NMR, whereas the amide proton of Ser¹⁰ does not seem to form a hydrogen bond to the phosphate as determined from the X-ray structure. The hydrogen bonds will contribute to the tight binding of the FMN molecule to the apoprotein ($K_d \approx 0.24$ mM) (Curley, et al., 1991). But perhaps more important, these hydrogen bonds will "solvate" the negatively charged (dianionic) phosphate group. These dipolar groups surrounding the phosphate are thought to contribute to the stabilization of the charged phosphate (Warshel, 1987). It is interesting to observe that a correlation seems to exist between the chemical shift values observed for the amide protons and the stabilization of the negative charge via local peptide dipoles. E.g. the amide proton of Thr¹⁵ is shifted strongly downfield indicating the formation of a partial negative charge on the nitrogen atom which via the peptide bond can be delocalized onto the carbonyl oxygen of Asn¹⁴. This carbonyl group is within hydrogen bonding distance of a water molecule as can be judged from the crystallographic studies. All amide protons involved in the hydrogen bonding network have either water molecules in the immediate neighbourhood of the carbonyl oxygen of their peptide bond (Thr¹¹, Thr¹² and Asn¹⁴) or have a strong hydrogen bonding interaction of the carbonyl group of the peptide bond with a nearby amide group (Ser¹⁰ and Thr¹⁵, the carbonyl group of Gly⁹ and Asn¹⁴ form strong hydrogen bonds with the amide protons of Ser⁵⁸ and Thr¹⁸ respectively). Although the amide proton of Gly¹³ is observed to form a hydrogen bond with the FMN phosphate in the X-ray structure, NMR results indicate that this proton apparently is not involved in the strong hydrogen bonding network of the phosphate group as can be judged from the chemical shift value (7.53 ppm). In previous NMR studies performed in our laboratory on *M. elsdenii* flavodoxin a similar result was observed: the amide proton of Gly¹¹ was shown not to be involved in the hydrogen bonding network of the phosphate group (Mierlo van, et al., 1990). Although this glycine residue has been observed to be absolutely conserved in all flavodoxins studied, Drummond et al. (1993) could show that this residue can be substituted by many other amino acids without affecting stability or function.

In addition to local peptide dipoles, it has been claimed that helix dipoles can stabilize charges on either the N-terminal end (negative charge) or the C-terminal end (positive charge) (Hol, et al., 1978). Indeed the phosphate group of the FMN moiety

is bound at the N-terminus of an α -helix, but on close examination of all published three dimensional X-ray structures it can be observed that the center of the phosphate group is offset from the helix axis. The stabilizing effect of the helix dipole has not been proven for flavodoxins but it is likely that some stabilization of the dianionic negative charge will occur. It should be mentioned that theoretically the helix dipole can stabilize only 0.5 net charge at either end (Hol, et al., 1978). Moreover, the overall net dipole moment of the *Clostridium beijerinckii* flavodoxin points with its negative part directly to the isoalloxazine ring and probably even will destabilize the negative charge on the phosphate group to a certain extent (dr. J.W. van Leeuwen, pers. commun.).

Upon reducing the flavodoxin all protons involved in hydrogen bond formation with the phosphate group shift 0.1-0.2 ppm to lower field, except the side-chain hydroxyls of Thr¹⁵ and Ser⁵⁸, which shift about 0.1 ppm to higher field (Table 2.1). This difference in chemical shift may be explained by a structural change or by change in the electronic configuration of the phosphate group, induced by the negative charge of the isoalloxazine moiety of the two-electron reduced FMN molecule (Vervoort, et al., 1985). However no differences in chemical shifts are observed between the protons involved in hydrogen bonding with the phosphate in the two-electron reduced state and the very broad, still observable, residues in the semiquinone state (data not shown). If the negative charge on the isoalloxazine ring in the two-electron reduced state would have an effect on the negative charge of the phosphate, this effect should not be present in the semiquinone form. As a result, different chemical shifts between these two redox-states for the amide and hydroxyl protons, which form hydrogen bonds with the phosphate group, would be expected. As this is not the case, it is most likely for the difference in chemical shifts between the two-electron reduced and the oxidized flavodoxin to originate from structural changes. These structural changes probably cause small changes in strength of the H-bonding network towards the FMN phosphate group. Such changes are not apparent in the X-ray structures because they fall within the uncertainty of atomic positioning.

It is interesting to speculate on the influence of protein-protein complexation on the stabilization of the negative charge of the dianionic phosphate group. It can be expected that upon complexation of the flavodoxin with an electron-acceptor protein water molecules which are involved in the stabilization of the negative charges become expelled from the interface. This then leads to a decreased

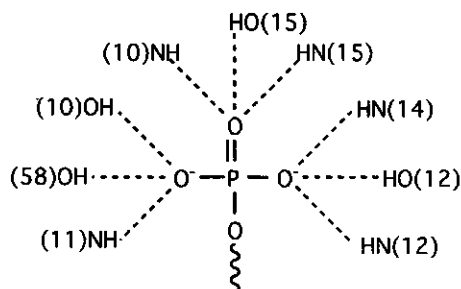


Fig. 2.4 Schematic representation of the H-bonding to the FMN phosphate group as determined by NMR.

stabilization of the dianionic phosphate group and to increased charge-charge interactions with the negatively charged N(1) atom of the isoalloxazine ring in the two-electron reduced state. The increase in charge-charge interaction will give rise to destabilization of this two-electron reduced state (i.e. lower redox-potential for the semiquinone-hydroquinone redox-couple) increasing thereby the driving force for electron transfer.

2.3.2 Isoalloxazine binding region

From the NOESY spectrum of the two-electron reduced flavodoxin (Fig. 2.3B) it is observed that the amide protons of Asp⁹⁵ and Cys¹⁰² resonate at very low field, 11.01 and 11.53 ppm respectively (Table 2.1; boxed resonances in Fig. 2.3B). These protons are in close proximity to the N(1) atom and C(2) carbonyl of the FMN ring (Watt, et al., 1991). In the oxidized flavodoxin these resonances are shifted to 9.51 and 9.73 ppm as compared to the two-electron reduced flavodoxin (Table 2.1; boxed resonances in Fig. 2.3A). The amide protons of these two residues have been shown to be involved in hydrogen bonding towards the N(1) and C(2) carbonyl region of the flavin ring (Watt, et al., 1991). In the two-electron reduced redox-state, using ¹³C and ¹⁵N labelled FMN derivatives, it could be shown that the isoalloxazine ring is anionic in the two-electron reduced state with its negative charge located at the N(1)-C(2) region of the flavin-ring (Vervoort, et al., 1985). The strong downfield shift of the amide protons of Asp⁹⁵ and Cys¹⁰² upon reduction indicates that these

protons are directly involved in the charge stabilization of the isoalloxazine moiety. Both amide groups can delocalize part of the negative charge via their peptide bond onto the carbonyl oxygens of Gly⁹⁴ and Phe¹⁰¹, which in the crystallographic structure both have a water molecule within hydrogen bonding distance. It can be visualized that decreased solvent accessibility to these residues, which are involved in the charge stabilization of the isoalloxazine ring, will lead to increased charge destabilization of the isoalloxazine ring and therefore to lower redox-potentials (Vervoort, 1991).

In previous studies on flavodoxins it could be shown that on reduction of the protein a conformational change of the peptide bond adjacent to the N(5) atom of the flavin ring occurs (Smith, et al., 1977). In recent crystallographic studies of *D. vulgaris* flavodoxin it was observed that the carbonyl group of Gly⁶¹ points away from the FMN N(5) in the oxidized protein, whereas it points towards the N(5)H in the hydroquinone state, forming a hydrogen bond interaction between the N(5)-H and the Gly⁶¹ carbonyl oxygen. Consequently, the amide proton of Asp⁶² points towards the FMN N(5) in the oxidized flavodoxin and points away towards the bulk solvent in the hydroquinone state. In the oxidized protein the Asp⁶² amide proton is close enough to the C(4) carbonyl oxygen to form a hydrogen bond. This Asp⁶² amide proton resonates at 8.62 ppm in the oxidized flavodoxin at pH 7.9. Upon increasing the pH the amide proton resonance of Asp⁶² decreases in intensity and at pH 8.3 the resonance has almost completely disappeared in the NOESY spectrum of the oxidized flavodoxin. This means that the hydrogen bond between the amide proton of Asp⁶² and the carbonyl oxygen of the FMN C(4) is a weak one. In the NOESY spectrum of the hydroquinone state the amide proton of Asp⁶² is not observed anymore. Probably this is due to the change in conformation in going from the oxidized to the two-electron reduced flavodoxin as observed in the X-ray structures. Due to this change in conformation the amide proton of Asp⁶² points towards the bulk water with which it is in fast exchange at pH 8.3 and 30 °C.

The amino acids Trp⁶⁰ and Tyr⁹⁸ are located close to the isoalloxazine ring but do not form hydrogen bonds with the flavin cofactor. Trp⁶⁰ is located above the xylene ring and the pyrazine ring of the isoalloxazine moiety of the FMN (Watt, et al., 1991). From the X-ray structures it is determined that there is no significant difference in orientation and distance of this tryptophan relative to the FMN ring between the oxidized and two-electron reduced protein. Moreover, low B-factors are determined both for Trp⁶⁰ and the isoalloxazine ring in both redox-states (B-factors < 14 Å²),

indicating that these two residues are well defined in the X-ray structure. Although small crystal contacts are observed for Trp⁶⁰ and FMN, it is very likely that, relative to the FMN, Trp⁶⁰ is orientated almost the same way in the solution structure. This because NOE contacts are observed between the FMN CH(6) and the C^α proton of Trp⁶⁰, and between both FMN CH₃(7) and CH₃(8) and the indole protons CH(5) and CH(6) of Trp⁶⁰ in both the oxidized and two-electron reduced protein. Thus the indole ring of Trp⁶⁰ must be located close to the FMN xylene ring, as also was observed in the X-ray structures. The intensity of the NOE cross-peak between FMN CH(6) and the C^α proton of Trp⁶⁰ hardly changes in going from the oxidized to the two-electron reduced flavodoxin. It is therefore very unlikely that the large downfield shift of 2.03 ppm for this proton (Table 2.1) upon reduction is caused by a structural change. It is more likely that, -although there are no appropriate ring current models for an isoalloxazine ring system-, the ring current (Johnson and Bovey, 1958) of the isoalloxazine ring decreases upon reduction. Probably this decrease in ring current is caused mainly by the pyrazine moiety of the isoalloxazine ring induced by protonation of the N(5) atom. Due to this protonation the N(5) atom changes from a sp²-type to a sp³-type nitrogen (Levy and Lichter, 1979) as can be deduced from ¹⁵N chemical shifts of ¹⁵N labelled FMN in *Desulfovibrio vulgaris* flavodoxin determined by Vervoort et al. (1985). Due to this change in hybridisation state of N(5) the pyrazine ring must become less aromatic in the reduced flavodoxin, this will lead to a decrease in ring current.

The ring of Tyr⁹⁸ is located below the pyrazine ring of the isoalloxazine ring-system. In the X-ray structure the ring of Tyr⁹⁸ is almost coplanar with the FMN ring (Watt, et al., 1991). However in the 2D NOESY spectrum there is only one δ/ε NOE cross-peak of Tyr⁹⁸, meaning that in solution the tyrosine ring flips fast, on NMR time scale, around the C^β-C^γ axis, being not always coplanar with the FMN ring. The downfield shift of the ring protons of Tyr⁹⁸ upon reduction is in agreement with the decrease in ring current of the two-electron reduced isoalloxazine ring suggested above. However, this downfield shift is too small to unambiguously be assigned as caused by a decrease in ring current.

The proton of the N(3) of the pyrimidine moiety of the isoalloxazine ring shifts to higher field upon reduction (Table 2.1). From NMR studies using ¹⁵N labelled FMN it was concluded that the hydrogen bond formed by the N(3)H proton decreases in the reduced state as compared to the oxidized state (Vervoort, et al., 1985). The weaker

hydrogen bond present will cause the proton resonance of the N(3)H to shift upfield upon reduction as observed.

2.4 Conclusions

The results obtained by NMR for the solution structures of *Desulfovibrio vulgaris* flavodoxin resemble to a large extent the results obtained from the X-ray structures. Like for the crystal structure no changes outside the FMN binding region are observed between the three redox-states for the solution structure as judged from NOE intensities and chemical shift values. Small differences in the strength of the hydrogen bonds towards the phosphate group are observed by NMR between the oxidized and the semiquinone state. No changes are detected in the hydrogen bonding geometry between the semiquinone and the hydroquinone state. The NMR results suggest that the ring current of the isoalloxazine ring decreases upon reduction, probably because the pyrazine ring is less aromatic in the two-electron reduced flavodoxin, due to protonation of the N(5) atom.

2.5 References

- Braunschweiler, L. and Ernst, R.R. (1983) *J. Magn. Res.* **53**, 521-528.
- Brown, S.C., Weber, P.L. and Mueller, L. (1988) *J. Magn. Res.* **77**, 166-169.
- Curley, G.P., Carr, M.C., Mayhew, S.G. and Voordouw, G. (1991) *Eur. J. Biochem.* **202**, 1091-1100.
- Drummond, M., Huff, S. and Green, A. (1993) *Eur. J. Biochem.* **217**, 395-400.
- Dubourdieu, M. and LeGall, J. (1970) *Biochem. Biophys. Res. Commun.* **38**, 815-820.
- Hol, W.G.J., Duijnen van, P.T. and Berendsen, H.J.C. (1978) *Nature* **273**, 443-446.
- Jeener, J., Meier, B.H., Bachmann, P. and Ernst, R.R. (1979) *J. Chem. Phys.* **71**, 4546-4553.
- Johnson, C.E. and Bovey, F.A. (1958) *J. Chem. Phys.* **29**, 1012-1014.
- Levy, G.C. and Lichter, R.L. (1979) *Nitrogen-15 nuclear magnetic resonance spectroscopy*, Wiley, New York.
- Marion, D. and Wüthrich, K. (1983) *Biochem. Biophys. Res. Commun.* **113**, 967-724.

- Mierlo van, C.P.M., Sanden van der, B.P.J., Woensel van, P., Müller, F. and Vervoort, J. (1990) *Eur. J. Biochem.* **194**, 199-216.
- Piantini, U., Sørensen, O.W. and Ernst, R.R. (1982) *J. Am. Chem. Soc.* **104**, 6800-6801.
- Rance, M., Sørensen, O.W., Bodenhausen, G., Wagner, G., Ernst, R.R. and Wüthrich, K. (1983) *Biochem. Biophys. Res. Commun.* **117**, 479-485.
- Shaka, A.J., Lee, C.J. and Pines, A. (1988) *J. Magn. Res.* **77**, 274-293.
- Shaka, A.J. and Freeman, R. (1983) *J. Magn. Res.* **51**, 169-173.
- Smith, W.W., Burnett, R.M., Darling, G.D. and Ludwig, M.L. (1977) *J. Mol. Biol.* **117**, 195-225.
- Vervoort, J. (1991) *Current opinion in structural biology* **1**, 889-894.
- Vervoort, J., Mierlo van, C.P.M. and LeGall, J. (1991) *Proceedings of the 10th international symposium, Como, de Gruyter, Berlin.*
- Vervoort, J., Müller, F., LeGall, J., Bacher, A. and Sedlmaier, H. (1985) *Eur. J. Biochem.* **151**, 49-57.
- Warshel, A. (1987) *Nature* **330**, 15-16.
- Wassink, J.H. and Mayhew, S.G. (1975) *Anal. Biochem.* **68**, 609-616.
- Watt, W., Tulinsky, A., Swenson, R.P. and Watenpaugh, K.D. (1991) *J. Mol. Biol.* **218**, 195-208.
- Wüthrich, K. (1986) *NMR of proteins and nucleic acids*, Wiley & Sons Inc., New York.

3

Short extra loop of the long-chain flavodoxin from *Azotobacter chroococcum* may be important for electron transfer to nitrogenase. Complete ^1H , ^{15}N and ^{13}C backbone assignments and secondary solution structure of the flavodoxin

Sjaak Peelen, Sybren S. Wijmenga, Paul J. A. Erbel, Robert L. Robson, Robert R. Eady and Jacques Vervoort

Modified version published in *Journal of Biomolecular NMR* (1996).

*The ^1H , ^{15}N and ^{13}C backbone and ^1H and ^{13}C beta resonance assignments of the long-chain flavodoxin from *Azotobacter chroococcum* (the 20 kDa *nifF* product, flavodoxin-2) in its oxidized form were made at pH 6.5 and 30 °C using heteronuclear multi-dimensional NMR spectroscopy. Analysis of the NOE connectivities, together with amide exchange rates, $^3J_{\text{HNH}\alpha}$ coupling constants and secondary chemical shifts, provided extensive solution secondary structure information. The secondary structure consists of a five-stranded parallel β -sheet and five α -helices. One of the outer regions of the β -sheet shows no regular extended conformation, whereas the outer strand $\beta 4/6$ is interrupted by a loop, which is typically observed in long-chain flavodoxins. Two of the five α -helices are non-regular at the N-terminus of the helix. Loop regions close to the FMN are identified. Negatively charged amino acid residues are found to be mainly clustered around the FMN, whereas a cluster of positively charged residues is*

located in one of the α -helices. Titration of the flavodoxin with the Fe-protein of the *Azotobacter chroococcum* nitrogenase enzyme complex, revealed that the residues Asn¹¹, Ser⁶⁸ and Asn⁷² are involved in the complex formation between the flavodoxin and the Fe-protein. The interaction between the flavodoxin and the Fe-protein is influenced by MgADP and is of electrostatic nature.

3.1 Introduction

Flavodoxins are small redox proteins that serve as low potential electron carriers. They all contain a non-covalently bound FMN molecule, which acts as the electron accepting/donating group (Mayhew and Tollin, 1992). The FMN can exist in three redox states: oxidized, one-electron reduced (or semiquinone), and two-electron reduced (or hydroquinone). In the semiquinone redox-state (SQ) the isoalloxazine part of the FMN has a paramagnetic character due to the unpaired electron on the isoalloxazine (Fritz, et al., 1973). Three-dimensional structures of several flavodoxins are known (Burnett, et al., 1974; Fukuyama, et al., 1990; Ludwig, et al., 1976; Mierlo van, et al., 1990a; Smith, et al., 1977; Smith, et al., 1983; Stockman, et al., 1990; Watenpaugh, et al., 1973; Watt, et al., 1991). They all consist of a central parallel β -sheet consisting of five strands linked by four or five α -helical segments that occur in parallel pairs on the exterior of the molecule. In the obligate aerobe *Azotobacter chroococcum*, flavodoxin-2 acts as an electron donor to nitrogenase (Bagby, et al., 1991b; Yates, 1972): two-electron reduced flavodoxin transfers one electron to the dimeric Fe-protein of the nitrogenase enzyme complex (Kim and Rees, 1994). After this electron transfer reaction the flavodoxin returns to the one-electron reduced state. The midpoint potential of this semiquinone-hydroquinone couple is -522 mV, which is the most negative redox-potential observed for flavodoxins (Deistung and Thorneley, 1986). This potential of -522 mV is almost 400 mV more negative than the midpoint potential of the semiquinone-hydroquinone couple of free FMN, which is -124 mV (Curley, et al., 1991). The apoprotein, surrounding the FMN, is therefore very important in modulating this midpoint potential. Zhou and Swenson (1995) have found for the flavodoxin from *Desulfovibrio vulgaris* that negatively charged amino acid residues located near the FMN binding site contribute to the low midpoint potential of the semiquinone-hydroquinone couple, because the mutation of some of these negatively charged amino acids to neutral residues, resulted in an increase of

the midpoint potential. Because of the very low semiquinone-hydroquinone midpoint potential of *Azotobacter chroococcum* flavodoxin, it is interesting to investigate if there are more negatively charged residues surrounding the FMN in this flavodoxin than in the flavodoxin from *Desulfovibrio vulgaris*. The *nifF* encoded flavodoxin from *Azotobacter chroococcum* (ACF1d2, molecular mass 20 kDa) contains 180 amino acids and is therefore one of the longer chain flavodoxins (Mayhew and Tollin, 1992), differing from the short-chain ones mainly by an insertion of 20 residues in a loop in the fifth strand of the β -sheet (Fig. 3.1b; residues 129-148). This flavodoxin is the largest one studied by multi-dimensional NMR.

This study reports the ^1H , ^{15}N and ^{13}C backbone and ^1H and ^{13}C beta assignments and the solution secondary structure of oxidized *Azotobacter chroococcum* flavodoxin, determined by heteronuclear multi-dimensional NMR spectroscopy. Also the interaction of the flavodoxin with the Fe-protein of the nitrogenase complex was studied by NMR in order to gain insight as to which residues are involved in complex formation between flavodoxin and the Fe-protein.

3.2 Materials and methods

Molecular cloning, protein expression and purification of flavodoxin. The flavodoxin encoding gene for flavodoxin-2 is located on the major nitrogen-fixation (*nif*) gene cluster from *Azotobacter chroococcum*. It was located 1.5 kb downstream of the *nifM* gene sequenced earlier (Evans, et al., 1991). The entire *nifF* gene on a 1.6 kb *Pst*I fragment was cloned from the recombinant cosmid pACB1 (Jones, et al., 1984) into plasmid pEMBL19+ (Dente, et al., 1983) to give pMOY10a. The insert was sequenced by the dideoxynucleotide chain termination method (Sanger, et al., 1977) with 5'-[α - ^{35}S]dATP (600 Ci/mmol; Amersham International), dequenase (U.S. Biochemical Corp.) and 7-deaza-dGTP in place of dGTP to eliminate compressions. Sequencing was performed from deletions and completed using oligonucleotide primers. The sequence (Fig. 3.1a) was compiled using the University of Wisconsin Genetics Computer Group programmes (Deveraux, et al., 1985). The sequence shows an open reading frame of 180 amino acid residues with a calculated pI of 4.27. The deduced amino acid sequence for the *Azotobacter chroococcum* flavodoxin showed 10 differences and overall 94.4 % identity with the sequence of the comparable gene product from *Azotobacter vinelandii* (Bennet, et al., 1988). For overexpression, the

a

```

      10              30              50
      |              |              |
CACGCAGCCAGAGGTTTAAGTTATGGCCAAGATTGGACTCTTCTTCGGTAGCAACACCGG
      |              |              |
      M A K I G L F F G S N T G ( 13 )
      70              90              110
      |              |              |
TAAACCCCGCAAGGTCGCCAAGTCGATCAAGAAGCGTTTCGACGACGAAACCATGTCCGA
      |              |              |
      K T R K V A K S I K K R F D D E T M S D ( 33 )
      130             150             170
      |              |              |
TGCAGTGAACGTC AACCGCGTTTCCGCGGAAGACTTCGCCCCAGTACCAGTTCCTGATCCT
      |              |              |
      A V N V N R V S A E D F A Q Y Q F L I L ( 53 )
      190             210             230
      |              |              |
GGGTACCCCGACCCTTGGCGAAGGCGAACTCCCGGCCCTCCTCCGACTGCGAGAACGA
      |              |              |
      G T P T L G E G E L P G L S S D C E N E ( 73 )
      250             270             290
      |              |              |
GAGCTGGGAAGAGTTCCTGCGAAAATCGAAGGCCTGGACTTCAGCGGCAAGACCGTGGC
      |              |              |
      S W E E F L P K I E G L D F S G K T V A ( 93 )
      310             330             350
      |              |              |
TCTGTCGGTCTGGGCGACCAGGTCGGCTATCCCGAGAACTTCCTCGATGCCATGGGGGA
      |              |              |
      L F G L G D Q V G Y P E N F L D A M G E ( 113 )
      370             390             410
      |              |              |
ACTGCATTCTTCTTCCACCGAGCGGGTGCCAAGGTCGTAGGCCCTGGTTCGACCGACGG
      |              |              |
      L H S F F T E R G A K V V G A W S T D G ( 133 )
      430             450             470
      |              |              |
CTACGAGTTCGAAGGCTCCACCGCAGTGGTTGACGGCAAGTTCGTCGGCTGGCGCTGGA
      |              |              |
      Y E F E G S T A V V D G K F V G L A L D ( 153 )
      490             510             530
      |              |              |
TCTGGACAACCAGAGCGGCAAGACCGACGAGCGCGTCGCTGCCTGGCTGGCACAGATCGC
      |              |              |
      L D N Q S G K T D E R V A A W L A Q I A ( 173 )
      550             570
      |              |
TCCCGAGTTCGGCCTGTCCCTGTAAGGGTCGATCCGGTCATGCAGCTTT
      |              |
      P E F G L S L

```

Fig. 3.1a Nucleotide sequence and deduced amino acid sequence of the *nifF* gene encoding the flavodoxin AcFld2 from *Azotobacter chroococcum*. The putative ribosome binding site for the *nifF* gene is underlined. The sequence is deposited with Genbank with the accession number M73019.

entire *nifF* coding region was amplified by the polymerase chain reaction using an N-terminal primer (5'-TGCACATATGGCCAAGATTGGACT-3') and a C-terminal primer (5'-TGCAGGATCCTTACAGGGACAGGCCG-3') which contained extensions which allowed the amplified product to be digested with the restriction enzymes *NdeI* and *BamHI* and cloned into the equivalent sites in the overexpression vector pT7.7

b

<i>D. vulgaris</i>	MPKALIVYGSTTGNTTEYTAETIARELADAGYEVDSRDAASVEAGGLFEGFDLVLL (55)
<i>A. nidulans</i>	MAKIGLFYGTOTGVTQTIAESIQQEFGGESIV-DLNDIANADASD-LNAYDYLLI (53)
<i>A. chroococcum</i>	MAKIGLFFGSNTGKTRKVAKSIKRFDDEETMS-DAVNVNRVSAED-FAQYQFLIL (53)
	1 10 20 30 40 50
<i>D. vulgaris</i>	GCSTWGD-----DSIELQDDFIPLFDSL-EETGAQGRKVACFGCGDS-SYE-YF (101)
<i>A. nidulans</i>	<u>GCPTWNVGEL</u> -----QSDWEGIYDD-LDSVNFQGGKVVAYFGAGDQVGYSDNE (99)
<i>A. chroococcum</i>	GTPTLGEGLPGLSSDCENESWEEFL-PKIEGLDFSGKTVALFGLGDQVGYPENF (107)
	60 70 80 90 100
<i>D. vulgaris</i>	CGAVDAIEEKLKLNLAETVQD-----GLRIDGDP--RAAR (134)
<i>A. nidulans</i>	<u>QDAMGILEEKISSLGSQTVGYWPIEGYDFNESKAVRNNQFVGLAIDEDNQPD LTK</u> (154)
<i>A. chroococcum</i>	LDAMGELHSFPTERGAKVVGAWSTDGYEFEGSTAVVDGKVFVGLALDLDNQSGKTD (162)
	110 120 130 140 150 160
<i>D. vulgaris</i>	DDIVGWAHDVRGAI---- (148)
<i>A. nidulans</i>	<u>NRIKTWVSQKSEFG--L</u> (170)
<i>A. chroococcum</i>	<u>ERVAAWLAQIAPEFGLSL</u> (180)
	170 180

Fig. 3.1b Sequence alignment of flavodoxins from *Desulfovibrio vulgaris*, *Anacystis nidulans* and *Azotobacter chroococcum*. The extra loop, characteristic for long-chain flavodoxins is found in *A. chroococcum* from residue Trp¹²⁹ to Val¹⁴⁸. Consensus flavin binding site residues in *A. nidulans* flavodoxin are underlined (Stockman, et al., 1990).

(Tabor and Richardson, 1985). In this recombinant plasmid (pGP1.2), expression of the *nifF* gene is under control of the strong T7 ϕ 10 transcriptional machinery and is induced in *Escherichia coli* strain K38(pGP1.2) which expresses T7-polymerase after heat induction at 42 °C. This *E. coli* strain (K38(pGP1.2/pT7.7/1.1/9) was used for the biosynthesis of the uniformly ¹³C/¹⁵N labelled and ¹⁵N labelled flavodoxin.

Cultures were routinely grown aerobically (dissolved air concentration of 50%) in a simple glucose salts medium containing in 24 l: 480 g glucose; 1.2 g yeast extract; 2.4 g MgSO₄·7H₂O; 167.7 g K₂HPO₄; 7.3 g KH₂PO₄; 12 g NH₄Cl; 200 mg/l carbenicillin and 25 mg/l kanamycin. For ¹⁵N labelling of flavodoxin, cultures were grown in 24 l N-limiting medium, where the concentration was decreased to 6.0 g NH₄Cl. Growth of the cultures stopped after 18 hours at which time 4.8 g ¹⁵NH₄Cl was added, and controlled at a dissolved air concentration of 50%. After 1 hour synthesis of flavodoxin was induced and the culture harvested 2.5-4 hours later.

For the $^{13}\text{C}/^{15}\text{N}$ labelling two 5 ml cultures of the *E. coli* strain were grown aerobically for 24 hours at 29 °C in Difco Nutrient Broth containing 200 mg/l carbenicillin and 25 mg/l kanamycin. These cultures each were used to inoculate a 1 l culture of the same medium. These two 1 l cultures were aerobically grown in a BiofloIII (NewBrunswick Scientific) fermentor for 15 hours at 29 °C. After this time the cultures were centrifuged for 5 minutes at 7500 g, 17 °C. The pellet was resuspended in saline phosphate and again centrifuged under the same conditions. After this washing step the cell pellet was resuspended in 1 l containing 6.25 g $^{13}\text{C}/^{15}\text{N}$ ISOGRO (ISOTEC inc., Miamisburg, OH), 1.8 g K_2HPO_4 , 1.4 g KH_2PO_4 , 1.0 g MgSO_4 , 11.1 mg $\text{CaCl}_2 \cdot 2\text{H}_2\text{O}$, 200 mg carbenicillin and 25 mg kanamycin at pH 7.0 and 29 °C in a BiofloIII fermentor. The culture was left to agitate slowly at 50 rpm with minimal aeration of 10 ml/min for 30 minutes, then the agitation and aeration were increased to 150 rpm and 100 ml/min respectively for the next 30 minutes, and finally the cells were grown at a dissolved air concentration of 50% for another 30 minutes. This preliminary growth was to ensure that any residual unlabelled media was utilised before induction. The cells were induced by increasing the temperature to 44 °C for 30 minutes, followed by 4 hours growth at a dissolved air concentration of 50% and 40 °C. The cells were harvested by centrifugation at 15000 g, 4 °C.

The cells were resuspended in 50 mM Tris/HCl buffer, pH 7.5 and a small amount of DNAase added. The suspension was then passed through a French press at 27 MPa and centrifuged for 30 minutes at 15000 g, 4 °C. The resulting pellet was resuspended in the same buffer and disrupted for a second time and then centrifuged. The supernatant was then loaded onto a DEAE cellulose column and equilibrated with 50 mM Tris/HCl pH 7.5. The flavodoxin was eluted as a blue/green coloured band by the equilibration buffer, subsequently containing 0.1 M NaCl, 0.25 M NaCl and 0.4 M NaCl. The flavodoxin containing fraction was then dialysed overnight against 20 mM 2-[bis(2-hydroxyethyl)amino]-2-(hydroxymethyl-propane-1,3-diol) buffer at pH 6.4, and purified on a Mono Q HR 5/5 anion exchange column (Pharmacia-LKB Biotechnology) as described previously (Bagby, et al., 1991a). The purified flavodoxin was concentrated in an Amicon centriprep concentrator. The final yields were 11 mg and 173 mg for the $^{13}\text{C}/^{15}\text{N}$ labelled and ^{15}N labelled flavodoxin, respectively.

The Fe-protein of the vanadium-nitrogenase complex from *Azotobacter chroococcum* was purified as described by Eady et al. (1988).

NMR sample preparation. Four samples were prepared for the NMR experiments. One contained 4.8 mM oxidized flavodoxin uniformly labelled (>80% as determined from a ^{15}N coupled 1D proton spectrum) with ^{15}N , dissolved in 90% $\text{H}_2\text{O}/10\%$ D_2O , 150 mM potassium pyrophosphate/HCl pH 6.5 and 0.4 mM TSP. The second sample contained 0.9 mM oxidized flavodoxin uniformly labelled (> 80% as determined from a ^{13}C and ^{15}N coupled 1D proton spectrum) with $^{13}\text{C}/^{15}\text{N}$, dissolved in 90% $\text{H}_2\text{O}/10\%$ D_2O , 150 mM potassium pyrophosphate/HCl pH 6.5 and 0.4 mM TSP. A third sample for the identification of slowly exchanging amide protons was prepared by lyophilization of 3.8 ml 0.3 mM oxidized flavodoxin uniformly labelled (>80%) with ^{15}N , dissolved in 20 mM potassium pyrophosphate/HCl pH 6.85. The lyophilized flavodoxin was dissolved in 0.5 ml D_2O , giving an NMR sample containing 2.5 mM oxidized flavodoxin uniformly labelled (>80%) with ^{15}N in 150 mM potassium pyrophosphate/HCl pH 6.5. All samples were evacuated and filled with argon for at least four times. The pH was not corrected for isotope effects. The last sample which contained 2.5 mM oxidized flavodoxin uniformly labelled (>80%) with ^{15}N , dissolved in 90% $\text{H}_2\text{O}/10\%$ D_2O , 150 mM potassium phosphate pH 7.0 and 0.2 mM TSP, was made anaerobic by five cycles of evacuation and filling with argon. To reduce the flavodoxin to its semiquinone form, an anaerobic sodium dithionite solution was added to a final concentration of about 12 mM.

Titration of flavodoxin with the Fe-protein. A sample containing 1.5 mM oxidized flavodoxin uniformly labelled (>80%) with ^{15}N , dissolved in 90% $\text{H}_2\text{O}/10\%$ D_2O , 50 mM potassium phosphate pH 7.1 and 0.4 mM TSP, was made anaerobic by five cycles of evacuation and filling with argon. The purified Fe-protein (dimer) of the vanadium nitrogenase complex, dissolved in 50 mM potassium phosphate pH 7.1 and 1 mM sodium dithionite, was left at room temperature for at least two hours in order to allow the dithionite to be oxidized by the Fe-protein. Since the Fe-protein is unstable under aerobic conditions it is important to work anaerobically. Stock solutions of 0.15 M MgADP at pH 7 and 2 M KCl in 50 mM potassium phosphate pH 7.1 were made anaerobic by extensive flushing with argon. The oxidized flavodoxin was titrated with the dithionite free Fe-protein, MgADP and KCl under anaerobic conditions according to Table 3.1. Two dimensional ^1H - ^{15}N HSQC spectra (Bodenhausen and Ruben, 1980) were recorded for each titration at 25 °C, acquiring 128 real t_1 points (^{15}N ; spectral width 1672 Hz), 1024 complex t_2 points (^1H ; spectral width 8064 Hz) with 16 scans per t_1 increment, using time-proportional phase

Table 3.1 Titration of oxidized flavodoxin with the Fe-protein from Azotobacter chroococcum at pH 7.1 and 25 °C.

Experiment number	[Flavodoxin] (mM)	[Fe-protein] (mM)	$\frac{[\text{Fe-protein}]}{[\text{Flavodoxin}]}$	[MgADP] (mM)	[KCl] (mM)	Volume (μl)
1	1.5	0.00	0.00	-	-	500
2	1.43	0.13	0.09	-	-	525
3	1.36	0.25	0.18	-	-	550
4	1.25	0.45	0.36	-	-	600
5	1.15	0.62	0.54	-	-	650
6	1.07	0.77	0.72	-	-	700
7	0.96	0.96	1.00	-	-	778
8	0.95	0.95	1.00	2.8	-	793
9	0.90	0.90	1.00	2.7	96.0	833

incrementation (TPPI) (Marion and Wüthrich, 1983). Presaturation of the water signal was employed during the 1.5 s relaxation delay.

NMR spectroscopy. Unless otherwise stated, all experiments were performed at 30 °C on a Bruker AMX-500 or AMX-600 spectrometer using either a triple-resonance 5 mm inverse probe or a triple-resonance 5 mm inverse probe with a self-shielding z-gradient. Presaturation of the water signal during the 1-1.5 s relaxation delay was employed for the non-gradient enhanced NMR experiments. No presaturation during the 1s relaxation delay was employed for the gradient enhanced experiments.

To identify fast and slowly exchanging amide protons a series of 2D ^1H - ^{15}N HSQC experiments was recorded at 25 °C, 0.5 hour, 7 hours, 53 hours and 43 days after dissolving the ^{15}N labelled flavodoxin in D_2O . For each HSQC experiment 128 real t_1 points (^{15}N ; spectral width 1600 Hz), 1024 complex t_2 points (^1H ; spectral width 8064 Hz) with 16 scans per t_1 increment, using TPPI were recorded. Amide protons which could still be observed 53 hours after dissolving in D_2O were marked as slowly exchangeable in Fig. 3.5.

Also 2D ^1H - ^{15}N HSQC spectra of ^{15}N labelled flavodoxin in 90% H_2O /10% D_2O in its oxidized and semiquinone redox-states were recorded. For the oxidized flavodoxin 128 complex t_1 points (^{15}N ; spectral width 1672 Hz), 1024 complex t_2 points (^1H ; spectral width 8064 Hz) with 128 scans per hypercomplex t_1 increment, using States-TPPI (Marion, et al., 1989c) were recorded. For the one-electron reduced flavodoxin, 148 complex t_1 points (^{15}N ; spectral width 1672 Hz), 1024 complex t_2 points (^1H ; spectral width 8064 Hz) with 16 scans per hypercomplex t_1 increment,

using States-TPPI were recorded. Due to the paramagnetic character of the isoalloxazine part of the FMN in the semiquinone redox-state, resonances of residues within about 15 Å of this isoalloxazine are broadened to a large extent. For the *A. chroococcum* flavodoxin (at 30 °C and 500 MHz) a theoretical extra line broadening of 10 Hz can be calculated for the resonance of a proton at a distance of about 15 Å from the paramagnetic center, by using the Solomon-Bloembergen equation (Bloembergen, 1957; Solomon, 1955). This line broadening is caused by a dipole-dipole interaction between the proton and the unpaired electron on the isoalloxazine part of the FMN. In this way residues surrounding to the FMN can be determined. Resonances that became broadened to a large extent are marked as 'SQ affected' in Fig. 3.5.

The following 3D experiments were recorded with the 4.8 mM ^{15}N labelled flavodoxin sample. Two 3D ^{15}N -separated NOESY-HMQC (Marion, et al., 1989a; Zuiderweg and Fesik, 1989) experiments with NOE mixing times of 75 and 100 ms were recorded, each acquired with 128 complex t_1 points (^1H ; spectral width 8064 Hz), 45 complex t_2 points (^{15}N ; spectral width 1672 Hz), 512 complex t_3 points (^1H ; spectral width 8064 Hz) and 16 scans per hypercomplex t_1/t_2 increment. A 3D ^{15}N -separated TOCSY-HMQC (Marion, et al., 1989a) experiment, changed to incorporate two different mixing times of 30 and 50 ms using the clean-MLEV-17 (Bax and Davis, 1985; Griesinger, et al., 1988) mixing sequence surrounded by trim pulses, was recorded, acquiring 128 complex t_1 points (^1H ; spectral width 8064 Hz), 48 complex t_2 points (^{15}N ; spectral width 1672 Hz), 512 complex t_3 points (^1H ; spectral width 8064 Hz) and 32 scans per hypercomplex t_1/t_2 increment. To resolve NOE cross peaks of degenerate amide protons a 3D ^{15}N -separated HMQC-NOESY-HMQC (Frenkiel, et al., 1990; Ikura, et al., 1990) experiment with a NOE mixing time of 75 ms was recorded, acquiring 64 complex t_1 points (^{15}N ; spectral width 1672 Hz), 38 complex t_2 points (^{15}N ; spectral width 1672 Hz), 512 complex t_3 points (^1H ; spectral width 8064 Hz) and 64 scans per hypercomplex t_1/t_2 increment. A 3D HNHA (Vuister and Bax, 1993) experiment was recorded for measuring $^3J_{\text{HNH}\alpha}$ coupling constants. Homonuclear de- and rephasing delays according to Vuister and Bax (1993) were used. In combination with the HAHB(CO)NH (Grzesiek and Bax, 1993) experiment the HNHA was also used for the sequential assignment (Vuister, et al., 1994). The HNHA was acquired with 47 complex t_1 points (^1H ; spectral width 5580 Hz), 24 complex t_2 points (^{15}N ; spectral width 2068 Hz), 512 complex t_3 points (^1H ; spectral width 9615 Hz) and 64 scans per hypercomplex t_1/t_2 increment. The determination of

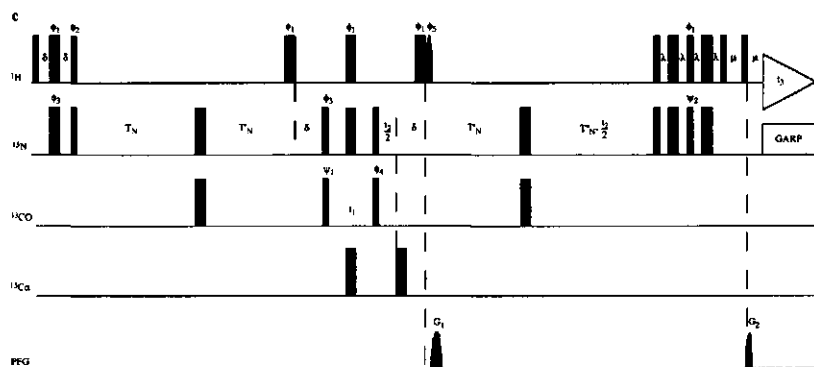


Fig. 3.2 Pulse sequences for the modified triple-resonance experiments with gradient enhancement: CBCANH (a), CBCA(CO)NH (b) and *ct*-HNCO (c). Narrow and wide pulses correspond to 90° and 180° flip angles, respectively. The 90° (grey) water flip-back pulse has a Gaussian profile (with a duration of 2.1 ms). Pulses for which the phase is not indicated are applied along the x-axis. The ^1H carrier is positioned at the H_2O frequency (4.71 ppm), the carrier for the $^{13}\text{C}^{\alpha\beta}$, $^{13}\text{C}^\alpha$ and ^{13}CO pulses are positioned at 47 ppm, 59 ppm and 176 ppm, respectively. The power of the $^{13}\text{C}^\alpha$ and $^{13}\text{C}^{\alpha\beta}$ pulses is adjusted such that they do not excite the ^{13}CO nuclei. The power of the ^{13}CO pulses is adjusted such that they do not excite the $^{13}\text{C}^\alpha$ nuclei. The shaped ^{13}CO pulses have an amplitude profile corresponding to the center lobe of a sinc function (with a duration of 202 μs). ^{15}N decoupling is accomplished using GARP modulation with a 2.1 kHz RF field. CBCANH (a): $\delta = 1.5$ ms; $\varepsilon = 2.4$ ms; $\zeta = 11$ ms; $\xi = 11.4$ ms; $\kappa = 3.2$ ms; $\lambda = 2.65$ ms; $\mu = 1$ ms; $T_{AB} = 3.55$ ms; $T_N = 5.7$ ms and $T'_N = 8.2$ ms. Phase cycling is as follows: $\phi_1 = y$; $\phi_2 = x, -x$; $\psi_1 = x$; $\phi_3 = x, x, -x, -x$; $\phi_4 = -y$; $\psi_2 = -y$; receiver = $x, -x, -x, x$. CBCA(CO)NH (b): $\delta = 1.5$ ms; $\varepsilon = 2.4$ ms; $\zeta = 3.9$ ms; $\eta = 4.5$ ms; $\theta = 11.1$ ms; $\xi = 11.4$ ms; $\kappa = 3.2$ ms; $\lambda = 2.65$ ms; $\mu = 1$ ms; $T_{AB} = 3.55$ ms; $T_N = 5.65$ ms and $T'_N = 8.1$ ms. Phase cycling is as follows: $\phi_1 = y$; $\phi_2 = x, -x$; $\psi_1 = x$; $\phi_3 = x, x, -x, -x$; $\phi_4 = 120^\circ$ (Bloch-Siegert phase error compensation); $\phi_5 = -y$; $\psi_2 = -y$; receiver = $x, -x, -x, x$. *ct*-HNCO (c): $\delta = 2.75$ ms; $\lambda = 2.75$ ms; $\mu = 1$ ms; $T_N = 13.75$ ms and $T'_N = 11$ ms; $T''_N = T_N - (t_2/2)$. Phase cycling is as follows: $\phi_1 = y$; $\phi_2 = y, -y$; $\phi_3 = x, -x$; $\psi_1 = x, x, -x, -x$; $\phi_4 = 325^\circ$; $\phi_5 = -x$; $\psi_2 = y$; receiver = $x, x, -x, -x$. Quadrature detection in t_1 is obtained by changing phase ψ_1 in a States-TPPI manner. For t_2 , N- and P-type spectra are recorded interleaved; N-type spectra with the gradient pulses as shown and $\psi_2 = y$ and P-type spectra with the gradient pulse G_2 inverted and $\psi_2 = -y$. Pulsed field gradients have a sine-bell shape, with a duration of $G_1 = 1$ ms and $G_2 = 0.5$ ms. Gradient strengths are set to $G_1 = 80$ and $G_2 = 16$, where a gradient strength of 100 corresponds to ca. 60 G/cm at the center of the gradient.

selective pulse is required. Fig. 3.2 shows three of the modified pulse sequences, which are representative for all triple-resonance experiments used in this study. The CBCANH (Grzesiek and Bax, 1992b) experiment (Fig. 3.2a) was recorded with 64 complex t_1 points ($^{13}\text{C}^{\alpha\beta}$; spectral width 10000 Hz), 48 complex t_2 points (^{15}N ; spectral width 2235 Hz), 512 complex t_3 points (^1H ; spectral width 9615 Hz) and 40 scans per hypercomplex t_1/t_2 increment. The CBCA(CO)NH (Grzesiek and Bax, 1992a) experiment (Fig. 3.2b) was recorded with 64 complex t_1 points ($^{13}\text{C}^{\alpha\beta}$; spectral width 10000 Hz), 48 complex t_2 points (^{15}N ; spectral width 2235 Hz), 512 complex t_3 points (^1H ; spectral width 9615 Hz) and 16 scans per hypercomplex t_1/t_2 increment. The ct-HNCO (Grzesiek and Bax, 1992c; Jahnke and Kessler, 1994) experiment (Fig. 3.2c) was recorded with 50 complex t_1 points (^{13}CO ; spectral width 1502 Hz), 55 complex t_2 points (^{15}N ; spectral width 2008 Hz), 512 complex t_3 points (^1H ; spectral width 9615 Hz) and 8 scans per hypercomplex t_1/t_2 increment. A ct-HNCA (Grzesiek and Bax, 1992c; Jahnke and Kessler, 1994) experiment was recorded with 50 complex t_1 points ($^{13}\text{C}^{\alpha}$; spectral width 1502 Hz), 52 complex t_2 points (^{15}N ; spectral width 2008 Hz), 512 complex t_3 points (^1H ; spectral width 9615 Hz) and 16 scans per hypercomplex t_1/t_2 increment. The ct-HNCA experiment is similar to the ct-HNCO experiment (Fig. 3.2c), except that the ^{13}CO and $^{13}\text{C}^{\alpha}$ frequency labels in Fig. 3.2c are interchanged. A HBHA(CO)NH (Grzesiek and Bax, 1993) experiment was recorded with 64 complex t_1 points ($^1\text{H}^{\alpha\beta}$; spectral width 4316 Hz), 44 complex t_2 points (^{15}N ; spectral width 2235 Hz), 512 complex t_3 points (^1H ; spectral width 9615 Hz) and 40 scans per hypercomplex t_1/t_2 increment. The HBHA(CO)NH experiment is identical to the CBCA(CO)NH experiment in Fig. 3.2b, except for the part up to the first ζ -delay. This part is recorded as given by Grzesiek and Bax (1993). Quadrature detection in the t_1 dimension of all 3D experiments and in the t_2 dimension of the non-enhanced 3D experiments was obtained by using the States-TPPI acquisition scheme (Marion, et al., 1989c). Quadrature detection in the t_2 dimension (^{15}N) of the triple-resonance experiments was obtained by alternate N- and P-type selection (Cavanagh, et al., 1991; Kontaxis, et al., 1994).

NMR processing and data analysis. The spectra were processed on a Silicon Graphics IndigoII workstation using FELIX 2.3 (Biosym, San Diego, CA). For processing States-TPPI and P/N-type spectra macros written in-house were used. The data were apodized in the acquisition dimension using a Gaussian multiplication with a line broadening of -7 Hz and a Gaussian multiplication factor of 0.1, before zero-filling to 1024 real points for the 3D and 2048 real points for the 2D spectra. For the

indirectly detected dimensions the data were apodized using a squared cosine-bell window function. After the apodization the data were zero-filled to the next power of 2, Fourier transformed and phased. A FLATT baseline correction (Güntert and Wüthrich, 1992) was applied to F_1 of the ^{15}N -separated TOCSY- and NOESY-HMQC's and to the F_2 dimension of the 2D ^1H - ^{15}N HSQC's. Solvent suppression by convolution of the time domain data (Marion, et al., 1989b) in the acquisition dimension was applied to the 3D triple-resonance spectra and to the ^{15}N -separated TOCSY-HMQC. The data were analyzed using the program XEASY (ETH, Zürich, Switzerland) (Bartels, et al., 1995). A consensus chemical shift index for assigning protein secondary structure, was calculated using the Chemical Shift Index program (Wishart and Sykes, 1994; Wishart, et al., 1992). ^1H chemical shifts were referenced using internal TSP as a standard. TSP was set to -0.014 ppm, which is the pH corrected chemical shift value when DSS is set to 0 ppm. ^{15}N and ^{13}C chemical shifts were referenced indirectly using the following, temperature corrected, δ -values of 0.251449533 and 0.101329118 for ^{13}C and ^{15}N , respectively (Wishart, et al., 1995).

3.3 Results

Fig. 3.3 shows a 2D ^1H - ^{15}N HSQC spectrum of uniformly ^{15}N labelled *Azotobacter chroococcum* flavodoxin in the oxidized form. For a protein of 180 amino acids the dispersion of the ^1H - ^{15}N cross peaks is rather good. Nevertheless, some cross peaks in Fig. 3.3 are composed of two or three overlapping ^1H - ^{15}N resonances (boxed regions): a (Val³⁷, Phe⁴⁵, Lys⁹⁰); b (Thr⁹¹, Ala¹⁶⁷); c (Leu⁶³, Glu¹³⁷); d (Asp²⁸, Ser⁸⁸, Ser¹¹⁶); e (Ser²¹, Leu⁷⁹); f (Ala⁴⁶, Glu⁷³); g (Tyr¹⁰³, Met¹¹¹); h (Ser¹⁰, Thr¹³¹); i (Gly¹⁰², Asn¹⁵⁶(N^δH^δ)). All these degeneracies, however, could be resolved in a 3D ct-HNCO experiment. Out of a total of 175 non-proline residues 172 ^1H - ^{15}N amide cross peaks could be observed. The only amide cross peaks missing are the ones from Ala² and Gly¹⁵⁹. This is either caused by rapid exchange of the amide proton or by slow conformational averaging processes. When no presaturation is employed by recording a gradient enhanced 2D ^1H - ^{15}N HSQC (Kay, et al., 1992), Ala² and Gly¹⁵⁹ are still unobserved. The N-terminal part of a polypeptide chain often is somewhat flexible and therefore slow conformational averaging processes probably cause the amide proton of Ala² to be unobserved. Ser¹⁵⁸ is affected by presaturation, meaning that this part of the protein must be accessible to the solvent.

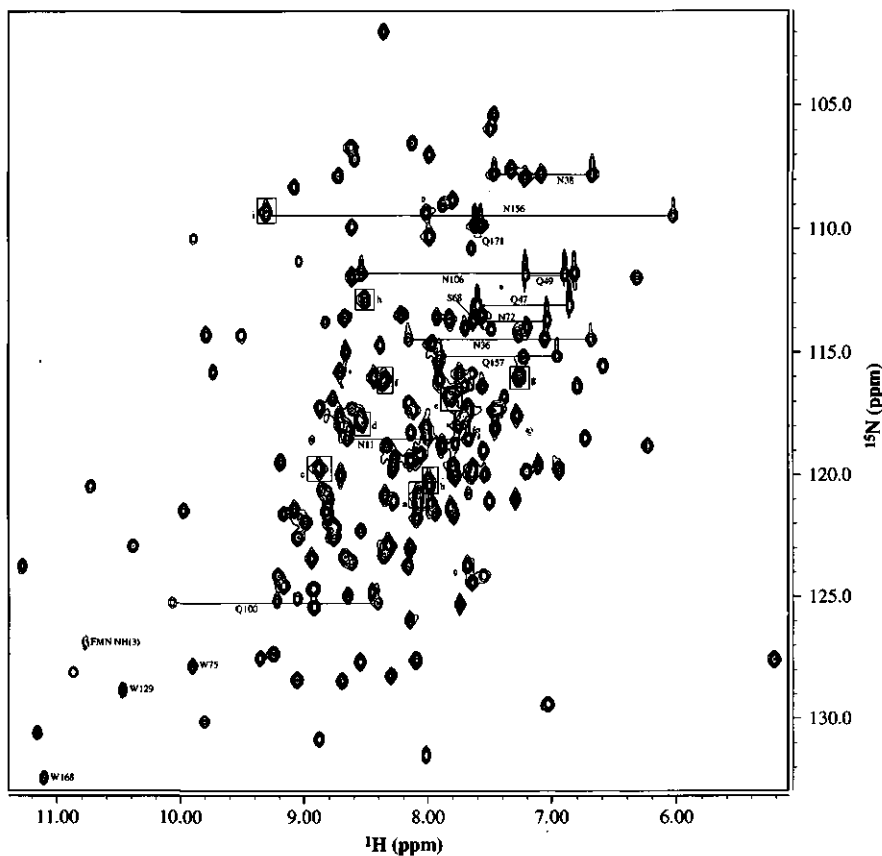


Fig. 3.3 2D ^1H - ^{15}N HSQC spectrum of 4.8 mM oxidized *Azotobacter chroococcum* flavodoxin. Cross peaks of the Asn and Gln sidechain amino groups are labelled, as are the Trp indole NH correlations. The aliased FMN NH(3) cross peak as well as the amide cross peak of Ser⁶⁸ are labelled as well. Negative resonances are marked by dashed contours. ^1H - ^{15}N cross peaks which consist of two or three resonances are marked by rectangles: a (Val³⁷, Phe⁴⁵, Lys⁹⁰); b (Thr⁹¹, Ala¹⁶⁷); c (Leu⁶³, Glu¹³⁷); d (Asp²⁸, Ser⁸⁸, Ser¹¹⁶); e (Ser²¹, Leu⁷⁹); f (Ala⁴⁶, Glu⁷³); g (Tyr¹⁰³, Met¹¹¹); h (Ser¹⁰, Thr¹³¹); i (Gly¹⁰², Asn¹⁵⁶(N ^{δ} H ^{δ})).

Fast exchange of the amide proton of Gly¹⁵⁹ therefore, probably causes this proton not to be observed in a 2D ^1H - ^{15}N HSQC spectrum. Also, the fact that Gly¹⁵⁹ is close to the N-terminal part of an α -helix (Fig. 3.5), can increase its amide proton exchange rate (Eriksson, et al., 1995). Flavodoxin from *Azotobacter chroococcum* contains 6

asparagines, 5 glutamines and 3 tryptophans. Cross peaks of all the 11 sidechain amino groups of the asparagines and the glutamines as well as the 3 indole NH groups of the tryptophans are observed in the ^1H - ^{15}N HSQC spectrum (Fig. 3.3). Besides ^1H - ^{15}N cross peaks from the apoprotein, one cross peak from the FMN, i.e. NH(3), is observed. All these cross peaks are indicated in Fig. 3.3. The FMN NH(3) ^1H and ^{15}N frequencies resonate at 10.77 ppm and 159.9 ppm, respectively; the ^1H - ^{15}N cross peak is therefore aliased in the ^{15}N dimension of the spectrum shown in Fig. 3.3. The ^1H - ^{15}N cross peaks of the backbone amides are not labelled to prevent Fig. 3.3 from becoming too crowded, their chemical shifts are listed in Table 3.2.

3.3.1 Sequential assignments

The sequential assignments were achieved through the use of the CBCANH experiment in combination with the CBCA(CO)NH experiment and the combined use of the ^{15}N -TOCSY-HMQC, HNHA and HBHA(CO)NH experiments. The assignment started by picking all amide peaks in a 2D ^1H - ^{15}N HSQC spectrum. The picked peaks were transferred to a 3D ct-HNCO spectrum in order to resolve overlapping resonances. The ^1H and ^{15}N frequencies of the picked peaks in the ct-HNCO spectrum next were transferred to the CBCANH spectrum and adjusted to the corresponding intra-residue $^{13}\text{C}^\alpha$ and $^{13}\text{C}^\beta$ resonances by making use of the CBCA(CO)NH spectrum. Analogously, the ^1H - ^{15}N frequencies of the picked ct-HNCO peaks were transferred to the HNHA and ^{15}N -TOCSY-HMQC spectra and adjusted to the intra-residual $^1\text{H}^\alpha$ and $^1\text{H}^\beta$ resonances, using the HBHA(CO)NH spectrum. Next spin system information was obtained from the ^{15}N -TOCSY-HMQC as described by Wüthrich (1986). Due to the size of *Azotobacter chroococcum* flavodoxin it was not possible to assign all spin systems, but those that were assigned were categorized in the following classes: Gly, Ala, Val, AMX and long-chain. Owing to their characteristic $^{13}\text{C}^\alpha$ and $^{13}\text{C}^\beta$ chemical shift values Gly, Ala and Ser/Thr could be assigned from the CBCANH/CBCA(CO)NH experiments (Grzesiek and Bax, 1993). Cross peaks of $^{13}\text{C}^\alpha$ resonances of Ser and Thr, which overlap with their intra-residual $^{13}\text{C}^\beta$ resonance are not observed in a CBCANH experiment, because they cancel one another due to their opposite signs. In this case the ct-HNCA experiment was used to determine the $^{13}\text{C}^\alpha$ resonance. Gly and Ala were used as starting points in the sequential assignment using the CBCANH and CBCA(CO)NH spectra. In this

Table 3.2 Chemical shifts of assigned ^1H , ^{15}N , ^{13}C backbone and $^1\text{H}^\beta$ and $^{13}\text{C}^\beta$ resonances of oxidized *Azotobacter chroococcum flavodoxin* at pH 6.5 and 30 °C.

Residue	Chemical shift (ppm)						
	^{15}N	H^N	$^{13}\text{C}^\alpha$	H^α	$^{13}\text{C}^\beta$	H^β	^{13}CO
Met ¹							
Ala ²			51.3	4.23	20.9	1.43	174.0
Lys ³	120.8	7.66	59.3	4.30	33.9	2.24, 2.10	176.3
Ile ⁴	117.4	8.10	59.9	4.68	40.6	1.64	174.3
Gly ⁵	117.2	8.60	44.1	3.26, 1.97			169.7
Leu ⁶	129.4	7.03	53.3	5.31	44.1	1.56, 0.93	174.2
Phe ⁷	122.5	8.74	55.6	5.92	43.9	2.84, 2.84	174.7
Phe ⁸	114.7	7.96	55.4	5.96	42.3	2.94, 2.63	171.7
Gly ⁹	106.0	7.49	43.6	4.35, 3.28			171.4
Ser ¹⁰	113.0	8.49	58.9	4.66	66.2	3.57, 4.00 ^a	172.8
Asn ¹¹	128.1	10.84	55.0	5.53	43.4	3.19, 2.72	176.7
Thr ¹²	110.4	9.89	60.4	4.74	68.1	4.80	175.4
Gly ¹³	109.0	7.86	47.0	4.30, 3.65			176.2
Lys ¹⁴	130.6	11.15	61.4	3.88	31.3	2.31, 1.54	179.1
Thr ¹⁵	120.4	10.72	67.8	3.65	68.0	4.20	177.1
Arg ¹⁶	118.8	6.23	58.9	2.22	29.4	4.37, 1.69	176.2
Lys ¹⁷	119.7	7.61	59.8	3.74	32.0	1.95, 1.95	180.0
Val ¹⁸	119.6	7.79	66.5	3.37	31.2	2.08, 1.91 ^a	178.4
Ala ¹⁹	122.8	8.32	55.9	3.71	18.3	1.16	178.9
Lys ²⁰	116.0	8.42	60.0	3.77	31.9	1.69, 1.69	179.2
Ser ²¹	116.9	7.79	61.5	4.12	62.9	3.94 ^a , 3.79 ^a	176.4
Ile ²²	124.4	7.63	66.3	3.47	37.9	2.00	176.5
Lys ²³	117.5	7.28	57.6	4.49	30.4	2.38, 1.81	177.4
Lys ²⁴	116.4	7.55	58.9	3.99	32.8	1.81 ^a , 1.81 ^a	177.0
Arg ²⁵	114.5	7.06	56.7	3.90	30.6	1.09	176.1
Phe ²⁶	117.0	8.14	57.4	5.04	44.3	3.14, 2.73	175.3
Asp ²⁷	121.9	8.75	53.5	4.68	41.7	3.31 ^a	176.6
Asp ²⁸	117.5	8.53	56.2	4.47	40.3	2.82, 2.68	177.4
Glu ²⁹	119.1	8.05	58.4	4.27	29.7	2.05, 2.05	178.6
Thr ³⁰	118.3	8.12	66.4	3.94	69.1	4.15	173.6
Met ³¹	121.0	8.25	54.3	5.11	38.0	2.03, 1.49	174.2
Ser ³²	124.9	8.63	58.9	4.37	65.2	4.06, 3.86	172.4
Asp ³³	115.4	7.89	54.8	4.34	40.9	2.54, 2.45	175.7
Ala ³⁴	123.1	8.29	52.3	4.03	18.6	1.15	177.4
Val ³⁵	127.5	8.08	61.7	4.18	35.2	1.74	173.5
Asn ³⁶	128.2	8.25	51.6	3.16	38.8	2.55, 2.26	177.1
Val ³⁷	121.2	8.06	63.6	3.13	30.1	0.46	175.4
Asn ³⁸	116.1	7.89	53.5	4.28	37.6	2.90, 2.44	176.8
Arg ³⁹	118.0	8.01	54.9	4.54	31.6	1.95, 1.78	176.0
Val ⁴⁰	119.7	6.93	60.6	4.54	34.7	1.83	173.9
Ser ⁴¹	121.4	8.79	56.5	4.75	65.9	4.34, 4.05	175.5
Ala ⁴²	125.2	9.19	56.3	3.88	18.8	1.32	179.2
Glu ⁴³	115.0	8.65	60.0	3.96	29.3	2.07, 1.97	179.0
Asp ⁴⁴	119.9	7.75	56.8	4.51	40.9	3.01, 2.89	178.7
Phe ⁴⁵	120.7	8.06	61.7	4.13	41.0	3.31, 2.97	177.0

Table 3.2 Continued.

Residue	Chemical shift (ppm)						
	¹⁵ N	H ^N	¹³ C ^α	H ^α	¹³ C ^β	H ^β	¹³ CO
Ala ⁴⁶	116.0	8.32	53.7	4.13	19.5	1.54	177.4
Gln ⁴⁷	114.0	7.19	57.2	4.10	29.0	1.95, 1.86	176.4
Tyr ⁴⁸	116.4	6.80	59.5	4.47	40.4	3.43, 2.65	176.5
Gln ⁴⁹	121.4	9.94	56.0	4.17	29.8	1.98, 1.98	173.5
Phe ⁵⁰	115.2	7.22	56.1	5.45	43.1	3.16, 2.99	175.0
Leu ⁵¹	124.5	9.15	53.9	5.43	48.6	1.68, 1.28	175.1
Ile ⁵²	121.9	8.98	61.5	5.22	39.9	1.59	174.5
Leu ⁵³	124.7	8.91	52.5	5.86	45.1	1.83, 1.30	175.6
Gly ⁵⁴	106.7	8.60	42.2	4.56, 1.69			175.4
Thr ⁵⁵	116.5	7.75	59.1	5.40	72.0	3.54	
Pro ⁵⁶			62.5	5.64	32.4	2.65, 1.78	176.5
Thr ⁵⁷	112.0	6.32	62.6	4.39	70.8	3.54	172.2
Leu ⁵⁸	130.8	8.85	51.8	3.26	44.1	1.42, 0.93	174.8
Gly ⁵⁹	106.5	8.09	48.1	4.10, 3.72			174.5
Glu ⁶⁰	121.3	9.05	56.4	4.41	27.9	2.22, 2.22	175.9
Gly ⁶¹	107.0	7.97	46.8	4.47, 3.64			173.9
Glu ⁶²	118.8	8.30	55.1	4.56	33.5	2.07, 1.59	176.5
Leu ⁶³	119.9	8.84	53.6	5.52	31.9		
Pro ⁶⁴			62.9	4.28	31.8	2.15, 1.91 ^a	173.7
Gly ⁶⁵	110.8	7.63	45.8	5.09, 4.01			174.6
Leu ⁶⁶	123.8	11.25	58.3	4.05	40.4	1.86, 1.33	182.6
Ser ⁶⁷	115.8	9.71	61.4	4.46	61.5	4.03, 3.81	174.7
Ser ⁶⁸	114.1	7.48	56.4	4.66	62.4	3.84, 3.48	173.5
Asp ⁶⁹	114.0	7.68	56.2	4.35	38.9	3.06, 2.72	176.1
Cys ⁷⁰	114.4	7.26	59.9	4.37	28.7	2.82, 2.60	174.3
Glu ⁷¹	120.8	8.34	58.9	3.94	30.5	2.05, 2.05	175.7
Asn ⁷²	113.6	7.79	51.1	4.87	43.2	2.75, 2.5	173.3
Glu ⁷³	116.4	8.36	57.2	3.83	30.9	1.90, 1.90	175.8
Ser ⁷⁴	114.3	9.79	57.4	4.00	62.0	3.67, 3.43	176.9
Trp ⁷⁵	123.7	8.15	61.3	4.27	33.0	3.30, 2.93	176.6
Glu ⁷⁶	117.6	8.70	60.0	3.69	30.0	1.88	177.4
Glu ⁷⁷	115.8	8.68	59.5	4.05	28.8	2.14, 1.95	177.2
Phe ⁷⁸	121.7	8.08	60.3	4.32	41.3	2.87, 2.46	176.8
Leu ⁷⁹	116.7	7.83	59.2	4.13	37.9	1.69 ^a	
Pro ⁸⁰			65.9	4.35	31.6	2.38, 1.60	178.6
Lys ⁸¹	113.5	7.55	58.4	4.03	32.3	1.68, 1.68	178.7
Ile ⁸²	108.0	7.22	61.0	4.51	39.9	2.44	176.7
Glu ⁸³	121.0	7.28	58.9	4.10	29.5	2.17, 2.17	177.1
Gly ⁸⁴	107.2	8.60	44.8	4.22, 3.55			174.2
Leu ⁸⁵	121.1	7.49	54.5	4.23	42.2	1.95	175.3
Asp ⁸⁶	119.6	8.10	53.2	4.71	42.2	2.79, 2.63	177.6
Phe ⁸⁷	125.0	9.03	58.9	4.39	39.4	3.48, 2.63	174.1
Ser ⁸⁸	117.9	8.56	61.2	4.32	62.9	3.88	175.9
Gly ⁸⁹	113.8	8.80	45.5	4.17, 3.72			174.2
Lys ⁹⁰	120.9	8.05	56.3	4.70	34.0	1.50	175.4

Table 3.2 Continued.

Residue	Chemical shift (ppm)						
	¹⁵ N	H ^N	¹³ C ^α	H ^α	¹³ C ^β	H ^β	¹³ CO
Thr ⁹¹	120.2	7.99	62.7	5.04	70.2	3.65	172.4
Val ⁹²	127.3	9.24	60.0	5.29	36.1	1.66	172.9
Ala ⁹³	128.4	9.05	51.3	5.43	24.2	1.52	175.3
Leu ⁹⁴	122.9	10.37	53.2	5.58	45.6	1.68, 1.11	174.5
Phe ⁹⁵	113.6	8.67	55.4	4.88	43.1	2.07, 2.07	173.3
Gly ⁹⁶	109.9	8.60	44.4	5.00, 3.14			170.6
Leu ⁹⁷	124.1	7.53	54.9	5.22	44.8	2.05, 1.18	178.0
Gly ⁹⁸	109.4	8.00	46.3	5.34, 4.58			172.2
Asp ⁹⁹	120.6	8.83	52.4	5.45	43.0	3.76, 2.99	176.0
Gln ¹⁰⁰	122.3	8.53	58.4	3.57	28.4	2.26, 2.26	174.3
Val ¹⁰¹	119.9	7.2	64.7	3.69	32.6	1.88	178.6
Gly ¹⁰²	108.3	9.08	46.3	3.50, 3.10			174.1
Tyr ¹⁰³	116.0	7.25	56.2	4.80	37.8	2.84, 2.63	
Pro ¹⁰⁴			65.3	4.62	32.4	2.67, 1.98	179.1
Glu ¹⁰⁵	116.7	8.74	57.4	4.37	30.5	2.21, 1.98	176.4
Asn ¹⁰⁶	120.0	7.63	53.6	5.48	42.4	3.37, 2.26	177.0
Phe ¹⁰⁷	125.9	8.12	57.8	5.34	38.5	3.42, 2.85	174.3
Leu ¹⁰⁸	118.5	8.00	56.7	3.55	38.0	1.42, 0.86	177.4
Asp ¹⁰⁹	119.6	7.11	57.6	4.46	41.4	2.70, 2.21	178.4
Ala ¹¹⁰	119.4	8.26	55.1	4.01	20.0	1.16	179.8
Met ¹¹¹	116.2	7.27	59.4	3.50	33.6	2.05, 1.30	178.4
Gly ¹¹²	107.6	7.34	47.3	3.77, 3.54			175.6
Glu ¹¹³	123.7	7.66	59.8	4.10	28.9	2.07, 1.93	179.8
Leu ¹¹⁴	117.3	7.64	57.9	3.91	41.6	1.71, 1.06	178.3
His ¹¹⁵	119.7	8.26	62.7	4.03	31.0	3.47, 3.06	178.8
Ser ¹¹⁶	117.8	8.51	62.3	4.00	63.0	3.47, 3.04	174.8
Phe ¹¹⁷	121.1	7.97	61.6	3.78	39.2	2.99, 2.79	178.3
Phe ¹¹⁸	113.4	8.21	63.6	3.84	38.1	2.65, 2.51	178.6
Thr ¹¹⁹	114.7	8.38	66.4	4.10	69.0	4.34 ^a	179.6
Glu ¹²⁰	122.9	8.12	59.0	4.13	29.2	2.07, 1.90	177.4
Arg ¹²¹	115.6	6.59	55.7	4.49	30.8	2.67 ^a , 1.23	175.4
Gly ¹²²	105.4	7.46	46.2	4.32, 3.74			174.4
Ala ¹²³	121.4	7.81	52.5	4.46	20.0	1.15	176.7
Lys ¹²⁴	123.2	8.35	55.7	4.50	33.4	1.93, 1.79	174.8
Val ¹²⁵	127.6	8.52	61.0	5.45	31.7	2.07	177.2
Val ¹²⁶	122.5	9.03	59.3	4.90	34.7	2.34	175.0
Gly ¹²⁷	108.0	8.69	46.7	4.61, 3.76			174.0
Ala ¹²⁸	121.6	7.76	53.8	4.37	19.6	1.47	177.8
Trp ¹²⁹	123.4	8.66	56.2	5.34	35.6	3.40, 3.04	174.3
Ser ¹³⁰	119.9	7.51	58.8	4.41	63.2	3.88, 3.52	175.1
Thr ¹³¹	112.7	8.47	62.4	4.58	69.5	4.63	176.0
Asp ¹³²	124.7	8.43	56.3	4.54	40.8	2.58, 2.58	177.8
Gly ¹³³	111.3	9.01	45.5	4.12, 3.65			173.2
Tyr ¹³⁴	117.6	7.70	56.4	5.14	41.3	3.28, 2.97	175.0
Glu ¹³⁵	124.2	9.20	55.4	4.73	31.2	1.86, 1.86	173.3

Table 3.2 Continued.

Residue	Chemical shift (ppm)							
	¹⁵ N	H ^N	¹³ C ^α	H ^α	¹³ C ^β	H ^β		¹³ CO
Phe ¹³⁶	118.7	7.75	56.5	4.80	39.2	3.43, 3.13		172.5
Glu ¹³⁷	119.6	8.86	56.8	4.44	32.5	2.05, 1.64		176.8
Gly ¹³⁸	109.2	9.28	45.6	4.59, 3.89				170.7
Ser ¹³⁹	113.6	7.91	58.1	5.00	66.9	4.25, 3.38		177.5
Thr ¹⁴⁰	121.6	9.16	63.1	4.49	67.8	4.54		174.7
Ala ¹⁴¹	122.1	8.74	51.0	4.13	20.1	1.27		174.8
Val ¹⁴²	118.5	6.72	61.7	4.44	32.4	1.79		175.2
Val ¹⁴³	128.4	8.69	61.6	4.08	35.5	1.61		175.6
Asp ¹⁴⁴	127.5	9.31	55.7	4.25	39.6	2.97, 2.60		176.5
Gly ¹⁴⁵	102.0	8.33	45.8	4.06, 3.47				173.2
Lys ¹⁴⁶	119.0	7.54	55.2	4.63	36.6	1.93, 1.61		176.2
Phe ¹⁴⁷	119.4	9.18	59.1	5.19	41.6	3.42, 3.19		180.4
Val ¹⁴⁸	112.0	8.59	62.4	3.96	32.2	2.03		174.6
Gly ¹⁴⁹	107.7	7.08	45.3	4.59, 4.08				171.8
Leu ¹⁵⁰	117.5	7.45	55.9	2.69	38.1			173.9
Ala ¹⁵¹	127.6	5.22	50.0	3.98	22.3	-0.05		175.7
Leu ¹⁵²	125.4	8.90	53.3	4.73	46.0	1.93, 1.15		174.1
Asn ¹⁵³	116.0	7.61	53.5	5.46	43.1	2.85, 2.85		175.8
Leu ¹⁵⁴	130.2	9.76	57.5	3.98	42.1	1.23		176.6
Asp ¹⁵⁵	123.6	8.61	57.9	4.64	41.8	2.96, 2.67		177.6
Asn ¹⁵⁶	114.3	9.50	53.5	4.95	42.6	2.89, 2.36		175.9
Gln ¹⁵⁷	116.8	7.36	53.5	5.09	29.8	2.07, 1.93		179.2
Ser ¹⁵⁸	118.6	8.91	63.1	4.58	62.2			
Gly ¹⁵⁹			46.5	4.20, 4.02				174.9
Lys ¹⁶⁰	117.3	7.41	55.9	4.61	33.2	2.07, 1.68		176.8
Thr ¹⁶¹	117.1	7.67	68.1	3.54	69.4	4.32		174.4
Asp ¹⁶²	121.0	8.76	58.8	4.25	40.1	2.63, 2.63		179.0
Glu ¹⁶³	120.0	8.66	59.1	4.17	29.6	2.14, 2.14		179.6
Arg ¹⁶⁴	121.4	7.92	60.3	4.32	31.1	1.88 ^a , 1.68 ^a		176.9
Val ¹⁶⁵	118.0	8.67	67.3	3.33	32.0	2.03		177.7
Ala ¹⁶⁶	119.3	8.08	56.1	3.93	18.4	1.50		180.8
Ala ¹⁶⁷	120.5	7.98	55.1	4.34	19.3	1.95		180.5
Trp ¹⁶⁸	123.5	8.91	62.5	4.39	29.5	3.04		178.4
Leu ¹⁶⁹	117.2	8.86	57.5	3.71	41.9	1.98, 1.16		178.7
Ala ¹⁷⁰	118.2	7.45	55.1	4.05, 3.00	18.0	1.56		179.8
Gln ¹⁷¹	118.8	7.87	59.1	4.17	29.5	2.48, 2.48		179.1
Ile ¹⁷²	110.3	7.97	62.7	4.34	38.2	1.79		177.0
Ala ¹⁷³	125.3	7.75	57.5	3.91	16.6	1.61		
Pro ¹⁷⁴			66.0	4.52	31.4	2.46, 1.97		180.0
Glu ¹⁷⁵	115.8	7.71	58.0	4.27	29.6	2.05, 1.98		177.6
Phe ¹⁷⁶	116.3	7.69	58.1	4.03	40.6	2.79, 2.44		174.8
Gly ¹⁷⁷	108.8	7.78	46.9	3.83, 3.67				174.9
Leu ¹⁷⁸	118.0	7.74	53.8	4.37	43.2	1.50, 1.32		176.4
Ser ¹⁷⁹	117.8	8.59	57.6	4.54	63.8	3.89, 3.76		173.1
Leu ¹⁸⁰	131.4	7.98	56.5	4.25	43.9	1.54		

^a Tentative assignment

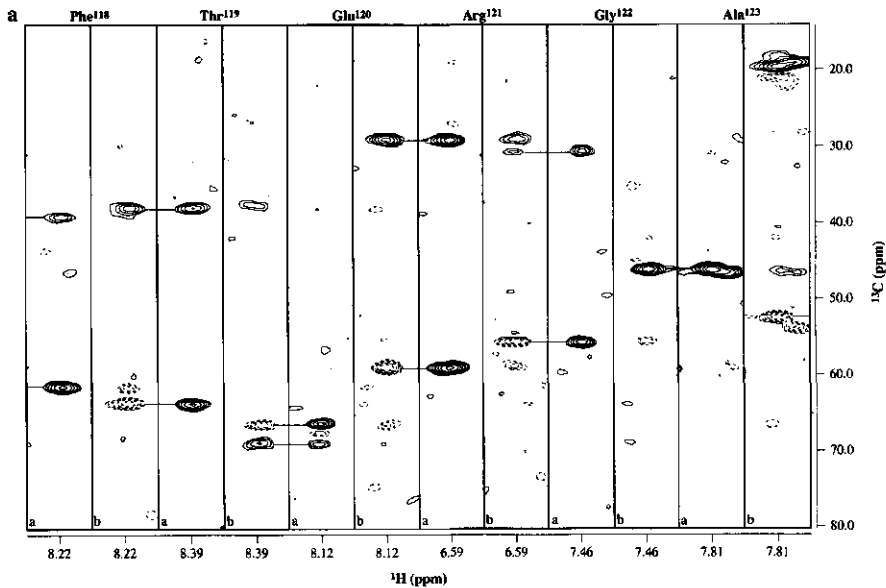


Fig. 3.4a Strips along the ¹³C axes of the CBCA(CO)NH (a) and CBCANH (b) spectra taken at the ¹H-¹⁵N resonance frequencies of Phe¹¹⁸-Ala¹²³ showing sequential connectivities. Resonances of negative intensity are marked by dashed contours.

way stretches of sequential residues were obtained. In Fig. 3.4a this sequential assignment procedure is illustrated. In this figure strips are shown along the ¹³C axes of the CBCANH and the CBCA(CO)NH spectra taken at the ¹H-¹⁵N resonance frequencies of Phe¹¹⁸-Ala¹²³. In combination with the spin system information these stretches were mapped onto the primary sequence. Ambiguities of what the next sequential neighbour will be, cause the stretch to end. These ambiguities mainly arise from simultaneous degeneracy of ¹³C^α and ¹³C^β resonances, or degeneracy of ¹³C^α Gly resonances, of different spin systems. However, if a stretch can be mapped uniquely onto the primary sequence, ¹³C^α and ¹³C^β chemical shift information (Grzesiek and Bax, 1993) of residue n-2 can be used to identify which of the degenerate n-1 candidates is the correct one. In this way almost all amide resonances could be sequential assigned. Ambiguities in the CBCANH/CBCA(CO)NH based assignments were solved by assignments based on the HNHA and ¹⁵N-TOCSY-

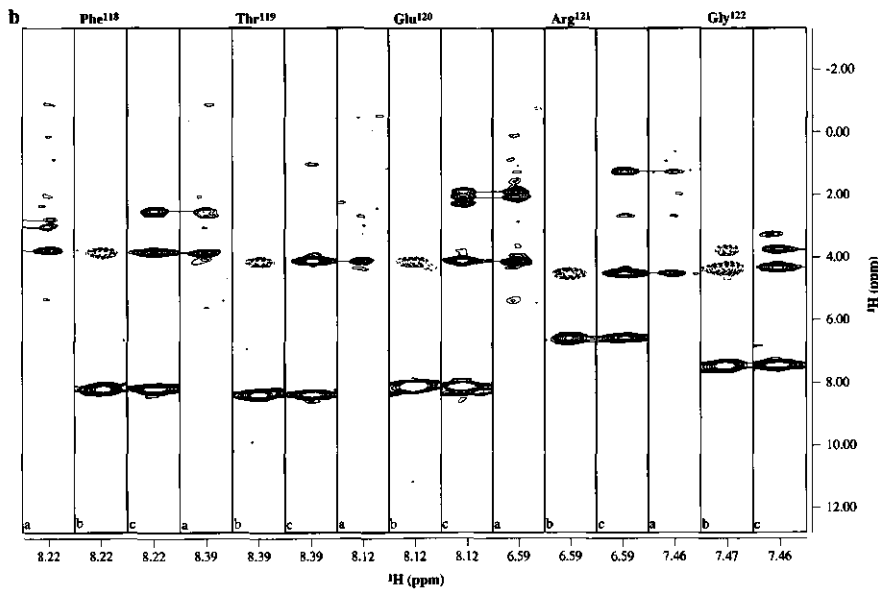


Fig. 3.4b Strips along the ^1H axes of the HBHA(CO)NH (a), HNHA (b) and ^{15}N -TOCSY-HMQC (c) spectra taken at the ^1H - ^{15}N resonance frequencies of Phe¹¹⁸-Gly¹²² showing sequential connectivities. Resonances of negative intensity are marked by dashed contours.

HMQC in combination with the HBHA(CO)NH spectra. An example of the sequential assignment based on these three experiments is given in Fig. 3.4b. This combination of experiments also served as a check for the assignments obtained from the CBCANH and CBCA(CO)NH spectra. Furthermore, it yielded the chemical shifts of the $^1\text{H}^\alpha$ and $^1\text{H}^\beta$ protons. Finally, the ^{13}CO chemical shifts were determined from the ct-HNCO spectrum. A list of the chemical shifts of $^1\text{H}^\text{N}$, ^{15}N , $^{13}\text{C}^\alpha$, $^1\text{H}^\alpha$, $^{13}\text{C}^\beta$, $^1\text{H}^\beta$ and ^{13}CO derived from these experiments, is given in Table 3.2. Due to overlap and missing correlations 14 $^1\text{H}^\beta$ resonances could not be assigned.

The ^1H - ^{15}N cross peaks in the HSQC spectrum of the sidechain amino groups of Asn and Gln were assigned by comparing the TOCSY and NOESY ladders correlated to the backbone amide proton with those correlated to the sidechain amino protons. The ^1H - ^{15}N cross peaks in the HSQC spectrum of the indole NH's were assigned on

the basis of observed NOE's between the Trp β -protons with the intra-residual indole NH proton in a ^{15}N -NOESY-HMQC spectrum.

3.3.2 Secondary structure

The solution secondary structure was determined from NOE connectivity patterns, amide proton exchange, $^3\text{J}_{\text{HNH}\alpha}$ coupling constants (Wüthrich, 1986) and $^1\text{H}\alpha$, $^{13}\text{C}\alpha$, $^{13}\text{C}\beta$ and ^{13}CO chemical shifts (Wishart and Sykes, 1994; Wishart, et al., 1992). These data and the secondary structure elements derived from them are shown in Fig. 3.5. The NOE connectivity patterns were obtained from the ^{15}N -NOESY-HMQC and the HMQC-NOESY-HMQC experiments, the $^3\text{J}_{\text{HNH}\alpha}$ couplings from the HNHA experiment and the amide proton exchange from 2D ^1H - ^{15}N HSQC experiments in D_2O . Instead of displaying secondary chemical shift values, the calculated consensus chemical shift (Wishart and Sykes, 1994) is given in Fig. 3.5. In combination with the chemical shift information, helical regions are characterized by the presence of $d_{\alpha\text{N}(i,i+3)}$, $d_{\alpha\text{N}(i,i+2)}$, strong or medium $d_{\alpha\text{N}(i,i+1)}$ and strong $d_{\text{NN}(i,i+1)}$ NOE connectivities as well as by small $^3\text{J}_{\text{HNH}\alpha}$ (< 5 Hz) coupling constants (Wüthrich, 1986). Whereas extended conformations are characterized by strong $d_{\alpha\text{N}(i,i+1)}$, weak $d_{\text{NN}(i,i+1)}$ and the absence of $d_{\alpha\text{N}(i,i+2)}$ and $d_{\alpha\text{N}(i,i+3)}$ NOE connectivities, as well as by large $^3\text{J}_{\text{HNH}\alpha}$ (> 8 Hz) coupling constants (Wüthrich, 1986). Five helical regions are observed: $\alpha 1$ (Gly¹³-Lys²⁴), $\alpha 2$ (Ala⁴²-Tyr⁴⁸), $\alpha 3$ (Ser⁷⁴-Lys⁸¹), $\alpha 4$ (Glu¹⁰⁵-Glu¹²⁰) and $\alpha 5$ (Thr¹⁶¹-Ala¹⁷³). In Fig. 3.5 only $d_{\alpha\text{N}(i,i+2)}$ and $d_{\alpha\text{N}(i,i+3)}$ NOE connectivities which did not show overlap with other sequential NOE connectivities are indicated. Due to overlap in the HNHA spectrum $^3\text{J}_{\text{HNH}\alpha}$ coupling constants from only 96 out of 175 non-proline residues could be determined. Between the extended conformations several strong $d_{\alpha\text{N}(i,j)}$ and medium $d_{\text{NN}(k,l)}$ interstrand NOE connectivities could be identified, indicating that these strands form a parallel β -sheet. Besides interstrand long range NOE connectivities also strong connectivities are observed between strand $\beta 1$ and residues 32-37. These observed long range (interstrand) NOE connectivities are given in Fig. 3.6. The small extended conformation $\beta 5$ is not part of the β -sheet, because no long range interstrand NOE connectivities could be observed. Due to the large number of hydrogen bonds in secondary structure elements, a large number of slowly exchangeable amide protons are observed for these secondary structure elements (Fig. 3.5). For the central β -sheet these slowly

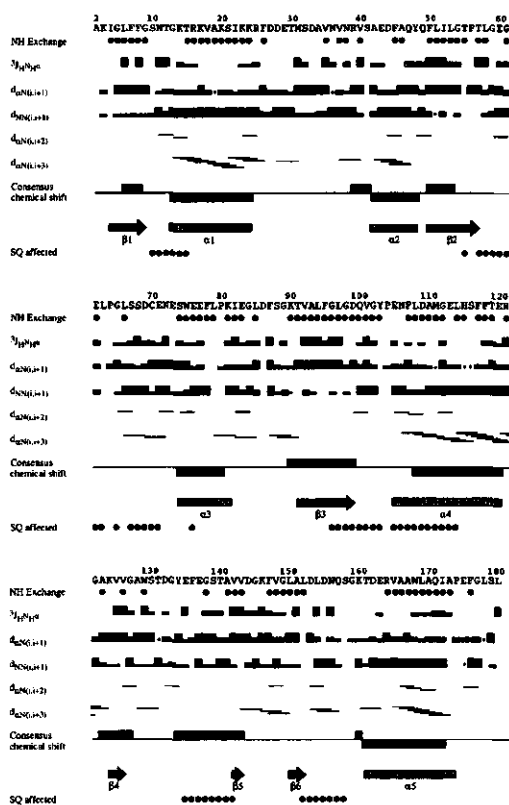
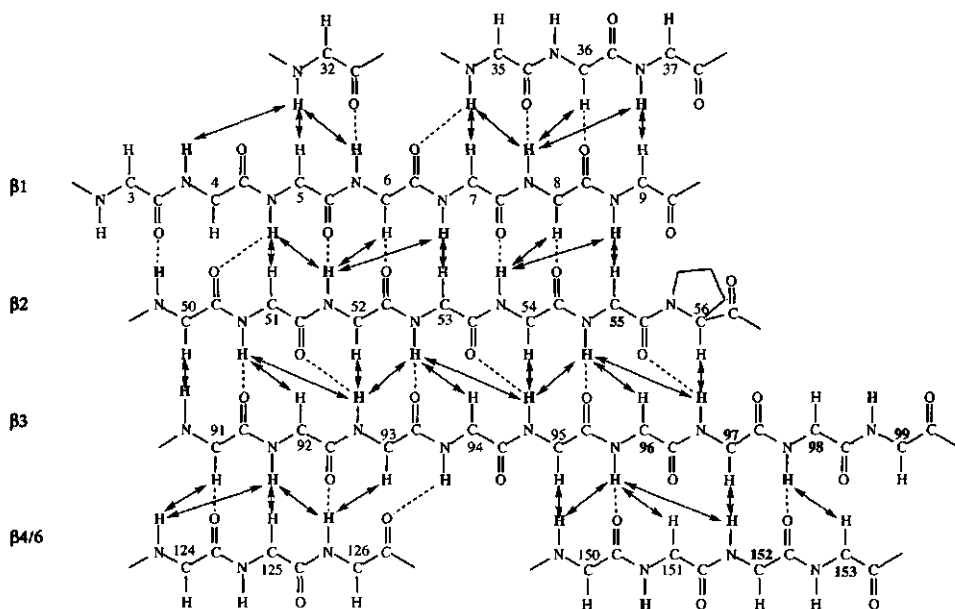


Fig. 3.5 Summary of the NMR data obtained for oxidized *Azotobacter chroococcum* flavodoxin on amide proton exchange, sequential and medium range NOE connectivities, $^3J_{HNHa}$ coupling constants, $^1H^\alpha$, $^{13}C^\alpha$, $^{13}C^\beta$ and $^{13}C^O$ secondary shifts depicted as consensus chemical shifts, the secondary structure elements deduced from these data and the amide protons broadened by the one-electron reduced FMN. Amide protons which are still observed 53 hours after dissolving lyophilized flavodoxin in D_2O in a 2D 1H - ^{15}N HSQC spectrum are marked by dots. $^3J_{HNHa}$ coupling constants as determined from the HNHA experiment are given by black and shaded boxes for non-overlapping and slightly overlapping resonances, respectively. Large boxes: $^3J_{HNHa} > 8$ Hz; medium sized boxes: $5 \text{ Hz} < ^3J_{HNHa} < 8$ Hz; small boxes: $^3J_{HNHa} < 5$ Hz. Strong, medium and weak sequential NOE connectivities are indicated by large, medium sized and small boxes. Shaded boxes denote partial overlap and stars denote uncertain connectivities due to overlap. Consensus chemical shift: Positive and negative boxes denote chemical shift derived β -sheet and α -helix conformations, respectively. Residues of which the amide protons are affected by the one-electron reduced FMN are indicated by dots.



*Fig. 3.6 Topology of central β -sheet of *Azotobacter chroococcum* flavodoxin. Interstrand long range NOE connectivities are indicated by double arrows. Slowly exchangeable amide protons are in bold letter type. Hydrogen bonds, as expected on the basis of NOE's and slow amide proton exchange, are indicated by dashed lines. Amide protons of residues of which the residue-number is in bold letter type are affected by the one-electron reduced FMN.*

exchangeable amide protons and their most probable hydrogen bond acceptor are indicated in Fig. 3.6.

Fig. 3.5 also shows the residues of which the amide proton resonance is broadened by the paramagnetic FMN of the flavodoxin in the one-electron reduced redox-state. These residues therefore, are located close to the isoalloxazine part of the FMN (within about 15 Å). From this and Fig. 3.6 it can be concluded that the FMN ring is located at the C-terminal part of the strands β 2, β 3 and β 6. Furthermore it is observed that residues Glu¹³⁵, Phe¹³⁶, Ser¹³⁹ and Val¹⁴² are only slightly affected by the paramagnetic FMN, meaning that this part of the protein is located further away from the isoalloxazine ring.

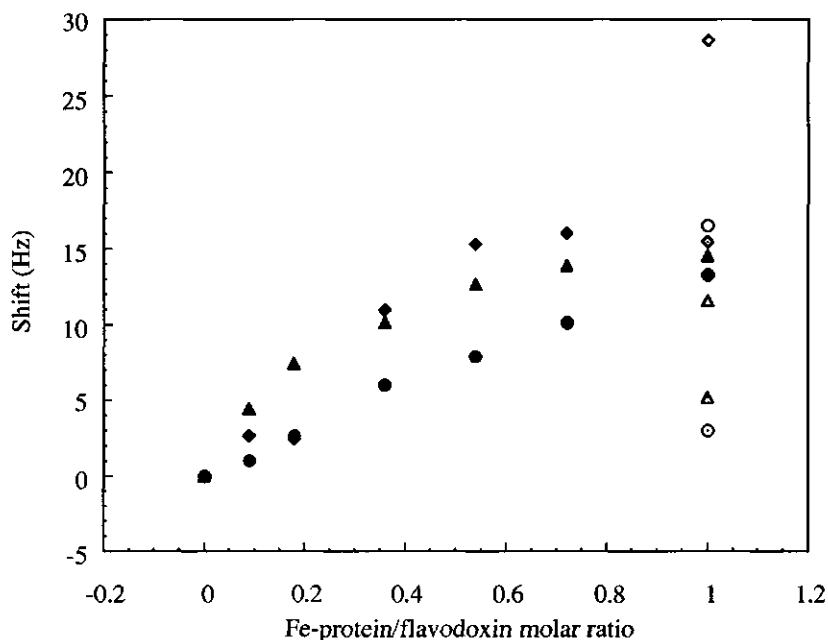


Fig. 3.7 Absolute ^{15}N chemical shift changes as a function of Fe-protein/flavodoxin ratio at 25 °C, pH 7.1. The chemical shifts of the uncomplexed flavodoxin are taken as reference. \blacklozenge : sidechain amino group of Asn¹¹; \blacktriangle : amide group of Ser⁶⁸; \bullet : sidechain amino group of Asn⁷². Open symbols denote the sample containing 2.8 mM MgADP and open symbols with a dot denote the sample containing 96 mM KCl (and 2.7 mM MgADP).

3.3.3 Titration of flavodoxin with Fe-protein

The titration of oxidized ^{15}N labelled flavodoxin with dimeric Fe-protein (molecular mass 60 kDa for the homodimer) as indicated in Table 3.1, was monitored by recording 2D ^1H - ^{15}N HSQC spectra after each titration. The intensities of the ^1H - ^{15}N correlations in these spectra decrease with increasing Fe-protein/flavodoxin ratio. Partly this is an effect of dilution of the sample as more Fe-protein is added, but also it is caused by complexation of the flavodoxin with the Fe-protein, forming a 80 kDa complex (assuming a 1:1 stoichiometry). Complexation will cause broadening of the ^1H - ^{15}N resonances of the flavodoxin, and thus a decreased ^1H - ^{15}N cross peak

intensity. Upon addition of 96 mM KCl the intensities, despite the extra dilution, again increase, indicating that more uncomplexed flavodoxin is present in the NMR sample. Besides these changes in intensities hardly any significant changes in chemical shifts were detected during the titration, except for three residues. Small but significant chemical shift changes for the backbone amide ^{15}N of Ser⁶⁸ and the sidechain amino ^{15}N of Asn¹¹ and Asn⁷² (Fig. 3.3) were observed during the titration (Fig. 3.7). No significant chemical shift changes for the corresponding protons were observed. For the one-electron reduced flavodoxin from *Klebsiella pneumoniae* it was found that a stronger complex with its Fe-protein is formed when MgADP was present (Thorneley and Deistung, 1988). MgADP was therefore added at the end of the Fe-protein titration series. For the complexation of oxidized flavodoxin with the Fe-protein of *Azotobacter chroococcum*, MgADP also has an effect on the complex formation, as chemical shift changes of the above mentioned resonances are observed upon addition of MgADP (Fig. 3.7). An increase in ionic strength by addition of KCl causes the chemical shifts to shift towards their uncomplexed chemical shift values (Fig. 3.7).

3.4 Discussion

This study reports the ^1H , ^{15}N and ^{13}C backbone and ^1H and ^{13}C beta resonance assignments of the flavodoxin-2 from *Azotobacter chroococcum*. To date this is the largest flavodoxin studied by 2D and 3D heteronuclear NMR techniques. The NMR data (Fig. 3.5) indicate that like other flavodoxins *A. chroococcum* flavodoxin contains a central parallel β -sheet linked by α -helices, probably folded in an α/β doubly wound superfold (Orengo, et al., 1994). All the flavodoxin structures known thusfar have a five-stranded central parallel β -sheet. Although the central β -sheet of *Azotobacter chroococcum* flavodoxin also consists of five strands, one outer strand (Ser³²-Val³⁷) has no regular extended conformation as deduced from the NMR data. Especially the secondary chemical shifts and the presence of some medium sized $^3J_{\text{HNH}\alpha}$ coupling constants give an indication of deviation from a regular extended conformation. However, in view of the observed long range NOE's to strand β_1 (Fig. 3.6), the stretch Ser³²-Val³⁷ can still considered to be part of the central β -sheet. Besides long range NOE's, also strong sequential $d_{\alpha\text{N}(i,i+1)}$ NOE's, indicative for β -sheet conformation, are observed in this stretch. Furthermore, the absence of

interstrand NOE's between residues Asp³³, Ala³⁴ and strand β 1, is an indication for the irregularity of this stretch. The second outer strand also shows an irregularity, in that this strand is composed of two sequential stretches, Lys¹²⁴-Val¹²⁶ and Leu¹⁵⁰-Leu¹⁵², connected to each other by a loop region. This region contains the residues which form the extra loop in the long-chain flavodoxins. Furthermore, no β -sheet consensus chemical shifts for strand β 6 are observed. This means that either this strand also has an irregular extended conformation or that the strand is too short to be identified by the CSI program as β -sheet. From Fig. 3.5 it can be seen that the consensus chemical shift is a good indication for the secondary structure elements in the flavodoxin from *Azotobacter chroococcum*. Especially helical structures determined from the consensus chemical shifts are in good agreement with NOE's and $^3J_{\text{HNH}\alpha}$ coupling constants characteristic for α -helices. For the determination of the β -sheet in this flavodoxin, the consensus chemical shifts perform less well. The strands β 1 to β 5 are characterized by a β -sheet consensus chemical shift, however, the termination of these strands as determined by the absence of strong sequential $d_{\alpha\text{N}(i,i+1)}$ and weak $d_{\text{NN}(i,i+1)}$ NOE connectivities and large coupling constants differs from the termination on the basis of consensus chemical shifts. Based on former characteristics the following extended conformations were determined for the flavodoxin from *Azotobacter chroococcum* (Fig. 3.5): β 1(Ile⁴-Gly⁹), β 2(Phe⁵⁰-Thr⁵⁷), β 3(Thr⁹¹-Asp⁹⁹), β 4(Lys¹²⁴-Val¹²⁶), β 5(Val¹⁴²-Val¹⁴³) and β 6(Leu¹⁵⁰-Leu¹⁵²). The absence of long range NOE's between strand β 5 and the central β -sheet, shows that strand β 5 is not part of this sheet. No long range NOE connectivities between strand β 5 and any other part of the protein could be detected. The only NOE's observed where medium range NOE's between the amide protons of Val¹⁴³ and Lys¹⁴⁶ and between the α -proton of Val¹⁴² and the amide protons of Lys¹⁴⁶ and Phe¹⁴⁷. This indicates the presence of a reverse turn-like structure in that part of the protein.

Helices were characterized by the presence of $d_{\alpha\text{N}(i,i+3)}$, $d_{\alpha\text{N}(i,i+2)}$, strong or medium $d_{\alpha\text{N}(i,i+1)}$ and strong $d_{\text{NN}(i,i+1)}$ NOE connectivities as well as by small $^3J_{\text{HNH}\alpha}$ (< 5 Hz) coupling constants. In combination with the consensus chemical shifts five helical regions were determined: α 1(Gly¹³-Lys²⁴), α 2(Ala⁴²-Tyr⁴⁸), α 3(Ser⁷⁴-Lys⁸¹), α 4(Glu¹⁰⁵-Glu¹²⁰) and α 5(Thr¹⁶¹-Ala¹⁷³). Helices α 1, α 2 and α 5 show all the characteristics of a regular α -helix (it has to be borne in mind that not every $d_{\alpha\text{N}(i,i+3)}$ connectivity could be assigned, due to overlap). Fig. 3.5 only shows the unambiguously assigned $d_{\alpha\text{N}(i,i+3)}$ NOE's. Helices α 3 and α 4 show some deviation from a regular α -helix. The deviations for helix α 3 are found in the N-terminal part of

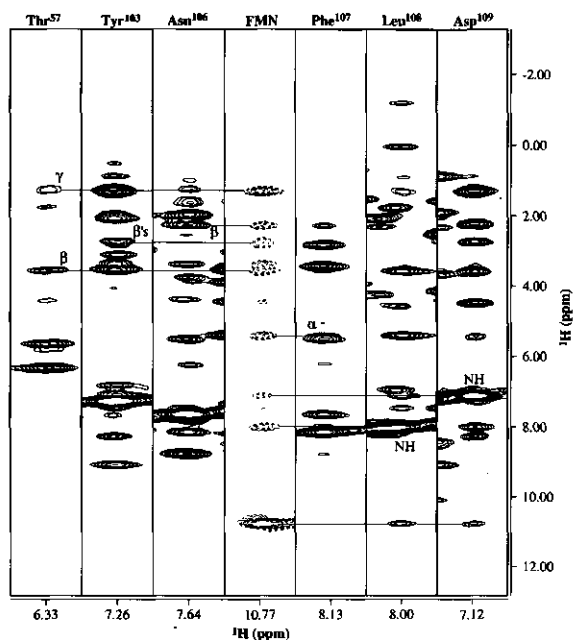


Fig. 3.8 Strips along the ^1H axis of the ^{15}N -NOESY-HMQC spectrum taken at the ^1H - ^{15}N resonance frequencies of Thr⁵⁷, Tyr¹⁰³, Asn¹⁰⁶-Asp¹⁰⁹ and FMN NH(3) showing NOE connectivities between these amino acids and the FMN NH(3) proton. Resonances of negative intensity are marked by dashed contours.

the helix, where some weak $d_{\text{NN}(i,i+1)}$ NOE connectivities are observed. The fact that hardly any $d_{\alpha\text{N}(1,1+3)}$ NOE connectivities are indicated for this helix in Fig. 3.5, merely arises from extensive overlap in this region. For helix α_4 some medium sized $d_{\text{NN}(i,i+1)}$ NOE's followed by a weak $d_{\alpha\text{N}(i,i+1)}$ NOE are observed, for the residues Phe¹⁰⁷-Ala¹¹⁰. This part therefore, deviates from a regular α -helix. However, due to the presence of $d_{\alpha\text{N}(i,i+3)}$ NOE's in combination with strong $d_{\text{NN}(i,i+1)}$ NOE's and small $^3J_{\text{HNH}\alpha}$ coupling constants for the residues Glu¹⁰⁵ and Asn¹⁰⁶, this helix is determined to start at Glu¹⁰⁵.

In Fig. 3.1b the consensus binding site residues of *Anacystis nidulans* flavodoxin are underlined (Stockman, et al., 1990). The corresponding residues in *Azotobacter chroococcum* flavodoxin also are located near the FMN molecule, since all of them are affected in the one-electron reduced flavodoxin (Fig. 3.5). As for other

flavodoxins (Clubb, et al., 1991; Mierlo van, et al., 1990b; Peelen and Vervoort, 1994; Stockman, et al., 1993) the loop containing the residues Ser¹⁰-Thr¹⁶ must be involved in the binding of the FMN phosphate, because low field amide proton chemical shift values, caused by hydrogen bonding to the negatively charged phosphate group, are observed for Ser¹⁰ (8.49 ppm), Asn¹¹ (10.84 ppm), Thr¹² (9.89 ppm), Lys¹⁴ (11.15 ppm) and Thr¹⁵ (10.72 ppm) (Table 3.2). A $d_{NN(i,i+2)}$ NOE connectivity between the amide protons of Asn¹¹ and Gly¹³ indicates the presence of a reverse turn (Wüthrich, 1986) between strand β 1 and helix α 1. This sheet-turn-helix motif is found in all flavodoxin structures as the FMN phosphate binding region (Burnett, et al., 1974; Fukuyama, et al., 1990; Ludwig, et al., 1976; Mierlo van, et al., 1990a; Smith, et al., 1977; Smith, et al., 1983; Stockman, et al., 1990; Watenpaugh, et al., 1973; Watt, et al., 1991). The residues in the regions of *Azotobacter chroococcum* flavodoxin, corresponding to the consensus FMN binding site residues, Pro⁵⁵-Glu⁶¹ and Ala⁸⁸-Gln⁹⁹, of the flavodoxin from *A. nidulans*, are located close to the FMN NH(3). This can be concluded because NOE connectivities between Thr⁵⁷, Tyr¹⁰³, Asn¹⁰⁶, Phe¹⁰⁷, Leu¹⁰⁸, Asp¹⁰⁹ and the FMN NH(3) proton are observed. These connectivities are shown in Fig. 3.8.

Zhou and Swenson (1995) have found for the flavodoxin from *Desulfovibrio vulgaris* that negatively charged amino acid residues located near the FMN contribute to the low midpoint potential of the semiquinone-hydroquinone couple (-440 mV (Curley, et al., 1991)). The midpoint potential of the semiquinone-hydroquinone couple of *A. chroococcum* flavodoxin is 82 mV more negative, i.e. -522 mV (Deistung and Thorneley, 1986). Zhou and Swenson (1995) observed an average increase in the midpoint potential of 15 mV when a negatively charged residue was mutated to a neutral residue. If this is extended to *A. chroococcum* flavodoxin, this means that this flavodoxin should have about five negatively charged residues more surrounding the FMN than the flavodoxin from *D. vulgaris*. From the residues in *A. chroococcum* flavodoxin affected by the one-electron reduced FMN, 13 are negatively charged (Fig. 3.5). From the corresponding residues, as deduced by the alignment in Fig. 3.1b, in *D. vulgaris* flavodoxin only 8 residues are negatively charged. Although this is exactly five negatively charged residues less, one should bear in mind that this way of comparison is only an estimate and that eventually the 3D structures should be compared. But it can safely be concluded that, indeed more negatively charged amino acids surround the FMN in *A. chroococcum* flavodoxin.

When compared with *D. vulgaris* flavodoxin it is interesting that the additional negatively charged residues in *A. chroococcum* flavodoxin are located mainly in the extra loops Gly⁶¹-Glu⁷¹ and Trp¹²⁹-Val¹⁴⁸. Mutations of the negatively charged residues in these loops need to be performed in order to test the hypothesis whether or not these extra loop residues in the flavodoxin from *A. chroococcum* are responsible for its low redox potential. A characteristic feature of the flavodoxins is the asymmetric distribution of the charged amino acid residues; the negatively charged residues are clustered around the FMN binding site, whereas no positively charged residues are observed in the vicinity of the isoalloxazine ring (Burnett, et al., 1974; Smith, et al., 1983; Watenpaugh, et al., 1973). For the flavodoxin of *A. chroococcum* 13 of the 29 acidic residues are located in the regions affected by the one-electron reduced FMN, whereas only one basic residue is located in these regions (Fig. 3.5). Positively charged residues are mainly located in helix α 1 (Fig. 3.5). Whether or not this is important for the stabilisation of the negatively charged FMN phosphate group, possibly in combination with the dipole moment of helix α 1 (Hol, et al., 1978), has to be investigated further. As no positively charged helix α 1 is observed in the flavodoxins from *D. vulgaris* and *A. nidulans* (Fig. 3.1b) (Stockman, et al., 1993; Watt, et al., 1991), the former seems not to be the case. On the other hand, this positively charged helix, in combination with the negatively charged cluster around the FMN, may play an important role in the formation of the electron-transfer complex, and thus for electron-transfer, with the Fe-protein of the nitrogenase enzyme system. For the electron transfer between flavodoxins and cytochrome *c*, electrostatic interactions were proven to be important (Simondson, et al., 1982; Weber and Tollin, 1985).

Indeed, electrostatic interactions are important for the complex formation between the flavodoxin and Fe-protein from *A. chroococcum*, as an increase in ionic strength leads to a weaker complex as the intensity of the uncomplexed flavodoxin amide resonances increase upon addition of KCl. Furthermore, the ¹⁵N chemical shifts of the flavodoxin amino acid residues involved in complex formation, return towards their uncomplexed chemical shift values (Fig. 3.7). Only a few flavodoxin chemical shift changes are observed upon titration of the flavodoxin with Fe-protein, and although they are small, they are significant. Larger effects would be expected if the Fe-protein were to have been in excess. However, for practical reasons this experiment could not be performed. It is interesting that the observed chemical shift changes all are located in the same part of the molecule, namely in the region of the

extra short loop Gly⁶¹-Glu⁷¹. This loop is located near the FMN binding site, since the amide resonances of the residues in this loop are affected by the one-electron reduced FMN (Fig. 3.5). Furthermore, this loop must be located at the surface of the protein, as most of the amide protons in this loop exchange within two hours after redissolving the protein in D₂O. The ¹⁵N chemical shifts of the amide of Ser⁶⁸ and the amino sidechains of Asn¹¹ and Asn⁷² significantly change when flavodoxin is titrated with Fe-protein. The residues Ser⁶⁸ and Asn⁷² both are located in the above mentioned extra loop, whereas Asn¹¹ is not. However, a clear NOE connectivity is observed between the amide proton of the extra loop residue Glu⁷¹ and one of the amino sidechain protons of Asn¹¹. It is therefore not unlikely that the sidechain of Asn¹¹ interacts with one of the extra loop residues via a hydrogen bond. The sidechain amino proton of Asn¹¹ exchanges within two hours after dissolving the protein in D₂O, and is therefore not involved in a strong hydrogen bond formation. The sidechain carbonyl oxygen on the other hand may form a hydrogen bond towards one of the extra loop amide protons. However, all the amide protons of Cys⁷⁰, Glu⁷¹ and Asn⁷² show fast exchange in D₂O, indicating that no strong hydrogen bond exists between the sidechain carbonyl oxygen of Asn¹¹ and any of these amide protons. The observation that the loop residues Ser⁶⁸ and Asn⁷² and the nearby Asn¹¹ are influenced upon the complexation of flavodoxin with Fe-protein indicates that this loop, which is missing in the shorter chain flavodoxins, must play an important role in the complex formation between flavodoxin and the nitrogenase enzyme system. For these residues only the ¹⁵N and not the ¹H chemical shifts change significantly, when Fe-protein is titrated. This indicates that the interaction of these residues with the Fe-protein is not via the amide and sidechain amino protons, but via the oxygen atoms of the backbone carbonyl of Ser⁶⁷ and the sidechain carbonyls of Asn¹¹ and Asn⁷². This hypothesis is reasonable, since interactions of acidic atoms are expected to be important for the complexation with Fe-protein, as the FMN is surrounded by acidic residues. For this reason, the acidic residues Glu⁶², Asp⁶⁹ and Glu⁷¹ in this extra loop may play an important role in the complex formation. However, due to the nature of a 2D ¹H-¹⁵N HSQC experiment the sidechain atoms of these residues can not be observed.

The flavodoxin from *Klebsiella pneumoniae* forms a stronger complex with its Fe-protein when MgADP is present (Thorneley and Deistung, 1988). The addition of MgADP shows an additional ¹⁵N chemical shift change for the three residues in *A. chroococcum* flavodoxin involved in complex formation with Fe-protein (Fig. 3.7),

indicating a change in the nature of this complex, possibly due to a stronger interaction. Especially, the sidechain amino group of Asn¹¹ is influenced by the addition of MgADP (Fig. 3.7). The binding of MgATP and MgADP to the Fe-protein results in a change in conformation of the protein which is accompanied by a decrease in the redox potential of the 4Fe4S cluster of the protein. The 2.9 Å resolution X-ray crystal structure of Fe-protein from *Azotobacter vinelandii* shows a nucleotide-binding site to be located at the subunit interface of the dimeric molecule (Georgiadis, et al., 1992). The change in stability of the flavodoxin-Fe-protein complex we observe most likely arises from a change in conformation of the Fe-protein resulting from MgADP binding at this site. Further studies have to be performed to elucidate the exact role of MgADP. Nevertheless, from this titration study it is clear that the extra short loop Gly⁶¹-Glu⁷¹ in the flavodoxin from *Azotobacter chroococcum* is of importance for the complexation with the Fe-protein of the nitrogenase enzyme complex, and therefore this loop may play an important role in the electron transfer to nitrogenase.

3.5 References

- Bagby, S., Barker, P., Hill, H.A.O., Eady, R.R. and Thorneley, R.N.F. (1991a) *Biochem. J.* **155**, 33-40.
- Bagby, S., Barker, P.D., Hill, H.A.O., Sanghera, G.S., Dunbar, B., Ashby, G.A., Eady, R.R. and Thorneley, R.N.F. (1991b) *Biochem. J.* **277**, 313-319.
- Bartels, C., Xia, T., Billeter, M., Güntert, P. and Wüthrich, K. (1995) *J. Biomol. NMR* **5**, 1-10.
- Bax, A. and Davis, D.G. (1985) *J. Magn. Reson.* **65**, 355-360.
- Bennet, L.T., Jacobson, M.R. and Dean, D.R. (1988) *J. Biol. Chem.* **263**, 1364-1369.
- Bloembergen, N. (1957) *J. Chem. Phys.* **27**, 572-573.
- Bodenhausen, G. and Ruben, D.J. (1980) *Chem. Phys. Lett.* **69**, 185-189.
- Burnett, R.M., Darling, G.D., Kendall, D.S., LeQuesne, M.E., Mayhew, S.G., Smith, W.W. and Ludwig, M.L. (1974) *J. Biol. Chem.* **249**, 4383-4392.
- Cavanagh, J., Palmer III, A.G., Wright, P.E. and Rance, M. (1991) *J. Magn. reson.* **91**, 429-436.
- Cavanagh, J. and Rance, M. (1990) *J. Magn. Reson.* **88**, 72-85.

- Clubb, R.T., Thanabal, V., Osborne, C. and Wagner, G. (1991) *Biochemistry* **30**, 7718-7730.
- Curley, G.P., Carr, M.C., Mayhew, S.G. and Voordouw, G. (1991) *Eur. J. Biochem.* **202**, 1091-1100.
- Deistung, J. and Thorneley, R.N.F. (1986) *Biochem. J.* **239**, 69-75.
- Dente, L., Cesareni, G. and Corteses, R. (1983) *Nucl. Acids Res.* **11**, 1645-1655.
- Deveraux, J., Haerberli, P. and Smithies, O. (1985) *Nucl. Acids Res.* **12**, 387-395.
- Eady, R.R., Richardson, T.H., Miller, R.W., Hawkins, M. and Lowe, D.J. (1988) *Biochem. J.* **256**, 189-196.
- Eriksson, M.A.L., Hård, T. and Nilsson, L. (1995) *Biophys. J.* **69**, 329-339.
- Evans, D.J., Jones, R., Woodley, P.R., Wilborn, J.R. and Robson, R.L. (1991) *J. Bacteriol.* **173**, 5457-5469.
- Frenkiel, T., Bauer, C., Carr, M.D., Birdsall, B. and Feeney, J. (1990) *J. Magn. Reson.* **90**, 420-425.
- Fritz, J., Müller, F. and Mayhew, S.G. (1973) *Helv. Chim. Acta* **56**, 2250-2254.
- Fukuyama, K., Wakabayashi, S., Matsubara, H. and Rogers, L.J. (1990) *J. Biol. Chem.* **265**, 15804-15812.
- Georgiadis, M.M., Komiya, H., Chakrabarti, P., Woo, D., Kornuc, J.J. and Rees, D.C. (1992) *Science* **257**, 1653-1659.
- Griesinger, C., Otting, G., Wüthrich, K. and Ernst, R.R. (1988) *J. Am. Chem. Soc.* **110**, 7870-7872.
- Grzesiek, S. and Bax, A. (1992a) *J. Am. Chem. Soc.* **114**, 6291-6293.
- Grzesiek, S. and Bax, A. (1992b) *J. Magn. Reson.* **99**, 201-207.
- Grzesiek, S. and Bax, A. (1992c) *J. Magn. Reson.* **96**, 432-440.
- Grzesiek, S. and Bax, A. (1993) *J. Biomol. NMR* **3**, 185-204.
- Güntert, P. and Wüthrich, K. (1992) *J. Magn. Reson.* **96**, 403-407.
- Hol, W.G.J., Duijnen van, P.T. and Berendsen, H.J.C. (1978) *Nature* **273**, 443-446.
- Ikura, M., Bax, A., Clore, G.M. and Gronenborn, A.M. (1990) *J. Am. Chem. Soc.* **112**, 9020-9022.
- Jahnke, W. and Kessler, H. (1994) *J. Biomol. NMR* **4**, 735-740.
- Jones, R., Woodley, P. and Robson, R.L. (1984) *Mol. Gen. Genet.* **197**, 318-327.
- Kay, L.E., Keifer, P. and Saarinen, T. (1992) *J. Am. Chem. Soc.* **114**, 10663-10665.
- Kim, J. and Rees, C.R. (1994) *Biochemistry* **33**, 389-397.
- Kontaxis, G., Stonehouse, J., Laue, E.D. and Keeler, J. (1994) *J. Magn. Reson. A* **111**, 70-76.

- Ludwig, M.L., Burnett, R.M., Darling, G.D., Jordan, S.R., Kendall, D.S. and Smith, W.W. (1976) in *Flavins and Flavoproteins* (Singer, T.P., Ed.) pp. 393-404, Elsevier, Amsterdam.
- Marion, D., Driscoll, P.C., Kay, L.E., Wingfield, P.T., Bax, A., Gronenborn, A.M. and Clore, G.M. (1989a) *Biochemistry* **28**, 6150-6156.
- Marion, D., Ikura, M. and Bax, A. (1989b) *J. Magn. Reson.* **84**, 425-430.
- Marion, D., Ikura, M., Tschudin, R. and Bax, A. (1989c) *J. Magn. Reson.* **85**, 393-399.
- Marion, D. and Wüthrich, K. (1983) *Biochem. Biophys. Res. Commun.* **113**, 967-724.
- Mayhew, S.G. and Tollin, G. (1992) in *Chemistry and Biochemistry of Flavoenzymes* (Müller, F., Ed.) pp. 389-426, CRC Press, Boca Raton.
- Mierlo van, C.P.M., Müller, F. and Vervoort, J. (1990a) *Eur. J. Biochem.* **189**, 589-600.
- Mierlo van, C.P.M., Sanden van der, B.P.J., Woensel van, P., Müller, F. and Vervoort, J. (1990b) *Eur. J. Biochem.* **194**, 199-216.
- Orengo, C.A., Jones, D.T. and Thornton, J.M. (1994) *Nature* **372**, 631-634.
- Palmer III, A.G., Cavanagh, J., Wright, P.E. and Rance, M. (1991) *J. Magn. Reson.* **93**, 151-170.
- Peelen, S. and Vervoort, J. (1994) *Arch. Biochem. Biophys.* **314**, 291-300.
- Sanger, F., Nicklen, S. and Coulson, A.R. (1977) *Proc. Natl. Acad. Sci. USA* **82**, 1074-1078.
- Simondson, R.P., Weber, P.C., Salemne, F.R. and Tollin, G. (1982) *Biochemistry* **21**, 6366-6375.
- Smith, W.W., Burnett, R.M., Darling, G.D. and Ludwig, M.L. (1977) *J. Mol. Biol.* **117**, 195-225.
- Smith, W.W., Patridge, K.A., Ludwig, M.L., Petsko, G.A., Tsernoglou, D., Tanaka, M. and Yasanobu, K.T. (1983) *J. Mol. Biol.* **165**, 737-755.
- Solomon, I. (1955) *Phys. Rev.* **99**, 559-565.
- Stockman, B.J., Euvrard, A., Kloosterman, D.A., Scahill, T.A. and Swenson, R.P. (1993) *J. Biomol. NMR* **3**, 133-149.
- Stockman, B.J., Krezel, A.M., Markley, J.L., Leonhardt, K.G. and Strauss, N.A. (1990) *Biochemistry* **29**, 9600-9609.
- Stonehouse, J., Shaw, G.L., Keeler, J. and Laue, E.D. (1994) *J. Magn. Reson. A* **107**, 178-184.
- Tabor, S. and Richardson, C.C. (1985) *Proc. Natl. Acad. Sci. USA* **82**, 1074-1078.
- Thorneley, R.N.F. and Deistung, J. (1988) *Biochem. J.* **253**, 587-595.
- Vuister, G.W. and Bax, A. (1993) *J. Am. Chem. Soc.* **115**, 7772-7777.
- Vuister, G.W., Kim, S.-J., Wu, C. and Bax, A. (1994) *Biochemistry* **33**, 10-16.

- Watenpaugh, K.D., Sieker, L.C. and Jensen, L. (1973) *Proc. Natl. Acad. Sci. USA* **70**, 3857-3860.
- Watt, W., Tulinsky, A., Swenson, R.P. and Watenpaugh, K.D. (1991) *J. Mol. Biol.* **218**, 195-208.
- Weber, P.C. and Tollin, G. (1985) *J. Biol. Chem.* **260**, 5568-5573.
- Wishart, D.S., Bigam, C.G., Yao, J., Abildgaard, F., Dyson, H.J., Oldfield, E., Markley, J.L. and Sykes, B.D. (1995) *J. Biomol. NMR* **6**, 135-140.
- Wishart, D.S. and Sykes, B.D. (1994) *J. Biomol. NMR* **4**, 171-180.
- Wishart, D.S., Sykes, B.D. and Richards, F.M. (1992) *Biochemistry* **31**, 1647-1651.
- Wüthrich, K. (1986) *NMR of proteins and nucleic acids*, Wiley & Sons Inc., New York.
- Yates, M.G. (1972) *FEBS Letters* **27**, 63-67.
- Zhou, Z. and Swenson, R.P. (1995) *Biochemistry* **34**, 3183-3192.
- Zuiderweg, E.R.P. and Fesik, S.W. (1989) *Biochemistry* **28**, 2387-2391.

4

¹⁹F-NMR study on the pH-dependent regioselectivity and rate of the *ortho*-hydroxylation of 3-fluorophenol by phenol hydroxylase from *Trichosporon cutaneum*: Implications for the reaction mechanism

Sjaak Peelen, Ivonne M.C.M. Rietjens, Willem J.H. van Berkel, Wilbert A.T. van Workum and Jacques Vervoort

Published in *European Journal of Biochemistry* **218** (1993), 345-353.

The regioselectivity and rate of the ortho-hydroxylation of 3-fluorophenol by phenol hydroxylase from Trichosporon cutaneum (EC 1.14.13.7) was studied using ¹⁹F-NMR. The regioselective hydroxylation as well as the rate of ortho-hydroxylation are pH-dependent with a pK_a of 6.5. At pH values below 6.5, 3-fluorophenol preferentially becomes hydroxylated at the C6 ortho position, resulting in a maximum C6 to C2 hydroxylation ratio of 6.7. Upon increasing the pH the total rate of conversion increases. Also, the C2 ortho-hydroxylation increases relatively to the C6 ortho-hydroxylation and yields a minimum C6/C2 hydroxylation ratio of 2.2 at pH values above 7.5.

Based on data from ¹⁹F-NMR binding studies and molecular orbital calculations, a hypothesis is put forward which explains the pH-dependent effects observed. A mechanism is proposed involving an active site amino acid residue acting as a base in the reduced form of the protein. Deprotonation of this residue results in hydrogen bond formation with the hydroxyl moiety of the phenolic substrate, leading to (partial) deprotonation of the substrate. Molecular orbital

calculations demonstrate that such a (partial) deprotonation increases (a) the overall reactivity of 3-fluorophenol for an electrophilic attack and (b) the reactivity of C2 relative to the C6 position. The hypothesis may explain the decrease in the C6/C2 hydroxylation ratio. Furthermore the increased amount of ortho-hydroxylated products formed with increasing pH can also be explained by this hypothesis.

4.1 Introduction

Phenol hydroxylase from *Trichosporon cutaneum* is one of the many flavin-dependent aromatic hydroxylases (Berkel van and Müller, 1991). The enzyme catalyses the conversion of phenol to 1,2-dihydroxybenzene (catechol). The monooxygenase phenol hydroxylase is a homodimer (molecular mass 152 kDa), each subunit containing a non-covalently bound FAD (Sejlitz and Neujahr, 1987). Unlike most bacterial flavin-dependent aromatic hydroxylases, eukaryotic phenol hydroxylase shows a rather broad substrate specificity. In addition to the parent substrate phenol, the enzyme also catalyses the hydroxylation of various substituted phenols such as *o*-, *m*- and *p*-fluorophenol, *m*- and *p*-chlorophenol, aminophenols, dihydroxybenzenes and cresol (Neujahr, 1991; Neujahr and Gaal, 1973).

The catalytic mechanism of the enzyme is reported to proceed by formation of a C(4a)-hydroperoxyflavin intermediate, formed upon two-electron reduction of the flavin prosthetic group by NADPH and incorporation of an oxygen molecule (Detmer and Massey, 1984; Neujahr, 1991). The mechanism by which the C(4a)-hydroperoxyflavin intermediate converts the substrate to its hydroxylated form is supposed to proceed analogously to the mechanism for other aromatic hydroxylases, i.e. by an electrophilic attack of the peroxide function on the substrate (Anderson, et al., 1987; Anderson, et al., 1991; Detmer and Massey, 1985; Entsch, et al., 1976; Kemal and Bruice, 1979). The nature in which the substrate reacts, however, is still a matter of debate. Despite the availability of the recently determined amino acid sequence (Kälin, et al., 1992), it is not clear which amino acid residues participate in catalysis. Binding of phenol was reported to be favored at higher pH values, and it was suggested that the substrate is bound in the phenolate form (Mörtberg and Neujahr, 1988; Neujahr, 1991). In contrast to this Detmer and Massey, based on binding experiments with the substrate analogue 4-nitrophenol at pH 7.1, concluded that the

substrate analogue is bound to the oxidized enzyme in its neutral form (Detmer and Massey, 1985). The ionisation state in which the substrate is bound to the enzyme could have implications for its conversion, because deprotonation of the hydroxyl moiety may result in activation of the substrate for electrophilic attack (Detmer and Massey, 1985; Vervoort, et al., 1992). For the related 4-hydroxybenzoate hydroxylase such an activation of the substrate by an active site tyrosine has been observed (Entsch, 1991). Molecular orbital calculations suggest that this activation originates from (a) an increase of the HOMO (highest occupied molecular orbital) electron density on the reaction centre C3 in the 4-hydroxybenzoate and (b) an increase in the energy of the HOMO electrons of the 4-hydroxybenzoate upon deprotonation, both phenomena favoring an electrophilic attack on C3 (Vervoort, et al., 1992). Thus, the theoretical reactivity of the reaction centres of a substrate molecule towards an electrophilic attack by the C(4a)-hydroperoxyflavin enzyme intermediate varies with the protonation state of the substrate. In analogy, ionisation of phenolic substrates of phenol hydroxylase may also influence their HOMO density distribution and, as a result, the relative reactivity of the various carbon centres in the phenol for electrophilic attack during conversion in the active site of phenol hydroxylase. This concept was used as a working hypothesis in the present study in order to obtain insight into the nature in which substrates are converted by phenol hydroxylase. To discriminate between the two possible sites for *ortho*-hydroxylation, 3-fluorophenol was used as the model substrate. Because the van der Waals radius of a fluorine substituent (0.135 nm) nearly equals that of a proton substituent (0.120 nm), possible differences in hydroxylation at the C2 and C6 *ortho* position in 3-fluorophenol are unlikely to result from sterical hindrance by the fluorine substituent at C3. Using this fluorinated substrate, hydroxylation by phenol hydroxylase was studied using ¹⁹F-NMR. Furthermore, binding characteristics of 3- and 4-fluorophenol to the enzyme were also studied using ¹⁹F-NMR.

4.2 Materials and methods

Chemicals. 2-Fluorophenol, 3-fluorophenol and 4-fluorophenol were purchased from Janssen Chimica (Beerse Belgium). NADPH and 1,4-dithiothreitol were purchased from Boehringer, FAD from Sigma and EDTA and ascorbate from Merck.

Enzyme purification. Phenol hydroxylase was isolated from the yeast *Trichosporon cutaneum*, essentially as described by Sejlitz and Neujahr (1987). The final preparation had a specific activity of 6.0 $\mu\text{mol NADPH oxidized}\cdot\text{min}^{-1}\cdot\text{mg protein}^{-1}$ and was over 90 % pure as judged by SDS/PAGE. The enzyme preparation contained no catechol oxygenase activity as only diol products were observed in hydroxylation studies.

Protein concentration was determined by the method of Lowry et al. (1951) using bovine serum albumin as the standard. For ^{19}F -NMR binding studies the enzyme concentration was determined from recording visible absorption spectra, using a molar absorption coefficient of $12.6\text{ mM}^{-1}\cdot\text{cm}^{-1}$ at 442 nm for protein-bound FAD (Neujahr, 1991).

Hydroxylation reactions. Hydroxylation reactions were carried out in closed reaction vessels to prevent evaporation of the substrate and contained (final concentrations) 50 mM potassium phosphate of varying pH (5.5-9.0, as indicated), 10 μM FAD, 1 mM 1,4-dithiothreitol, 0.1 mM EDTA, 1 mM 3-fluorophenol, 85 nM phenol hydroxylase and 2 mM ascorbate to prevent auto-oxidation of the fluorodihydroxybenzenes formed. The reaction was started by the addition of 0.17 mM NADPH. Reactions were carried out at 25 °C for 15 min and terminated by freezing the samples in liquid nitrogen. Under these conditions the reaction was linear in time. The samples were analysed using ^{19}F -NMR.

^{19}F -NMR. ^{19}F -NMR analysis of either 3-fluorophenol or 4-fluorophenol bound to oxidized or reduced phenol hydroxylase was performed using samples containing the highest possible concentration of enzyme (250 and 500 μM) and a one- or two-fold molar excess of 3- or 4-fluorophenol (it should be mentioned that, as the enzyme is a homodimer, the FAD concentration is twice the enzyme concentration). Exact concentrations for each experiment are indicated in the legend of each spectrum presented. Reduction of the enzyme was achieved by making the samples anaerobic by at least four cycles of evacuation and filling with argon, followed by the addition of three- to ten-fold molar excess of NADPH or dithionite.

After each ^{19}F -NMR analysis the protein was brought into the newly required buffer and made free of substrate and other added compounds by passing it twice over a Bio-gel P6 DG column equilibrated with 100 mM potassium phosphate buffer of the required pH containing 1 mM 1,4-dithiothreitol, 0.1 mM EDTA and 10 μM FAD. The collected protein fractions were concentrated over an Amicon YM 30 filter and used for the next ^{19}F -NMR binding experiment.

¹⁹F-NMR measurements were performed on a Bruker AMX 300 NMR spectrometer. Norell (Landisville, NJ, USA) 10-mm NMR tubes were used. The sample volume was 1.71 ml, containing 100 μ l ²H₂O for locking the magnetic field and 10 μ l 8.4 mM 4-fluorobenzoic acid, which served as an internal standard. Proton decoupling was achieved with the Waltz-16 pulse sequence (Shaka, et al., 1983) at -18 dB from 50 W. Nuclear Overhauser effects were eliminated using the inverse gated decoupling technique. Spectra were obtained with 25-30° pulses (5 μ s), a 50-kHz spectral width, 16k data points, repetition time of 1 s, quadrature phase detection and quadrature phase cycling (CYCLOPS). Between 5000 and 60 000 scans were recorded, depending on the concentration of the products and the signal/noise ratio required. Chemical shifts are reported relative to CFCl₃.

Molecular orbital computer calculations. Computer calculations were carried out on a Silicon Graphics Iris 4D/85 with Quanta/Charmm (Molecular Simulations, UK). The semi-empirical molecular orbital method was used, applying the AM1 Hamiltonian from the AMPAC program (Quantum Chemistry Program exchange no. 506; Indiana University, Bloomington, IN, USA). All calculations were carried out with PRECISE criteria. For all calculations the self-consistent field was achieved. Geometries were optimised for all bond lengths, bond angles and torsion angles with the Fletcher-Powell criteria. Frontier orbital densities for electrophilic attack were calculated from HOMO and HOMO-1 characteristics, using the equation given by Fukui et al. (1954).

4.3 Results

4.3.1 Regioselectivity of hydroxylation

Fig. 4.1 presents the ¹⁹F-NMR spectra of the incubations of phenol hydroxylase with 3-fluorophenol as the substrate at various pH values. The ¹⁹F-NMR resonances of the *ortho*-hydroxylated products formed, 3-fluoro-1,2-dihydroxybenzene and 4-fluoro-1,2-dihydroxybenzene, were identified on the basis of the ¹⁹F-NMR analysis of phenol hydroxylase incubations with respectively 2-fluorophenol and 4-fluorophenol (Fig. 4.2). Phenol-hydroxylase-dependent conversion of 2-fluorophenol results in formation of a fluoride anion (resulting from hydroxylation at the fluorinated position) but also in formation of a product at -140.4 ppm, identical to

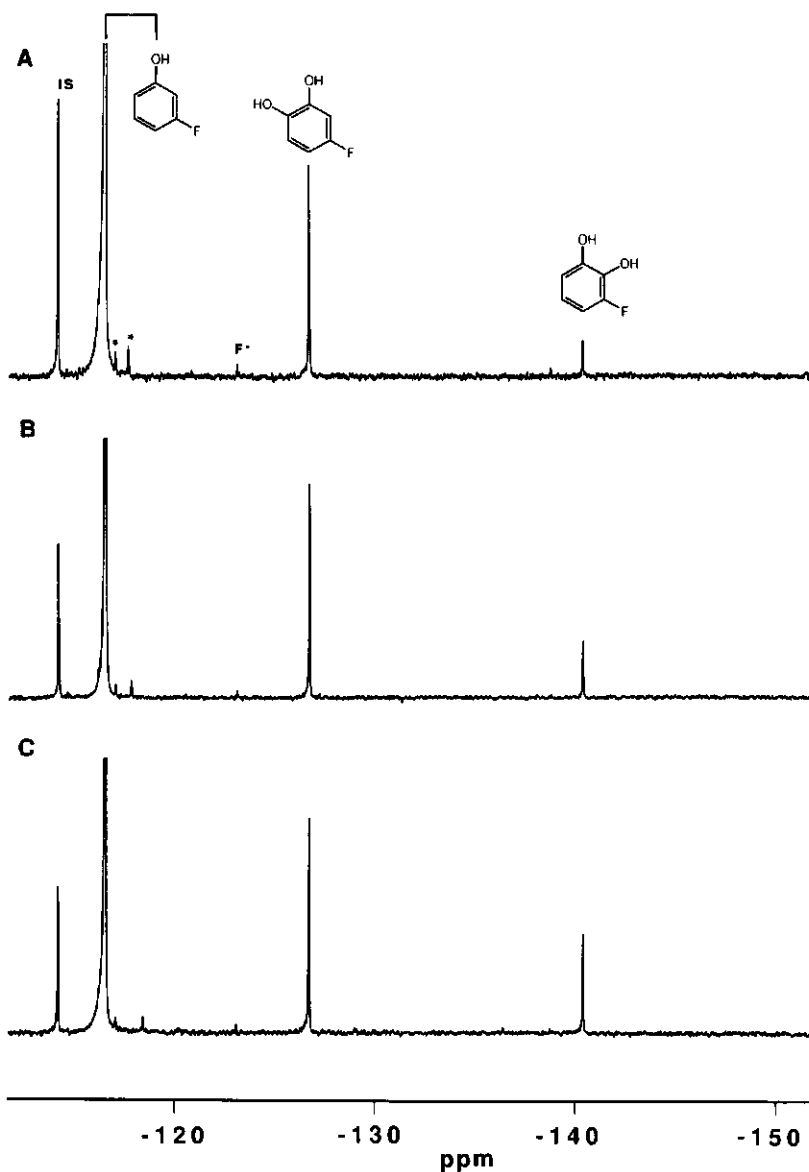


Fig. 4.1. ^{19}F -NMR spectra of the conversion of 3-fluorophenol at (A) pH 6.0, (B) pH 6.5, (C) pH 7.5 by phenol hydroxylase. The resonance marked IS is from the internal standard, 4-fluorobenzoate. The resonances marked with an asterisk are small impurities.

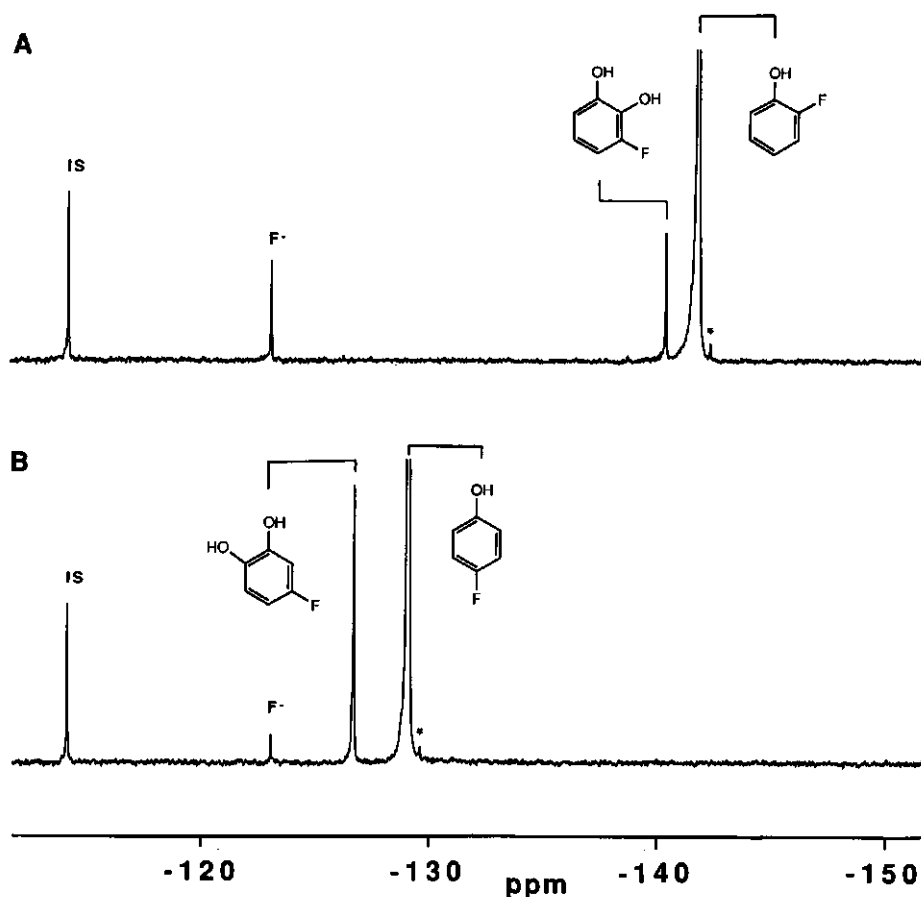


Fig. 4.2. ¹⁹F-NMR spectra of the conversion of (A) 2-fluorophenol and (B) 4-fluorophenol by phenol hydroxylase. The resonance marked IS is from the internal standard, 4-fluorobenzoate. The resonance marked with an asterisk is a small impurity.

the resonance observed in the spectrum from 3-fluorophenol (Fig. 4.2A). Based on the phenol-hydroxylase-dependent formation of the -140.4 ppm product from both 2- and 3-fluorophenol, this resonance is ascribed to 3-fluoro-1,2-dihydroxybenzene. In a similar way, based on the results presented in Fig. 4.1 and Fig. 4.2B, the resonance at -126.7 ppm is ascribed to 4-fluoro-1,2-dihydroxybenzene.

The spectra presented in Fig. 4.1 show that the regioselectivity of the 3-fluorophenol hydroxylation by phenol hydroxylase varies with pH. At pH 6.0 preferential hydroxylation at C6, leading to formation of 4-fluoro-1,2-dihydroxybenzene, is observed (Fig. 4.1A). Only a small amount of 3-fluoro-1,2-dihydroxybenzene, the C2 hydroxylation product, is formed. With increasing pH, the amount of 3-fluoro-1,2-dihydroxybenzene increases relative to the amount of 4-fluoro-1,2-dihydroxybenzene (Fig. 4.1B, C). Fig. 4.3A clearly shows that the regioselectivity of the hydroxylation of 3-fluorophenol changes with pH and that the preference for C6 hydroxylation decreases with increasing pH.

The results presented in Fig. 4.3A point at a protonation-deprotonation equilibrium which influences the regioselectivity of the 3-fluorophenol *ortho*-hydroxylation by phenol hydroxylase. Because the pK_a value for free 3-fluorophenol is 9.3 (Brown, et al., 1955), the pH effect depicted in Fig. 4.3A is likely to be due to the deprotonation of a group in the active site of the enzyme, influencing the hydroxylation of 3-fluorophenol. Assuming that this group regulates the deprotonation of 3-fluorophenol in the active site, Eqn (4.1) can be used. A similar equation, assuming one pK_a , has been used by Detmer and Massey (1985) for the change in the rate of formation of the so-called enzyme intermediate II from I and III from II during the conversion of resorcinol by phenol hydroxylase as a function of pH.

$$\frac{C6}{C2} = \frac{\left(\frac{C6}{C2}\right)_{\max}}{\frac{K_a}{[H^+]} + 1} + \frac{\left(\frac{C6}{C2}\right)_{\min}}{\frac{[H^+]}{K_a} + 1} \quad (4.1)$$

C6/C2 represents the ratio of the two *ortho*-hydroxylation products, $(C6/C2)_{\max}$ is the maximum value of C6/C2 at low pH and $(C6/C2)_{\min}$ is the minimum value of C6/C2 at high pH. Fitting of the data points in Fig. 4.3A by Eqn. 4.1 creates the curve presented in the figure, with an apparent pK_a of 6.5 and maximum and minimum C6/C2 ratios of 6.7 and 2.2, respectively.

In addition to the decrease in the C6/C2 hydroxylation ratio with increasing pH, the ^{19}F -NMR spectra presented in Fig. 4.1 also show an increase in the total amount of *ortho*-hydroxylation products formed with increasing pH. Fig. 4.3B gives a more detailed presentation of the effect of pH on the total amount of products formed. Combination of the results presented in Fig. 4.3A and B demonstrates that at pH 7.5,

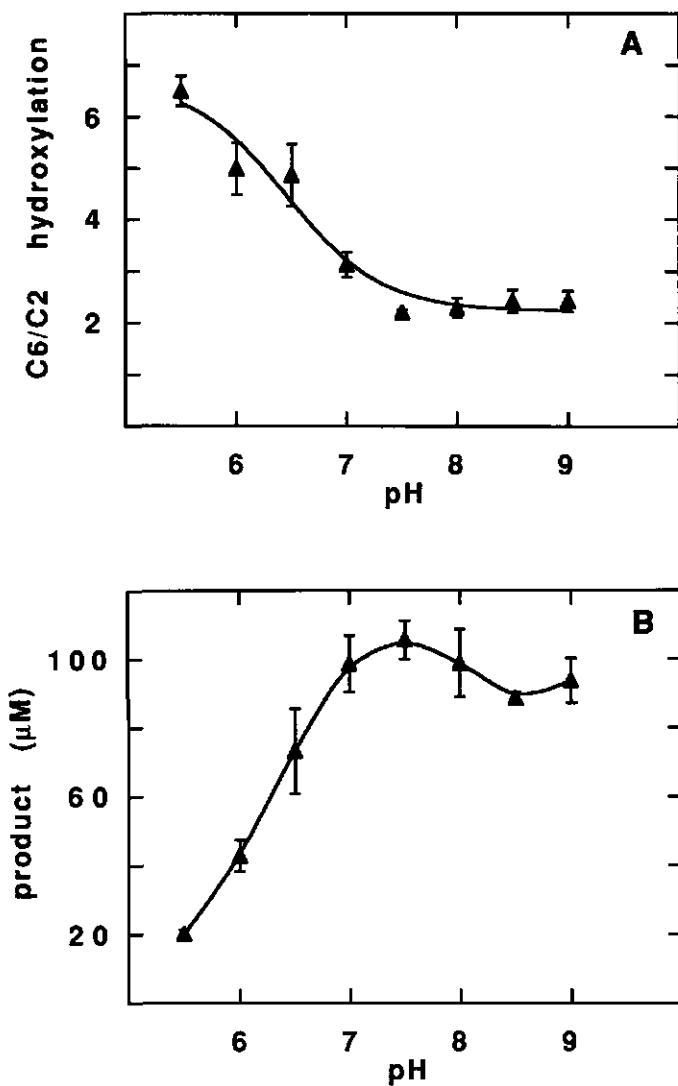


Fig. 4.3. (A) Ratio ortho-C6/ortho-C2 hydroxylation of 3-fluorophenol by phenol hydroxylase at increasing pH. (B) The amount of product formed by 0.14 nmol phenol hydroxylase after 15 min at 25 °C as a function of pH. Values presented are the mean \pm standard error of the mean of three independent measurements.

the C6/C2 ratio reaches a minimum value of 2.2 at a maximal rate of product formation.

4.3.2 NMR binding studies

From the data presented above it is evident that the enzyme shows a preferential *ortho* C6 over *ortho* C2 hydroxylation of 3-fluorophenol and a decrease in the C6/C2 hydroxylation ratio with increasing pH. In theory, these phenomena might be caused by binding of 3-fluorophenol in the active site in different orientations, leading to either C6 or C2 hydroxylation with the relative contribution of the orientations varying with pH. To investigate this possibility, ^{19}F -NMR spectra of oxidized and reduced phenol hydroxylase in the presence of 3-fluorophenol were recorded (Fig. 4.4). At pH 7.6 in the presence of oxidized phenol hydroxylase, 3-fluorophenol gives rise to a resonance at -116.4 ppm and a broad resonance at -112.4 ppm (Fig. 4.4A). The resonance at -116.4 ppm represents free 3-fluorophenol (cf. Fig. 4.1). Close comparison of the ^{19}F -NMR signal of free and bound 3-fluorophenol (Fig. 4.4A), demonstrates that the line width of free 3-fluorophenol is broadened from 5-8 Hz in the absence of protein to about 90 Hz in the presence of phenol hydroxylase. This line broadening in the presence of phenol hydroxylase arises from the fact that the 3-fluorophenol in solution is in equilibrium with the 3-fluorophenol bound to the enzyme. Because the rate of exchange is slow relative to the time scale of the NMR measurement, the free and protein bound fraction can be observed separately. Thus, the broad resonance at -112.4 ppm represents 3-fluorophenol bound to the protein. This broad resonance has no clear homogeneous Lorentzian line shape. Instead, a shoulder is observed at the low-field side of the resonance (Fig. 4.4A). This may point to the presence of two different orientations (which are not populated equally) of 3-fluorophenol bound to the active site of the oxidized enzyme at pH 7.6.

Fig. 4.4B presents the ^{19}F -NMR spectrum obtained from 3-fluorophenol when added to phenol hydroxylase in its reduced form in the absence of oxygen. A broad Lorentzian-type resonance at -113.4 ppm can be observed. If in the reduced form of the enzyme 3-fluorophenol is still bound in two different orientations their ^{19}F chemical shifts can apparently no longer be resolved (i.e. the chemical shift difference is $< 1-2$ ppm). On the other hand another explanation for the single (broad) Lorentzian-type resonance of 3-fluorophenol bound to the reduced form of the

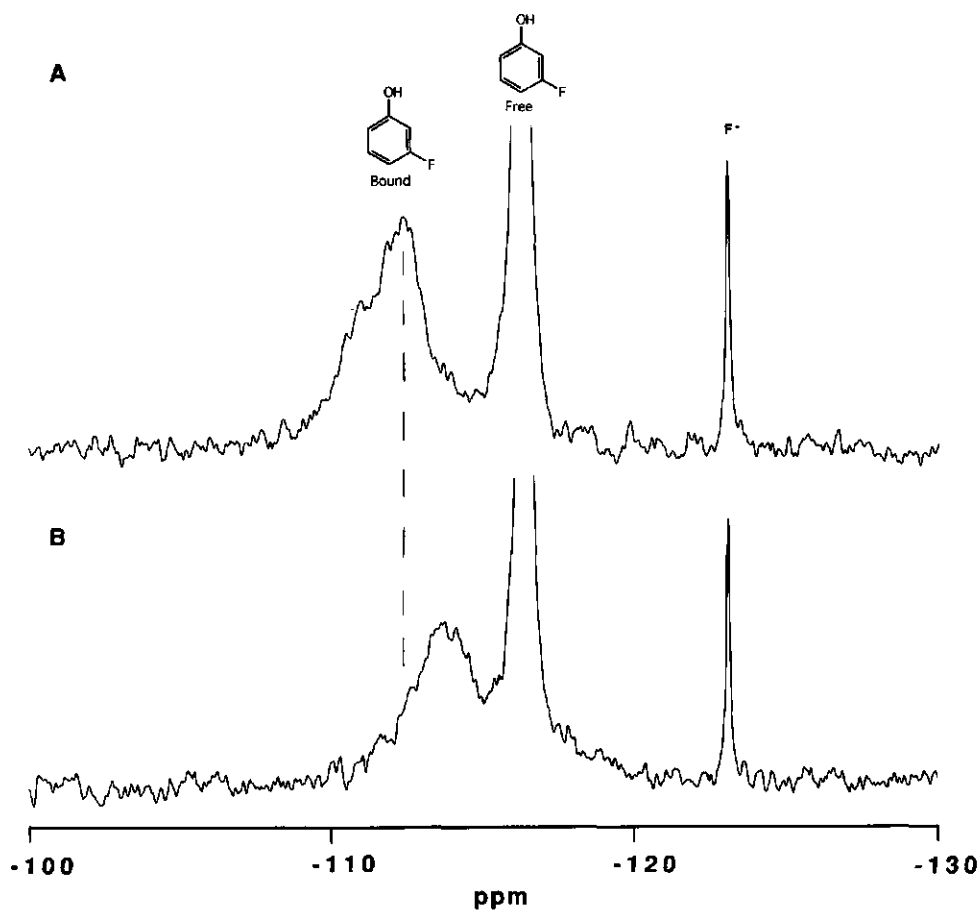


Fig. 4.4. ¹⁹F-NMR spectra of 500 μM 3-fluorophenol in the presence of 234 μM phenol hydroxylase in 100 mM potassium phosphate pH 7.6. (A) oxidized enzyme; (B) enzyme reduced by 2 mM NADPH.

enzyme at pH 7.6 (Fig. 4.4B) may be the existence of two fast (as compared to the maximum turnover rate for the conversion of 3-fluorophenol, i.e. 7 s⁻¹ (Neujahr and Kjellén, 1978)) interconverting conformations. In this case the line broadening results from phenomena like chemical shift anisotropy, dipole relaxation with other nuclear spins, exchange between free and bound substrate and flip-flop exchange between

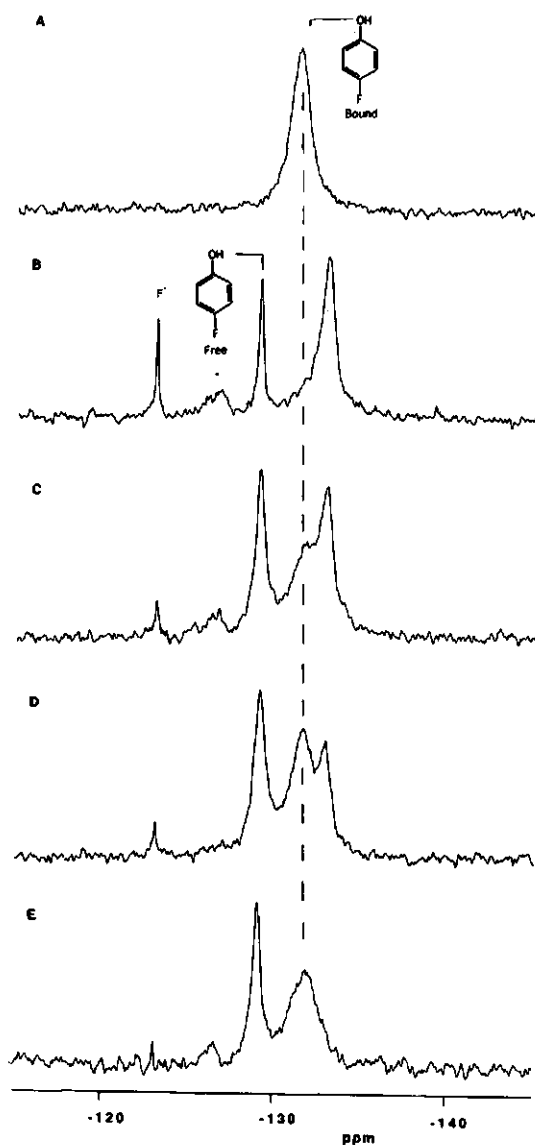


Fig. 4.5. ^{19}F -NMR spectra of 4-fluorophenol in the presence of phenol hydroxylase in 100 mM potassium phosphate. (A) 335 μM oxidized enzyme, 358 μM 4-fluorophenol, pH 7.6; (B) 265 μM reduced enzyme, 564 μM 4-fluorophenol, pH 7.6; (C) 283 μM reduced enzyme, 585 μM 4-fluorophenol, pH 6.6; (D) 321 μM reduced enzyme, 697 μM 4-fluorophenol, pH 6.4; (E) 232 μM reduced enzyme, 497 μM 4-fluorophenol, pH 6.2. The resonance marked with an asterisk presents a small amount of product formed.

the two binding orientations (Hull and Sykes, 1975).

Further comparison of Fig. 4.4B with Fig. 4.4A shows that reduction of the enzyme results in an about 1 ppm upfield shift of the ¹⁹F-NMR signal of the protein-bound substrate relative to the oxidized state. Because deprotonation of free 3-fluorophenol in solution also results in a 1.3 ppm upfield shift (results not shown), this upfield shift may be ascribed to (partial) deprotonation of the enzyme-bound 3-fluorophenol. The upfield shift of the ¹⁹F-NMR signal of the protein-bound 3-fluorophenol, however, may also result from a change in its protein surroundings. To study this possibility in more detail, the interaction of phenol hydroxylase with 4-fluorophenol (pK_a 10.0 (Brown, et al., 1955)) was studied. Free in solution, this substrate shows a more pronounced effect of deprotonation on its ¹⁹F-NMR signal, namely a 6.6 ppm upfield shift, than does 3-fluorophenol (results not shown).

Fig. 4.5A shows the ¹⁹F-NMR spectrum of 4-fluorophenol bound to oxidized phenol hydroxylase at pH 7.6. Upon binding of 4-fluorophenol to the oxidized enzyme its resonance shifts from -129.1 ppm (free 4-fluorophenol) to higher field by 2.3 ppm, resulting in a protein-bound-substrate peak at -131.4 ppm (Fig. 4.5A). From Fig. 4.5A and 4A it is clear that the ¹⁹F-NMR chemical shifts of 3- and 4-fluorophenol move in opposite directions upon binding of the substrate to the active site of the enzyme. This suggests that the change in the shift occurring upon binding of the compounds to the active site of the protein results from a change in chemical surroundings of their fluoro substituent and not from an effect on the protonation state of their hydroxyl moiety upon binding. If the latter were the case both substrates would have demonstrated an upfield shift of their ¹⁹F-NMR resonance upon binding to the oxidized form of the enzyme; this is not observed.

The ¹⁹F-NMR spectrum of 4-fluorophenol with oxidized phenol hydroxylase is identical at pH 7.6 and pH 6.2, indicating that, for the oxidized form of the enzyme, no change in the type of binding interaction occurs with a change in pH.

For the reduced state of the protein in the absence of oxygen, however, a different conclusion emerges. In the presence of reduced phenol hydroxylase at pH 7.6, the protein-bound 4-fluorophenol resonance shifts 1.6 ppm to higher field as compared to the substrate bound to the oxidized enzyme, resulting in a resonance at -133.0 ppm (Fig. 4.5B). This phenomenon is similar to the effect observed for the ¹⁹F-NMR resonance of 3-fluorophenol when bound to the reduced, compared to the oxidized, form of the enzyme at pH 7.6 (Fig. 4.4A and B). This similar effect of enzyme reduction on the ¹⁹F-NMR chemical shift of bound 3- and 4-fluorophenol

most likely arises from a comparable effect of the reduced enzyme on both substrates. A similar effect of enzyme reduction on the protein environment of both a C3 and a C4 fluoro substituent in the phenol molecule, influencing their chemical shift in a similar way, seems unlikely. This common upfield shift of the ^{19}F -NMR resonance of both 3- and 4-fluorophenol upon reduction of the enzyme could be explained by (partial) deprotonation of the substrates upon reduction of the phenol hydroxylase at pH 7.6. The actual chemical shift differences observed for the enzyme-bound 3- and 4-fluorophenol upon enzyme reduction are 1.0 ppm and 1.6 ppm, respectively, whereas the changes in chemical shift upon deprotonation of the free substrate show a larger difference between the two substrates, i.e. 1.3 ppm versus 6.6 ppm. Thus, either the extent of partial deprotonation is different for the two substrates, or there is an additional effect of a change in the protein surroundings on the fluorine substituents of the phenol substrates upon reduction of the enzyme. However, additional ^{19}F -NMR binding experiments of 4-fluorophenol bound to the reduced protein at varying pH further support the conclusion that the changes in shift upon reduction of the enzyme are at least in part due to deprotonation of the substrate. When the pH of the sample with reduced phenol hydroxylase and 4-fluorophenol is lowered stepwise from 7.6 to 6.2 (Fig. 4.5B-E), the 4-fluorophenol resonance at -133.0 ppm gradually shifts to -131.4 ppm (pH 6.2, Fig. 4.5E), i.e. a value similar to the ^{19}F -NMR chemical shift of the compound bound to the oxidized form of the protein (Fig. 4.5A). The spectra of the 4-fluorophenol bound to reduced phenol hydroxylase at intermediate pH values demonstrate both peaks at varying ratio (Fig. 4.5C and D). The results indicate that the effects of the pH on the ^{19}F -NMR chemical shift values shown in Fig. 4.5 are due, at least in part, to deprotonation of the fluorophenol substrates in the reduced form of the enzyme at pH 7.6. Furthermore they indicate the presence of the substrates in their protonated form in the reduced form of the enzyme at low pH as well as in the oxidized form of the enzyme at both pH 6.2 and 7.6. Clearly the reduced form of the enzyme demonstrates a pH-dependent effect on the ^{19}F -NMR chemical shift of the 4-fluorophenol bound to the active site. The changes occur in the same pH region as the changes observed for the regioselectivity and rate of the 3-fluorophenol hydroxylation (Fig. 4.3). This strongly suggests that these phenomena originate from the protonation/deprotonation of an active site amino acid residue.

4.3.3 Molecular orbital calculations

Molecular orbital calculations in combination with frontier orbital theory (Fleming, 1976) could provide insight into the reactivity of the C2 and C6 positions in 3-fluorophenol for electrophilic attack by the presumed C(4a)-hydroperoxyflavin intermediate of phenol hydroxylase. Molecular orbital calculations were performed to investigate whether a (partial) deprotonation of the substrate, implied by the results from the ¹⁹F-NMR binding studies, could explain the effects on regioselectivity and activity of the 3-fluorophenol conversion.

Table 4.1 presents the calculated HOMO and Coulomb characteristics of 3-fluorophenol and its phenolate anion which are of importance for an electrophilic attack (Fleming, 1976) by the enzyme peroxy-intermediate. Because the difference in energy between the HOMO and HOMO-1 of 3-fluorophenol is relatively small, 0.54 eV, the HOMO-1 density may also contribute to reactivity of the centres for electrophilic attack (Fukui, et al., 1954). Therefore, in addition to the HOMO characteristics, Table 4.1 also presents the frontier electron density distributions for electrophilic attack, calculated from the HOMO and HOMO-1 density distributions as described by Fukui et al. (1954).

From the calculations it is clear that both forms of 3-fluorophenol vary significantly in their HOMO density distribution on C2 and C6. For the neutral 3-fluorophenol the HOMO density on C6 is about seven times that on C2 (Table 4.1). Taking also into account the electron density distribution of the HOMO-1, the frontier electron density difference between C6 and C2 of 3-fluorophenol is still clearly observed, although it is less pronounced. These results indicate that in the neutral 3-fluorophenol both *ortho* positions vary significantly with respect to their intrinsic reactivity for an electrophilic attack by the C(4a)-peroxyflavin enzyme intermediate, C6 being more reactive than C2. Upon ionisation, however, this difference disappears. In the 3-fluorophenolate anion the C2 and C6 position contain similar HOMO and frontier electron density, making these centres equally reactive for electrophilic attack. This implies that the pH effect on the regioselectivity of the 3-fluorophenol hydroxylation can be explained by assuming that the deprotonation of the amino acid residue in the active site of the enzyme (pK_a 6.5) results in an ionisation of the 3-fluorophenol substrate and, as a result, in a decrease of the relatively higher reactivity of C6 compared to C2. The fact that the ultimate minimum C6/C2 hydroxylation ratio observed at $pH \geq 7.5$ equals 2.2 suggests that the

Table 4.1. Calculated Coulomb, HOMO and frontier orbital characteristics of 3-fluorophenol and its phenolate anion. Numbering of the carbon atoms was chosen in such a way that the fluoro substituent is situated at C3 and the oxygen/hydroxyl moiety at C1. The frontier electron density was calculated from the density distribution of the HOMO and the HOMO-1 as described by Fukui et al. (1954).

Compound	Atomic charge on carbon centre						E(HOMO) (eV)	E(HOMO-1) (eV)	
	C1	C2	C3	C4	C5	C6			
3-fluorophenol	+0.11	-0.23	+0.13	-0.20	-0.07	-0.20	-9.35	-9.89	
3-fluorophenolate	+0.29	-0.37	+0.14	-0.36	-0.05	-0.34	-3.05	-5.00	
	Orbital	Density on carbon centre							
		C1	C2	C3	C4	C5	C6		
3-fluorophenol	HOMO	0.18	0.03	0.11	0.29	0.01	0.22		
	frontier	0.32	0.18	0.23	0.49	0.09	0.41		
3-fluorophenolate	HOMO	0.03	0.22	0.00	0.31	0.00	0.23		
	frontier	0.06	0.44	0.01	0.62	0.00	0.46		

ionisation of the hydroxyl moiety is not complete, resulting in a C6/C2 hydroxylation ratio at pH ≥ 7.5 that is above the value of 1.0 expected on the basis of the calculated equal reactivity of C6 and C2 in the fully deprotonated form.

Table 4.1 also presents the calculated atomic charges of the carbon centres in 3-fluorophenol and its phenolate anionic form. No significant difference in the relative charge distribution on the two *ortho* C atoms is observed for either 3-fluorophenol or the 3-fluorophenolate anion. This implies that the Coulomb term (Fleming, 1976) does not contribute to the differential reactivity of C2 and C6 of the 3-fluorophenol molecule.

Furthermore, the data presented in Table 4.1 demonstrate an increase in HOMO energy upon ionisation of 3-fluorophenol, providing an explanation for the increased rate of conversion observed with increasing pH (Fig. 4.3B). Analogous to the proposed increased rate of conversion of a series of fluorinated 4-hydroxybenzoates by 4-hydroxybenzoate hydroxylase with increasing E(HOMO) (energy of the highest occupied molecular orbital) of the substrate (Vervoort, et al., 1992), reactivity of the 3-fluorophenol substrate increases with increasing E(HOMO) and, thus, upon its ionisation in the reduced form of the enzyme (Fleming, 1976; Vervoort, et al., 1992).

Altogether, the data from the molecular orbital calculations support the above proposal that deprotonation of an amino acid residue in the active site of the reduced protein results in ionisation of the bound 3-fluorophenol.

4.4 Discussion

Regioselective hydroxylation of substituted phenols by phenol hydroxylase from *Trichosporon cutaneum* has not been reported so far (e.g. Neujahr and Gaal, 1973; Neujahr and Kjellén, 1978). Two possible ways of hydroxylation of *meta*-substituted phenols have been suggested by Neujahr (Neujahr and Varga, 1970). This paper is the first to present evidence for the regioselective hydroxylation of 3-fluorophenol. Using ¹⁹F-NMR it is clearly demonstrated that the ratio of *ortho*-C6/*ortho*-C2 hydroxylation of 3-fluorophenol decreases with increasing pH (Fig. 4.3A) and that the rate of product formation increases with increasing pH (Fig. 4.3B).

In theory, the difference in *ortho*-C6/*ortho*-C2 hydroxylation ratio could be caused by different orientations of 3-fluorophenol in the active site, leading to either C6 or C2 hydroxylation. A change in the relative contribution of discrete orientations with changing pH might then explain the observed decrease in the C6/C2 hydroxylation ratio with increasing pH. If this is the actual mechanism underlying the effects of pH on the regioselectivity, then different orientations of the 3-fluorophenol substrate in the active site of the phenol hydroxylase should be visible in ¹⁹F-NMR binding studies. Such different orientations of 3-fluorophenol in the active site of the reduced enzyme at pH 7.6 could not be observed (Fig. 4.4B). However, due to the broad nature of the resonance of 3-fluorophenol bound to the reduced enzyme (and the observation of an inhomogeneous line shape of 3-fluorophenol bound to the oxidized enzyme, Fig. 4.4A), two different orientations with slightly different chemical shifts and independent line widths around 250-300 Hz cannot be ruled out and might be a factor contributing to the observed regioselectivity of the reaction. Different orientations of 3-fluorophenol bound to the enzyme may be caused by a flip-flop movement of the substrate. If the populations of the two orientations are different (i.e. different lifetimes of the two orientations) and, in addition, if these populations vary with a change in pH, regioselective binding might explain the effect of pH on the observed regioselectivity of the *ortho*-hydroxylation.

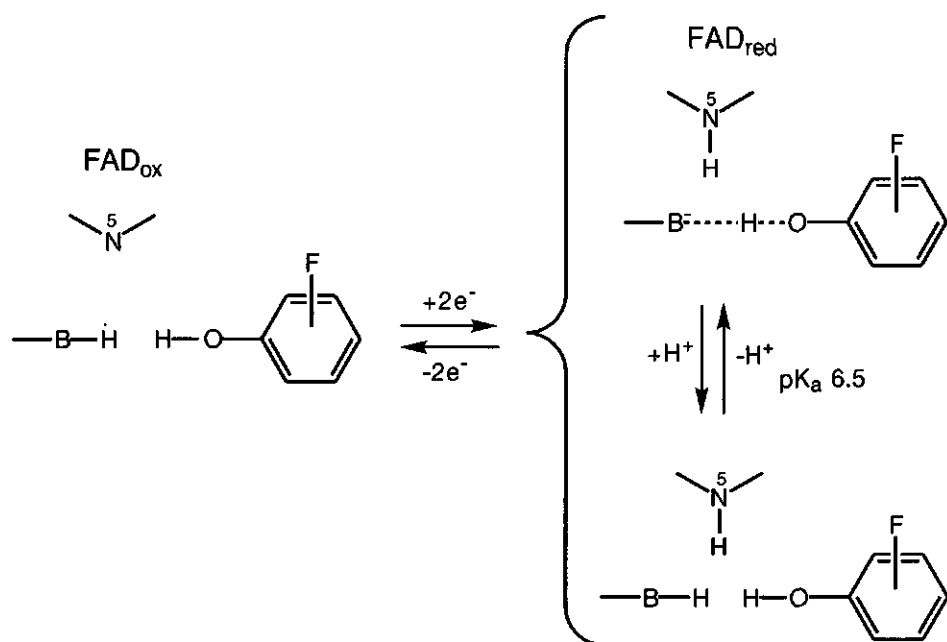


Fig. 4.6. Hypothetical scheme for the protonation/deprotonation equilibria of importance for the catalytic mechanism of phenol hydroxylase. Only part of the isoalloxazine moiety of FAD is depicted. For further details see text.

However, in addition to possible different binding orientations, results from molecular orbital calculations provide an alternative explanation for the observed pH-dependent regioselectivity and rate of the reaction. Based on this explanation, a working hypothesis is schematically presented in Fig. 4.6.

At physiological pH values, the fluorinated aromatic substrates are bound to the active site of the oxidized protein in their neutral forms. This conclusion is in accordance with data presented by Detmer and Massey, reporting that 4-nitrophenol binds to the oxidized enzyme also in its unionised form (Detmer and Massey, 1985). Upon reduction of the enzyme, however, the situation changes. A pH-dependent change in the ^{19}F -NMR chemical shift of 4-fluorophenol bound to the reduced protein points at a change in the nature of the bound substrate caused by deprotonation of an amino acid residue with a $\text{p}K_a$ of about 6.5. This effect and, thus,

deprotonation of this amino acid residue is not observed for the oxidized form of the enzyme. This difference in apparent pK_a of the amino acid residue involved suggests that deprotonation of the group is associated with the two-electron reduction of the nearby flavin cofactor. This amino acid then acts as a base facilitating the ionisation of the bound phenol substrate. Molecular orbital calculations give theoretical support for the change in protonation/deprotonation of the substrate in the active site of reduced phenol hydroxylase, explaining the pH-dependent effect on the increase in product formation with increasing pH and probably also on the C6/C2 hydroxylation ratio of 3-fluorophenol. The pK_a value of the actual responsible protein residue was determined from fitting the data in Fig. 4.3A with Eqn. 4.1. This resulted in a pK_a of 6.5 and maximum and minimum C6/C2 *ortho*-hydroxylation ratios of 6.7 and 2.2, respectively. This pK_a value is in fair agreement with the pK_a value reported for the change in the rate of formation of the so-called enzyme intermediate II from I and III from II during the conversion of resorcinol by phenol hydroxylase (Detmer and Massey, 1985). This strengthens the idea that the pK_a value in question belongs to an amino acid residue involved in enzyme catalysis. It could be argued that the data presented in Fig. 4.3A reflect two pK_a values. Looking at the data of Detmer and Massey (1985) for the change in the rate of formation of the so-called enzyme intermediate II from I and III from II during the conversion of resorcinol by phenol hydroxylase, it is also possible to derive two different pK_a values for one intermediate formation. However, two pK_a values would not change the proposed mechanism (Fig. 4.6) that an active site amino acid is involved in substrate deprotonation. The data of the present study corroborate the conclusion of Detmer and Massey (1985), based on stopped-flow experiments, that both a protonated and a deprotonated form of phenol hydroxylase can catalyse the conversion of the phenolic substrates, only with different rates. Using our working hypothesis, the results of the present study imply that the deprotonated form would lead to the highest rate of conversion.

4.5 References

- Anderson, R.F., Patel, K.B. and Stratford, M.R.L. (1987) *J. Biol. Chem.* **262**, 17475-17479.
- Anderson, R.F., Patel, K.B. and Vojnovic, B. (1991) *J. Biol. Chem.* **266**, 13086-13090.

- Berkel van, W.J.H. and Müller, F. (1991) in *Chemistry and biochemistry of flavoenzymes* (Müller, F., Ed.) Vol. 2, pp. 1-29, CRC Press, Boca Raton.
- Brown, H.C., McDaniel, D.H. and Häfliger, O. (1955) *Determination of organic structures by physical methods*, Academic Press, New York.
- Detmer, K. and Massey, V. (1984) *J. Biol. Chem.* **259**, 11265-11272.
- Detmer, K. and Massey, V. (1985) *J. Biol. Chem.* **260**, 5998-6005.
- Entsch, B. (1991) *J. Biol. Chem.* **266**, 17341-17349.
- Entsch, B., Ballou, D.P. and Massey, V. (1976) *J. Biol. Chem.* **251**, 2550-2563.
- Fleming, I. (1976) *Frontier orbitals and organic chemical reactions*, John Wiley & Sons, Chichester.
- Fukui, K., Yonezawa, T., Nagata, C. and Shingu, H. (1954) *J. Chem. Phys.* **22**, 1433-1442.
- Hull, W.E. and Sykes, B.D. (1975) *J. Mol. Biol.* **98**, 121-153.
- Kälin, M., Neujahr, H.Y., Weissmahr, R.N., Sejlitz, T., Jöhl, R., Fiechter, A. and Reiser, J. (1992) *J. Bacteriol.* **174**, 7112-7120.
- Kemal, C. and Bruce, T. (1979) *J. Am. Chem. Soc.* **101**, 1635-1638.
- Lowry, O.H., Rosebrough, N.J., Far, A.L. and Randall, R.J. (1951) *J. Biol. Chem.* **193**, 265-275.
- Mörtberg, M. and Neujahr, H.Y. (1988) *FEBS Lett.* **242**, 75-78.
- Neujahr, H.Y. (1991) in *Chemistry and biochemistry of flavoenzymes* (Müller, F., Ed.) Vol. 2, pp. 65-85, CRC Press, Boca Raton.
- Neujahr, H.Y. and Gaal, A. (1973) *Eur. J. Biochem.* **35**, 386-400.
- Neujahr, H.Y. and Kjellén, K.G. (1978) *J. Biol. Chem.* **253**, 8835-8841.
- Neujahr, H.Y. and Varga, J.M. (1970) *Eur. J. Biochem.* **13**, 37-44.
- Sejlitz, T. and Neujahr, H.Y. (1987) *Eur. J. Biochem.* **170**, 343-349.
- Shaka, A.J., Keeler, J. and Freeman, R. (1983) *J. Magn. Reson.* **53**, 313-340.
- Vervoort, J., Rietjens, I.M.C.M., Berkel van, W.J.H. and Veeger, C. (1992) *Eur. J. Biochem.* **206**, 479-484.

5

Conversion of phenol derivatives to hydroxylated products by phenol hydroxylase from *Trichosporon cutaneum*

A comparison of regioselectivity and rate of conversion with calculated molecular orbital substrate characteristics

Sjaak Peelen, Ivonne M.C.M. Rietjens, Marelle G. Boersma and Jacques Vervoort

Published in *European Journal of Biochemistry* 227 (1995), 284-291.

*This study describes the regioselective hydroxylation and the rates of conversion of a series of fluorinated phenol derivatives by phenol hydroxylase from the yeast *Trichosporon cutaneum*. The natural logarithm of the k_{cat} value for the conversion of the phenolic substrates correlates with the calculated energy of the reactive electrons in the highest occupied molecular orbital of the substrate ($r = 0.85$). This observation supports the hypothesis that at physiological pH (7.6) and 25 °C, in the absence of monovalent anions, the nucleophilic attack of the electrons in the highest occupied molecular orbital of the substrate on the C(4a)-hydroperoxyflavin enzyme intermediate is of major importance in determining the overall rate of catalysis. Results from ^{19}F -NMR analysis of the incubation mixtures demonstrate for phenols with two identical ortho substituents, that the ortho position which becomes preferentially hydroxylated is the one with the highest density of the reactive electrons in the highest occupied molecular orbital. A halogen substituent at a meta position decreases the chances for hydroxylation at the adjacent ortho position further than expected on the basis of the calculated reactivity. This result indicates a contribution of a protein/substrate dipolar*

interaction, influencing the time-averaged orientation of the substrate with respect to the reactive C(4a)-hydroperoxyflavin intermediate.

5.1 Introduction

Phenol hydroxylase (EC 1.14.13.7) is a flavin-dependent monooxygenase that can be isolated from a variety of sources, e.g. bacteria, actinomycetes and yeasts. The present study focuses on the phenol hydroxylase from the strictly aerobic yeast *Trichosporon cutaneum* (Neujahr, 1991).

The catalytic mechanism of the enzyme is reported to proceed by formation of a C(4a)-hydroperoxyflavin intermediate, formed upon two-electron reduction of the flavin prosthetic group by NADPH, incorporation of an oxygen molecule, and protonation of the peroxy moiety (Detmer and Massey, 1984; Maeda-Yorita and Massey, 1993; Neujahr, 1991). The mechanism by which the C(4a)-hydroperoxyflavin intermediate converts the substrate to its hydroxylated form is supposed to proceed analogously to the mechanism for other aromatic hydroxylases, i.e. by an electrophilic attack of the hydroperoxide function on the substrate (Detmer and Massey, 1985; Entsch, et al., 1976; Kemal and Bruce, 1979). The enzyme has been reported to catalyse the hydroxylation of a variety of substituted phenols, such as fluoro-, chloro-, amino- and methyl-phenols and also dihydroxybenzenes, at the *ortho* position with respect to the hydroxyl moiety (Neujahr and Gaal, 1973; Neujahr and Kjellén, 1978). The reaction cycle consists of various separate steps and is supposed to proceed by successive substrate binding, NADPH binding, flavin reduction, NADP⁺ release, oxygen binding, formation of reaction intermediates I, II and III, I representing the activated C(4a)-hydroperoxyflavin enzyme intermediate and III representing the C(4a)-hydroxyflavin intermediate formed after oxygen transfer to the substrate (Maeda-Yorita and Massey, 1993). The reaction cycle ends by release of the product and a molecule of water. Characterisation of the rate-limiting step is still a matter for considerable debate. A substrate-induced conformational change (Mörtberg and Neujahr, 1988; Neujahr, 1988; Neujahr, 1991), the conversion of intermediate II to III (Detmer and Massey, 1985), or the loss of water from intermediate III to regenerate the oxidized enzyme (Maeda-Yorita and Massey, 1993), have all been reported to be the rate-limiting step in the absence of monovalent anions at physiological pH.

The objective of the present study is to investigate a possible influence of substrate characteristics on the overall conversion rates of phenol derivatives by phenol hydroxylase. The rationale for this study was based on the so-called frontier orbital theory (Fleming, 1976) and recent molecular-orbital-based quantitative structure-activity relationship (MO-QSAR) results obtained for the 4-hydroxybenzoate-hydroxylase-catalysed conversion of fluorinated 4-hydroxybenzoates (Vervoort, et al., 1992), the cytochrome-P450-catalysed conversion of a series of aniline derivatives (Cnubben, et al., 1994), and the regioselectivity of the cytochrome-P450-catalysed hydroxylation of a series of fluorobenzenes (Rietjens, et al., 1993). This MO-QSAR approach is based on the following considerations. In the case where the electrophilic attack of the C(4a)-hydroperoxyflavin intermediate on the reactive π -electrons of the phenolic substrates is a major factor in determining the overall rate of catalysis, it can be expected that the reactivity of these frontier π -electrons will correlate with the overall rate of catalysis, whereas their density distribution might influence the actual site of hydroxylation. Following the so-called frontier orbital theory, the reactivity of these reactive π -electrons can be characterised by the energy of the orbital in which these electrons are located, i.e. the energy of the highest occupied molecular orbital [E(HOMO)] (Fleming, 1976). For the flavin-dependent monooxygenases, this approach provides a possibility to obtain information on rate-limiting factors under optimal turnover conditions, the enzymes generally being too active to allow accurate stopped-flow analysis, unless conditions such as low temperature, inhibition at low pH or the presence of monovalent anionic inhibitors are used (Detmer and Massey, 1985; Maeda-Yorita and Massey, 1993). In a previous study, a correlation between the $\ln k_{cat}$ value and E(HOMO) of the substrate already has been reported for the flavin dependent 4-hydroxybenzoate 3-hydroxylase (Vervoort, et al., 1992). The present study reports a similar MO-QSAR and its implications for the reaction cycle of phenol hydroxylase from *T. cutaneum*.

5.2 Materials and methods

Enzyme purification. Phenol hydroxylase was isolated from the yeast *T. cutaneum* (CBS-2466), essentially as described by Sejlitz and Neujahr (1987). The final preparation had a specific activity of 5.0 $\mu\text{mol NADPH oxidized}\cdot\text{min}^{-1}\cdot\text{mg}$

protein⁻¹ and was over 90 % pure as judged by SDS/PAGE. The enzyme preparation was free of any detectable catechol dioxygenase activity.

The protein concentration was determined by the method of Lowry et al. (1951) using bovine serum albumin as the standard. The concentration of the purified phenol hydroxylase was determined from recording visible absorption spectra, using a molar absorption coefficient of 12.6 mM⁻¹.cm⁻¹ at 442 nm for the protein-bound FAD (Neujahr, 1991).

Incubations with isolated phenol hydroxylase. Phenol hydroxylase incubations for ¹⁹F-NMR measurements were carried out in closed reaction vessels to prevent evaporation of the phenolic substrate and contained (final concentrations) 50 mM potassium phosphate, pH 7.6, 1 mM phenol, added from a 200 mM stock solution in dimethyl sulphoxide, 50 nM phenol hydroxylase, 0.1 mM EDTA, 10 μM FAD, 1 mM dithiothreitol and 2 mM ascorbic acid. Ascorbic acid provides possibilities for efficient chemical reduction of quinone-like metabolites, which are formed upon hydroxylation at a fluorinated *ortho* position, to dihydroxybenzenes, thus preventing further reaction of these electrophilic primary products (Husain, et al., 1980). The incubations were started by the addition of 0.17 mM NADPH. Reactions were carried out at 25 °C. Different incubation times (15 - 360 min) were used for the different substrates, the actual incubation time depending on the reactivity of the substrate.

Phenol hydroxylase incubations for kinetic analyses contained (final concentrations) 50 mM potassium phosphate, pH 7.6, concentrations of the various phenols varying from 2 μM to 2.5 mM, added from a 200 times concentrated stock solution in dimethyl sulphoxide, 0.1 mM EDTA, 10 μM FAD, 2 mM ascorbic acid, 1 mM dithiothreitol and different concentrations of NADPH (50, 75, 100, 170 or 340 μM). The incubations were started by the addition of 50 nM phenol hydroxylase. Final reaction volumes were 1 ml for spectroscopic measurements of NADPH oxidation (decrease at 340 nm) and 2 ml for measurement of oxygen consumption using a Clark electrode.

Determination of k_{cat} values. Turnover rates were determined by measuring both the rate of NADPH oxidation (spectrophotometrically) and the rate of oxygen consumption (Clark electrode). Rates of NADPH oxidation were corrected for uncoupling phenomena, i.e. electron transfer leading to H₂O₂ instead of product formation (Neujahr and Kjellén, 1978). The amount of electrons transferred to H₂O₂ was determined by quantification of the amount of oxygen reformed upon addition

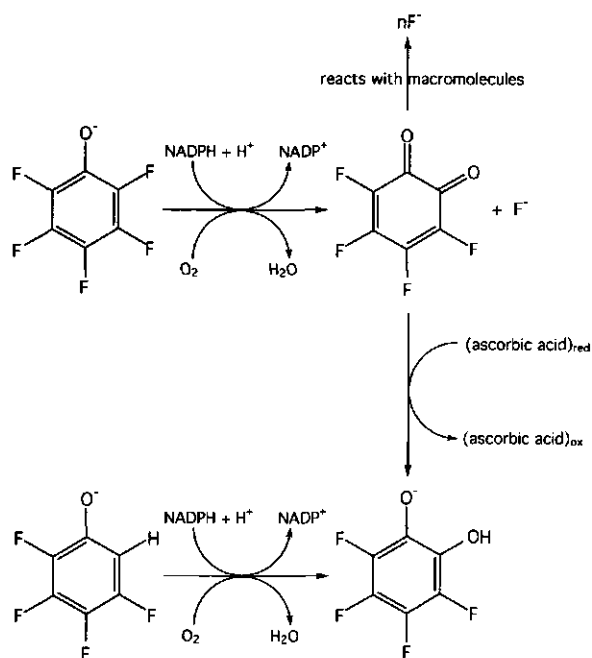
of catalase (from beef liver, 65 U/ml incubation medium; Boehringer Mannheim). The amount of uncoupling was calculated as the amount of oxygen reformed divided by the total amount of oxygen used at the time catalase was added. Since ascorbic acid is able to reduce part of the H_2O_2 , the amounts of uncoupling were determined in the absence of ascorbic acid. Apparent maximal conversion rates at saturating phenol concentrations (ranging from 2 μM to 2.5 mM for the different substrates) were determined at various NADPH concentrations. The maximal rate of conversion at saturating phenol and saturating NADPH concentrations (k_{cat}) was obtained from a fit of the maximal conversion rates at various NADPH concentrations to the Michaelis-Menten equation. The k_{cat} values thus obtained were used for MO-QSAR analysis.

Molecular orbital calculations. Molecular orbital (MO) calculations were carried out on a Silicon Graphics Indigo 2 workstation using Insight II (version 2.2.0; Biosym Technologies, San Diego, USA). The semi-empirical molecular orbital method was used, applying the AM1, MNDO or PM3 Hamiltonian from the MOPAC program (version 6.0). All calculations were carried out with PRECISE criteria. For all calculations, the self-consistent field was achieved. Geometries were optimised for all bond lengths, bond angles and torsion angles. When the difference in energy between the highest occupied molecular orbital (HOMO) and HOMO-1 of the substrate is relatively small (less than 1 eV), then the HOMO-1 density of the reaction center must also be taken into account. This was performed by calculating the so-called frontier orbital density, using the equation given by Fukui et al. (1954).

In this study, the outcomes of the semi-empirical calculations on molecules in a vacuum are related to the electronic characteristics of the substrates in the active site of phenol hydroxylase. Due to solvation effects and a different dielectric constant, the intrinsic properties of the compounds may be influenced upon binding to this active site. However, it is assumed that this phenomenon will not influence the relative differences of parameters between a series of closely related compounds to a significant extent. The outcomes of the *in vacuo* computer calculations can thus be used as an approach to study relative differences within a series of related compounds.

^{19}F -NMR. ^{19}F -NMR measurements were performed on a Bruker AMX 300 NMR spectrometer. Norell (Landisville, NJ, USA) 10-mm NMR tubes were used. The sample volume was 1.71 ml, containing 100 μl 2H_2O for locking the magnetic field and 10 μl 8.4 mM 4-fluorobenzoate, which served as an internal standard. Proton

decoupling was achieved with the Waltz-16 pulse sequence (Shaka, et al., 1983) at -18 dB from 50 W. Nuclear Overhauser effects were eliminated using the inverse-gated decoupling technique. Spectra were obtained at 7 °C with 25-30 ° pulses (5 μ s), a 50 kHz spectral width, 16 k data points, a relaxation delay of 1 s, quadrature phase detection and quadrature phase cycling (CYCLOPS). Between (1 - 60) $\times 10^3$ scans were recorded, depending on the concentration of the products and the signal-to-noise ratio required. Chemical shifts are reported relative to CFCl_3 .



Scheme 5.1. Formation of catechol and ortho quinone metabolites from phenolic substrates by phenol hydroxylase, as well as the non-enzymic conversion of the ortho quinone metabolite.

5.3 Results

5.3.1 Determination of k_{cat} values

Maximal rates of conversion of the various phenol derivatives were determined at pH 7.6 by measuring the rate of NADPH oxidation and oxygen consumption. When hydroxylation occurs at a fluorinated *ortho* position, the reaction can result in defluorination and formation of an *ortho* benzoquinone instead of a catechol metabolite. Subsequent chemical reduction of the *ortho* benzoquinone might give rise to formation of the catechol by a second route (Scheme 5.1) (Husain, et al., 1980). To prevent the use of NADPH for this chemical reduction, ascorbic acid is added, which is able to catalyse this reduction more efficiently (Besten den, et al., 1993).

Table 5.1. Average k_{cat} values for the conversion of phenol derivatives by phenol hydroxylase at saturating NADPH concentration, pH 7.6, 25 °C, determined by NADPH oxidation ($n = 2-3$) and oxygen consumption ($n = 2$). Maximal rates of conversion for nitrophenols could not be determined by the rate of NADPH oxidation due to the high absorbance of the nitrophenols at 340 nm. The data are corrected for uncoupling. The standard error of the mean is given in parentheses. n.d., not determined.

Phenol	k_{cat} for (min^{-1})		Average k_{cat} (min^{-1})
	NADPH oxidation	O ₂ consumption	
parent substrate	510 (30)	420 (6)	470
2-fluoro-	160 (14)	140 (6)	150
3-fluoro-	280 (7)	280 (11)	280
4-fluoro-	490 (51)	440 (23)	470
2,3-difluoro-	80 (11)	90 (10)	90
2,4-difluoro-	170 (1)	200 (9)	190
2,5-difluoro-	150 (10)	150 (0)	150
2,6-difluoro-	350 (10)	380 (18)	370
3,4-difluoro-	410 (24)	360 (12)	390
3,5-difluoro-	280 (9)	270 (20)	280
2,3,4-trifluoro-	150 (6)	150 (5)	150
2,3,5-trifluoro-	70 (10)	60 (5)	70
2,3,6-trifluoro-	140 (11)	150 (3)	150
3,4,5-trifluoro-	210 (7)	200 (8)	210
2,3,5,6-tetrafluoro-	50 (4)	50 (7)	50
pentafluoro-	40 (19)	40 (2)	40
3-chloro-4-fluoro-	180 (16)	190 (25)	190
4-chloro-3-fluoro-	260 (10)	270 (40)	270
2-fluoro-4-nitro-	n.d.	30 (0)	30
3-fluoro-4-nitro-	n.d.	30 (1)	30

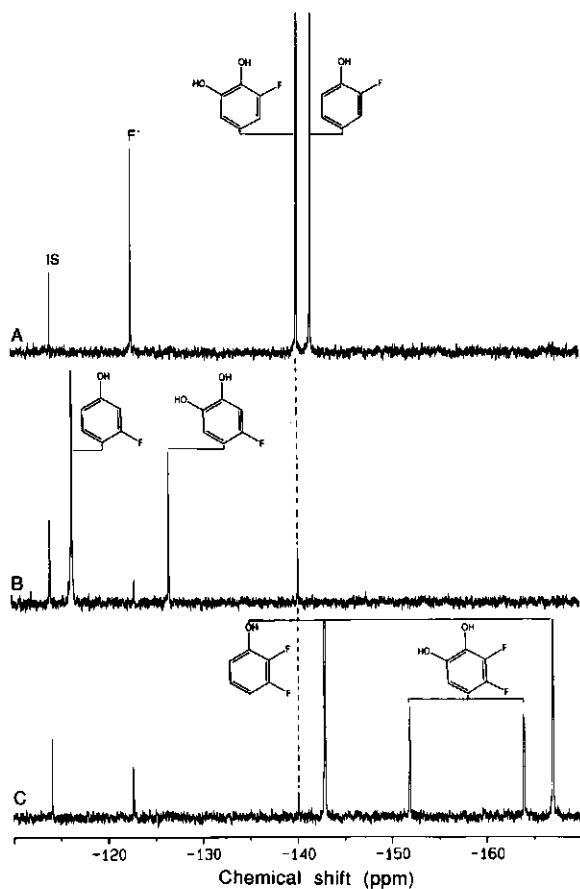


Fig. 5.1. ^{19}F -NMR spectra of the conversion of (A) 2-fluorophenol, (B) 3-fluorophenol and (C) 2,3-difluorophenol by phenol hydroxylase. The resonance marked IS is from the internal standard 4-fluorobenzoate.

From the k_{cat} values presented in Table 5.1, it follows that the maximal rate of conversion varies with the substituent pattern; an increase in the number of fluorine substituents, and especially incorporation of a nitro substituent, generally results in a decrease of the k_{cat} value.

5.3.2 Characterisation of the reaction products

To investigate to what extent the substituent patterns of the phenolic substrates not only influence the rates but also the regioselectivity of the conversion by phenol hydroxylase, reaction products formed from the various phenols were characterised by ^{19}F -NMR. Some of the ^{19}F -NMR spectra of incubations in which phenol hydroxylase was incubated with fluorinated phenol derivatives are shown (Fig. 5.1). Comparison of the ^{19}F -NMR spectra of incubations in the absence (data not shown) and presence of NADPH, clearly indicate NADPH-dependent product formation. The results of ^{19}F -NMR analysis of the phenol hydroxylase incubations with fluorinated phenol derivatives are summarised in Tables 5.2-5.4. Tables 5.2 and 5.3 present the chemical shift values for the various phenol and catechol derivatives, respectively. Table 5.3 also presents a short indication of how the ^{19}F -NMR resonances could be ascribed to specific catechol metabolites. Reference catechol derivatives are not commercially available, and their chemical synthesis is hampered by their rapid autooxidation. However, identification of the ^{19}F -NMR resonances of the various fluorinated catechol metabolites could be performed on the basis of their common formation from specific phenolic precursors and the knowledge that the enzyme hydroxylates a position *ortho* with respect to the hydroxyl moiety. For example, the ^{19}F -NMR resonance of 3-fluorocatechol was identified at -140.4 ppm on the basis of its formation as the only common metabolite in a phenol-hydroxylase-catalysed conversion of both 2-fluorophenol and 3-fluorophenol (Fig. 5.1A, B). In a similar way, the resonances of various other fluorinated catechol metabolites could be identified. From the chemical shift values determined this way (Tables 5.2 and 5.3), it could be derived that incorporation of the second hydroxyl moiety by phenol hydroxylase at a position *ortho*, *meta* or *para* with respect to a fluorine substituent, shifts its ^{19}F -NMR resonance position by -23.1 ± 0.3 ppm ($n=5$), $+1.3 \pm 0.4$ ppm ($n=11$) and -11.2 ± 0.7 ppm ($n=7$), respectively. Furthermore, if a hydroxyl moiety replaces a fluorine atom at a position *ortho*, *meta* or *para* with respect to another fluorine substituent, the chemical shift of this latter fluorine is changed by $+2.2 \pm 0.9$ ppm ($n=5$), $+1.0 \pm 0.9$ ppm ($n=7$) and -5.4 ± 0.9 ppm ($n=5$), respectively. These observations were used to identify catechol metabolites for which only one phenolic substrate was available. For example, the resonance at -141.9 ppm, representing a phenol hydroxylase metabolite from 4-chloro-3-fluorophenol, could in theory be either 4-chloro-3-fluorocatechol (resulting from hydroxylation at C2) or 4-chloro-5-

Table 5.2. Chemical shift values of ^{19}F -NMR resonances of fluorophenol derivatives in 50 mM potassium phosphate, pH 7.6 at 7 °C. Notice that for some fluorophenol derivatives, the number of resonances is less than the number of fluorine substituents; this is due to symmetry. Chemical shift values are reported relative to CFCl_3 .

Phenol	Chemical shift (ppm)		
2-fluoro-	-141.9		
3-fluoro-	-116.5		
4-fluoro-	-129.1		
2,3-difluoro-	-143.1 (F3)	-167.1 (F2)	
2,4-difluoro-	-126.3 (F4)	-137.4 (F2)	
2,5-difluoro-	-122.5 (F5)	-147.4 (F2)	
2,6-difluoro-	-139.1 (F2/F6)		
3,4-difluoro-	-140.9 (F3)	-154.2 (F4)	
3,5-difluoro-	-114.7 (F3/F5)		
2,3,4-trifluoro-	-153.6 (F4)	-162.5 (F2)	-164.9 (F3)
2,3,5-trifluoro-	-122.2 (F5)	-142.0 (F3)	-173.0 (F2)
2,3,6-trifluoro-	-144.4 (F3)	-148.5 (F6)	-164.1 (F2)
3,4,5-trifluoro-	-139.7 (F3/F5)	-177.9 (F4)	
2,3,5,6-tetrafluoro-	-149.3 (F3/F5)	-170.5 (F2/F6)	
pentafluoro-	-171.7 (F2/F6)	-173.2 (F3/F5)	-186.0 (F4)
3-chloro-4-fluoro-	-132.6		
4-chloro-3-fluoro-	-118.7		
2-fluoro-4-nitro-	-140.6		
3-fluoro-4-nitro-	-118.0		

fluorocatechol (resulting from hydroxylation at C6). Compared to the parent 4-chloro-3-fluorophenol, the ^{19}F -NMR resonance of the observed metabolite is shifted by -23.2 ppm. From this value it can be concluded that the hydroxyl moiety is incorporated *ortho* (expected shift -23.1 ± 0.3 ppm), not *para* (expected shift -11.2 ± 0.7 ppm) with respect to the fluorine substituent in 4-chloro-3-fluorophenol. This implies that the resonance at -141.9 ppm can be ascribed to 4-chloro-3-fluorocatechol. The identification of the second metabolite peak at -129.9 ppm as 4-chloro-5-fluorocatechol because of its common formation from both 4-chloro-3-fluorophenol and 3-chloro-4-fluorophenol, corroborates the assignment of the -141.9 ppm metabolite peak to the C2 hydroxylated metabolite from 4-chloro-3-fluorophenol. In the same way, various other resonances of fluorophenol-derived catechol metabolites could be identified (Table 5.3). The low $\text{p}K_a$ of nitrophenols and nitrocatechols (Brown, et al., 1955) results in deprotonation of their hydroxyl moiety at pH 7.6. Therefore chemical shifts of nitro-group-containing phenols and catechol metabolites were also determined at pH 2 at which their hydroxyl moieties are

protonated. The chemical shift values thus obtained could be used for the identification of chemical shift values of the catechol metabolites on the basis of the shift observed upon incorporation of the second *hydroxyl* moiety. Furthermore, F-F coupling constants determined for fluorine-substituted aromatics (Cooper, et al., 1971) were used, whenever necessary, for the identification of multi-fluorocatechols (Table 5.3).

5.3.3 Metabolite patterns

Upon identification of the ^{19}F -NMR resonances of the various catechols, the regioselectivity of the conversion of the various fluorophenols by phenol hydroxylase could be quantified from the ^{19}F -NMR spectra. The results obtained are presented in Table 5.4. Table 5.4 shows that C2 and C6 are not hydroxylated to the same extent for asymmetric phenols, demonstrating a regioselective *ortho* hydroxylation.

5.3.4 Molecular orbital characteristics of the substituted phenols

According to the frontier orbital theory, the chemical reactivity for an electrophilic attack by the C(4a)-hydroperoxyflavin, and, thus, chances for conversion of a phenol derivative in the active site of phenol hydroxylase will be dependent on the characteristics of its HOMO. The two characteristics of the HOMO that are of importance are (a) the HOMO density on the reaction centres (C2 and C6), reactivity increasing with increasing density, and (b) the energy of the reactive electrons in the HOMO, i.e. $E(\text{HOMO})$. A less negative $E(\text{HOMO})$ can be expected to result in a stronger interaction between the substrate HOMO and the C(4a)-hydroperoxyflavin lowest unoccupied molecular orbital (LUMO) and therefore in a reduction of the activation energy, which is related to $\ln k_{cat}$ of the reaction (Fleming, 1976).

The calculated HOMO characteristics of the various phenol derivatives are presented in Table 5.5. Values for both the protonated and the deprotonated forms of the phenol derivative are presented, because results of a previous study demonstrated that the phenolic substrates are likely to become partially deprotonated upon binding

Table 5.3. Chemical shift values of fluorinated catechol metabolites formed from fluorophenols by phenol hydroxylase in 50 mM potassium phosphate, pH 7.6, 7 °C. A short description of the strategy on which the identification was based is given. The fluorine atom to which the shift is compared is indicated in parentheses. Chemical shift values are reported relative to $CFCl_3$.

Catechol	Chemical shift (ppm)	Basis of identification
3-fluoro-	-140.4	formed from 2-, 3-fluorophenol, 2,3- and 2,6-difluorophenol <i>o</i> -OH: shift of -23.9 ppm (3-fluorophenol) <i>m</i> -OH: shift of +1.5 ppm (2-fluorophenol)
4-fluoro-	-126.7	formed from 3-, 4-fluorophenol, 2,4- and 2,5-difluorophenol <i>m</i> -OH: shift of +2.4 ppm (4-fluorophenol) <i>p</i> -OH: shift of -10.2 ppm (3-fluorophenol) <i>p</i> -OH/F: shift of -4.2 ppm (F5, 2,5-difluorophenol)
3,4-difluoro-	-152.1 (F4) -164.0 (F3)	formed from 2,3-, 3,4-difluorophenol and 2,3,6-trifluorophenol two signals of equal intensity $^3J_{F-F} = 21$ Hz <i>m</i> -OH shifts F4 by +2.1 ppm (F4, 3,4-difluorophenol) <i>p</i> -OH shifts F4 by -9.0 ppm (F4, 2,3-difluorophenol) <i>o</i> -OH shifts F3 by -23.1 ppm (F3, 3,4-difluorophenol) <i>p</i> -OH/F shifts F4 by -7.7 ppm (F3, 2,3,6-trifluorophenol)
3,5-difluoro-	-125.8 (F5) -137.9 (F3)	formed from 2,4-, 3,5-difluorophenol and 2,3,5-trifluorophenol two signals of equal intensity $^4J_{F-F} < 4$ Hz <i>o</i> -OH shifts F3 by -23.2 ppm (F3/5, 3,5-difluorophenol) <i>m</i> -OH shifts F3 by -0.5 ppm (F2, 2,4-difluorophenol) <i>m</i> -OH shifts F5 by +0.5 ppm (F4, 2,4-difluorophenol) <i>p</i> -OH shifts F5 by -11.1 ppm (F3/5, 3,5-difluorophenol) <i>p</i> -OH/F shifts F5 by -3.7 ppm (F5, 2,3,5-trifluorophenol)
3,6-difluoro-	-145.3 (F3/F6)	formed from 2,5-difluorophenol and 2,3,6-trifluorophenol two equivalent fluorine substituents <i>o</i> -OH shifts F3/6 by -22.8 ppm (F5, 2,5-difluorophenol) <i>m</i> -OH shifts F3/5 by +2.1 ppm (F2, 2,5-difluorophenol)
4,5-difluoro-	-152.2 (F4/F5)	formed from 3,4-difluorophenol two equivalent fluorine substituents <i>m</i> -OH shifts F4/5 by +2.0 ppm (F4, 3,4-difluorophenol) <i>p</i> -OH shifts F4/5 by -11.3 ppm (F3, 3,4-difluorophenol)
3,4,5-trifluoro-	-154.1 (F5) -162.2 (F3) -176.1 (F4)	formed from 2,3,4- and 3,4,5-trifluorophenol three signals of equal intensity $^3J_{F-F} = 21$ Hz <i>o</i> -OH shifts F3 by -22.5 ppm (F3, 3,4,5-trifluorophenol) <i>m</i> -OH shifts F3 by +0.3 ppm (F2, 2,3,4-trifluorophenol) <i>m</i> -OH shifts F4 by +1.8 ppm (F4, 3,4,5-trifluorophenol) <i>p</i> -OH shifts F4 by -11.2 ppm (F3, 2,3,4-trifluorophenol) <i>m</i> -OH shifts F5 by -0.5 ppm (F4, 2,3,4-trifluorophenol) <i>p</i> -OH shifts F5 by -14.4 ppm (F3/5, 3,4,5-trifluorophenol)

Table 5.3. Continued.

Catechol	Chemical shift (ppm)	Basis of identification
3,4,6-trifluoro-	-146.0 (F6) 153.1 (F4) -171.5 (F3)	formed from 2,3,5-trifluorophenol and 2,3,5,6-tetrafluorophenol three signals of equal intensity $^3J_{F-F} = 21$ Hz and $^5J_{F-F} = 8$ Hz <i>o</i> -OH shifts F6 by -23.8 ppm (F5, 2,3,5-trifluorophenol) <i>m</i> -OH shifts F3 by +2.3 ppm (F2, 2,3,5-trifluorophenol) <i>p</i> -OH/F shifts F4 by -3.8 ppm (F3/5, 2,3,5,6-tetrafluorophenol)
3,4,5,6-tetrafluoro-	-170.9 ^a (F3/F6) -180.8 (F4/F5)	formed from pentafluorophenol <i>p</i> -OH/F shifts F5 by -7.6 ppm (F5, pentafluorophenol)
3-chloro-4-fluoro-	-129.4	formed from 3-chloro-4-fluorophenol <i>m</i> -OH: shift of -3.2 ppm (3-chloro-4-fluorophenol)
4-chloro-3-fluoro-	-141.9	formed from 4-chloro-3-fluorophenol <i>o</i> -OH: shift of -23.2 ppm (4-chloro-3-fluorophenol)
4-chloro-5-fluoro-	-129.9	formed from 4-chloro-3-fluoro- and 3-chloro-4-fluorophenol <i>m</i> -OH: shift of +2.6 ppm (3-chloro-4-fluorophenol) <i>p</i> -OH: shift of -11.1 ppm (4-chloro-3-fluorophenol)
3-fluoro-4-nitro-	-145.6	formed from 3-fluoro-4-nitrophenol <i>o</i> -OH shifts F3 by -27.6 ppm (F3, 3-fluoro-4-nitrophenol) and shifts by -25.1 ppm at low pH
3-fluoro-5-nitro-	-141.9	formed from 2-fluoro-4-nitrophenol <i>m</i> -OH shifts F3 by -1.3 ppm (F2, 2-fluoro-4-nitrophenol)
4-fluoro-5-nitro-	-123.4	formed from 3-fluoro-4-nitrophenol <i>p</i> -OH shifts F4 by -5.4 ppm (F3, 3-fluoro-4-nitrophenol) and shifts by -9.4 ppm at low pH

^a calculated chemical shift, because the resonance is expected to overlap with the large F2/F6 substrate peak of pentafluorophenol (Table 5.2).

to the active site of phenol hydroxylase (Peelen, et al., 1993). The results in Table 5.5 indicate that in the protonated form, and thus also in the partially deprotonated form, the *ortho* positions in asymmetric phenols show different intrinsic theoretical reactivity for an electrophilic attack by the C(4a)-hydroperoxyflavin, i.e. different frontier orbital densities. Furthermore, the energy of the reactive π -electrons, represented by E(HOMO), varies with the substituent pattern (Table 5.5). In the next paragraph, these molecular orbital characteristics of the various phenolic substrates (Table 5.5) are compared to the outcomes of catalysis presented in Tables 5.1 and 5.4.

Table 5.4. Characterisation of the regioselectivity of the conversion of fluorophenols by phenol hydroxylase. The relative amount of fluoride anions observed in the ^{19}F -NMR spectra is presented. Whether or not a substrate contains a fluorine atom *ortho* with respect to the hydroxyl moiety, and therefore if it is expected to form F^- , is also indicated. -, + and ++ represent zero, one or two *ortho* fluorine substituents, respectively.

Phenol	C2:C6	F^- (%)	<i>ortho</i> F
2-fluoro-	29:71	29	+
3-fluoro-	29:71	6	-
4-fluoro-	50:50	0	-
2,3-difluoro-	12:88	19	+
2,4-difluoro-	20:80	26	+
2,5-difluoro-	66:34	57	+
2,6-difluoro-	50:50	72	++
3,4-difluoro-	7:93	17	-
3,5-difluoro-	50:50	0	-
2,3,4-trifluoro-	1:99	12	+
2,3,5-trifluoro-	37:63	31	+
2,3,6-trifluoro-	27:73	83	++
3,4,5-trifluoro-	50:50	3	-
2,3,5,6-tetrafluoro-	50:50	59	++
pentafluoro-	50:50	67	++
3-chloro-4-fluoro-	4:96	17	-
4-chloro-3-fluoro-	6:94	5	-
2-fluoro-4-nitro-	45:55	45	+
3-fluoro-4-nitro-	3:97	8	-

5.3.5 Comparison of calculated molecular orbital characteristics of phenolic substrates and the regioselectivity of their conversion by phenol hydroxylase

The regioselectivity of the hydroxylation of asymmetric phenols with two identical *ortho* substituents can be compared to the calculated frontier density on these centres. This demonstrates a qualitative relationship. The *ortho* position with the highest HOMO density in its protonated form, and thus also in its partially deprotonated form, is the position preferentially hydroxylated. For substrates with unequal *ortho* substituents, i.e. 2-fluoro-, 2,3-difluoro-, 2,4-difluoro-, 2,5-difluoro-, 2,3,4-trifluoro- and 2,3,5-trifluorophenol, this qualitative relationship no longer holds. Comparison of the actual regioselectivity (Table 5.4) to the calculated HOMO densities (Table 5.5) indicates that two factors cause a larger decrease in hydroxylation at an *ortho* position than expected on the basis of the calculated parameter. These factors are (a) the presence of a *meta* halogen substituent at a

Table 5.5. Molecular orbital characteristics of phenol derivatives of importance for a nucleophilic attack by the reactive electrons of the phenol on the C(4a)-hydroperoxyflavin intermediate, as calculated by the AM1 Hamiltonian. Results for both the phenol (OH) and the corresponding phenolate anion (O⁻) are presented.

Phenol	Frontier orbital density for		HOMO density for		E(HOMO) for (eV)	
	C2 OH	C6 OH	C2 O ⁻	C6 O ⁻	OH	O ⁻
parent substrate	0.27	0.27	0.23	0.23	-9.11	-2.70
2-fluoro-	0.39	0.14	0.24	0.20	-9.23	-2.88
3-fluoro-	0.18	0.40	0.22	0.23	-9.34	-3.05
4-fluoro-	0.20	0.20	0.21	0.21	-9.09	-2.87
2,3-difluoro-	0.35	0.25	0.24	0.20	-9.54	-3.22
2,4-difluoro-	0.29	0.13	0.22	0.19	-9.27	-3.05
2,5-difluoro-	0.48	0.10	0.24	0.19	-9.36	-3.22
2,6-difluoro-	0.26	0.26	0.22	0.22	-9.46	-3.06
3,4-difluoro-	0.12	0.30	0.20	0.21	-9.30	-3.21
3,5-difluoro-	0.33	0.33	0.22	0.22	-9.66	-3.41
2,3,4-trifluoro-	0.22	0.21	0.22	0.19	-9.53	-3.37
2,3,5-trifluoro-	0.48	0.17	0.25	0.19	-9.67	-3.55
2,3,6-trifluoro-	0.20	0.36	0.22	0.22	-9.65	-3.39
3,4,5-trifluoro-	0.21	0.21	0.21	0.21	-9.56	-3.54
2,3,5,6-tetrafluoro-	0.32	0.32	0.22	0.22	-9.87	-3.72
pentafluoro-	0.23	0.23	0.20	0.20	-9.94	-3.87
3-chloro-4-fluoro-	0.15	0.25	0.21	0.21	-9.26	-3.23
4-chloro-3-fluoro-	0.13	0.29	0.21	0.21	-9.31	-3.35
2-fluoro-4-nitro-	0.42	0.14	0.22	0.18	-10.12	-4.26
3-fluoro-4-nitro-	0.22	0.42	0.21	0.20	-10.27	-4.44

position adjacent to the *ortho* position in question and (b) the presence of a fluorine substituent at an *ortho* position when there is a hydrogen-substituted alternative. Furthermore, the results in Table 5.5 demonstrate that the summarised frontier densities on the two reaction centres C2 and C6 do not show differences between the various substrates that can account for the 20-fold variation in the rate of conversion (Table 5.1). However, the E(HOMO) values do vary to a significant extent. In Fig. 5.2, the natural logarithm of the k_{cat} value of conversion of the phenol derivatives by phenol hydroxylase (Table 5.1) is plotted against E(HOMO) of the substrates (Table 5.5). A correlation of 0.85 is obtained representing a molecular-orbital-based quantitative structure-activity relationship.

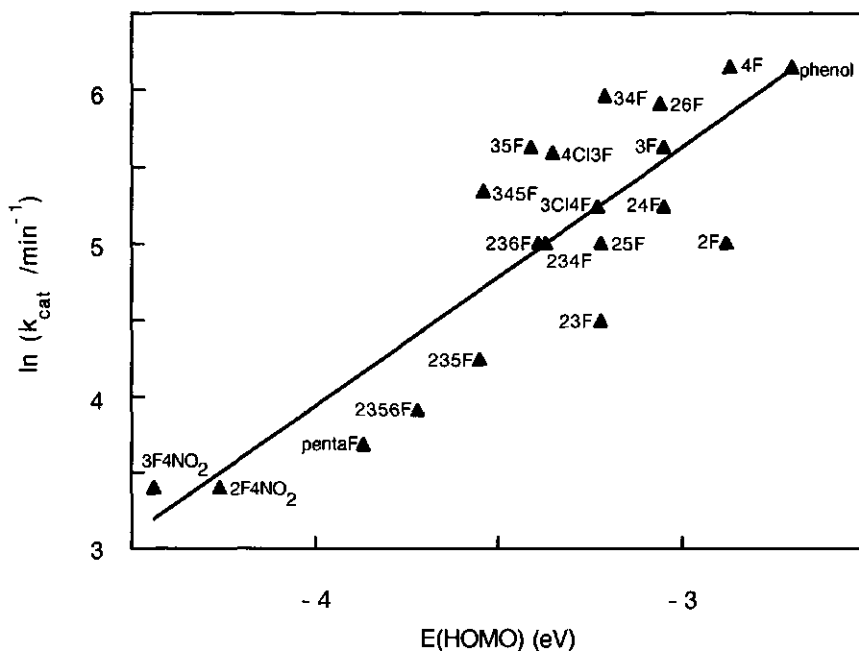


Fig. 5.2. Plot of $\ln k_{cat}$ values for the conversion of fluorinated phenols by phenol hydroxylase at pH 7.6, 25 °C, versus the calculated $E(\text{HOMO})$ of the phenolates, using the AM1 Hamiltonian. The average k_{cat} values in Table 5.1 are used. The correlation coefficient is 0.85.

5.4 Discussion

In the present study, the characteristics of the conversion of a series of halogenated phenol derivatives by phenol hydroxylase from *T. cutaneum* were investigated and compared to calculated molecular orbital parameters. Based on these studies, a molecular-orbital-based quantitative structure-activity relationship could be described in which the natural logarithm of the k_{cat} value, for maximal turnover of the phenol derivatives (Table 5.1), correlated ($r = 0.85$) with the $E(\text{HOMO})$ of the substrates (Table 5.5). The $E(\text{HOMO})$ represents the energy and,

thus, the reactivity of the π -electrons (Fleming, 1976) in the phenolic substrate that are involved in the nucleophilic attack on the C(4a)-hydroperoxyflavin cofactor of the activated form of the enzyme (Entsch, et al., 1976; Kemal and Bruice, 1979). Therefore, this MO-QSAR indicates that this nucleophilic attack is a major factor in determining the overall rate of catalysis. However, since that the correlation of the MO-QSAR is 0.85, it can be concluded that additional factors contribute to the fine-tuning of the overall rate of catalysis.

Before discussing this fine-tuning, it should be noticed that uncoupling is determined as the amount of oxygen reformed upon addition of catalase at the end of the phenolhydroxylase reaction, divided by the total amount of oxygen used. A different way to correct for uncoupling would be to include the catalase in the reaction mixture. Although this may give slightly different k_{cat} values, it will not affect the overall correlation as observed in Fig. 5.2.

The fact that the nucleophilic attack of the substrate on the C(4a)-hydroperoxyflavin has an important contribution to the rate-limiting steps in catalysis would be in accordance with the results of Maeda-Yorita and Massey (1993). They reported that the rate constant for this nucleophilic attack in the conversion of resorcinol (3-hydroxyphenol) was among the slowest in catalysis. The release of product and the decay of the C(4a)-hydroxyflavin are other slow steps in catalysis that could influence the overall rate of conversion. However, in this study, the stopped-flow kinetic data on separate rate constants in catalysis were determined for resorcinol at 4 °C, conditions chosen to decrease the overall reaction rate (Maeda-Yorita and Massey, 1993). Therefore, the reported kinetic constants do not necessarily represent the situation under more optimal turnover conditions. The MO-QSAR of the present study, determined under more physiological conditions, provides support for the conclusion that at 25 °C in the absence of inhibiting monovalent anions, the nucleophilic attack of the reactive π -electrons of the phenol on the C(4a)-hydroperoxyflavin intermediate is a major factor determining the overall rate of catalysis. Rate constants of other steps in the catalytic cycle might be in the same order of magnitude as the rate constant for the nucleophilic attack. These rate constants differ for different phenols and thus may result in a fine-tuning of the overall rate of catalysis and deviations from a perfect MO-QSAR correlation (Fig. 5.2). Possible reaction steps that contribute to this fine-tuning of the overall rate of catalysis are given below. First, the decay of the C(4a)-hydroxyflavin intermediate has been demonstrated to be a slow step in the catalytic cycle of resorcinol

conversion under sub-optimal conditions (Maeda-Yorita and Massey, 1993). However, it is unlikely that this step is different for various phenolic substrates, hence causing variable deviations from the MO-QSAR line, because at this stage in catalysis the product is already dissociated from the complex (Maeda-Yorita and Massey, 1993). Secondly, the actual dissociation rate of the product from the complex contributes to the fine-tuning (Maeda-Yorita and Massey, 1993). This step can be expected to be dependent on the nature of the phenol. Thirdly, the conversion of the dissociated cyclohexadienone to the actual catechol metabolite may be a factor that influences the rate of catalysis indirectly, resulting in higher concentrations of the cyclohexadienone when the conversion is hampered and, as a result, decreased possibilities for dissociation of the cyclohexadienone from the enzyme/product intermediate. Hampering the cyclohexadienone conversion to the reaction product may occur to some extent in the case of phenols with a fluorinated *ortho* position, because fluoride anion elimination, accompanied by formation of a quinone primary product, might be less efficient than formation of a catechol product from a cyclohexadienone with a hydrogen-containing *ortho* position (Scheme 5.1). Finally, as observed for other flavin-dependent monooxygenases (Entsch, et al., 1976; Escherich, et al., 1993), the actual initial reduction of the enzyme/substrate complex may be a step which varies and influences the overall rate of catalysis, depending on the nature of the substrate bound to the enzyme. The actual contribution of these factors to the deviation of the k_{cat} values of the various phenol derivatives from the MO-QSAR may vary with the type of phenol studied, and, therefore, has to await stopped-flow studies with each individual substrate under conditions where the reaction rate no longer needs to be decreased to provide possibilities for stopped-flow analysis. Clearly, this is beyond the scope of the present study.

Additional results of the present study characterise the regioselectivities of the conversion of the halogenated phenols by phenol hydroxylase. ^{19}F -NMR data clearly demonstrate that in all asymmetric phenols C2 and C6 both become hydroxylated although not to a similar extent (Table 5.4). The actual regioselectivities can be compared to the calculated differences in chemical reactivity of the two sites for a nucleophilic attack on the C(4a)-hydroperoxyflavin intermediate. This comparison demonstrates that for substrates with similar *ortho* substituents, i.e. two hydrogen or two fluorine *ortho* substituents, the preferential site for hydroxylation can be qualitatively predicted on the basis of the site with the highest calculated density of the reactive electrons in the partially deprotonated form

of the phenol. This result demonstrates that chemical reactivity of the two *ortho* positions for a nucleophilic attack on the C(4a)-hydroperoxyflavin intermediate is a factor influencing the regioselectivity of the phenol-hydroxylase-catalysed hydroxylation of the asymmetric phenol derivatives. Closer comparison of the regioselectivity observed to the regioselectivity that would be predicted on the basis of the calculated chemical reactivity of the two *ortho* sites in the partially deprotonated phenol, demonstrates that the presence of a *meta* halogen substituent adjacent to the *ortho* position decreases the possibilities for hydroxylation of this *ortho* position. Thus, compared to the C6 position, the C2 position in 3-fluorophenol, 3,4-difluorophenol, 2,3,6-trifluoro-phenol, 3-chloro-4-fluorophenol, 4-chloro-3-fluorophenol and 3-fluoro-4-nitrophenol becomes hydroxylated to a smaller extent than expected on the basis of the difference in chemical reactivity between the C2 and C6 positions. Steric effects, at least for a fluorine substituent, can be ruled out (Rietjens, et al., 1993). It is more likely, due to local dipole-dipole interactions of the halogen substituent at C3 of the substrate with the enzyme active site, that one of the two binding modes [i.e. C2 or C6 closer to the reactive hydroperoxide group of the C(4a)-hydroperoxyflavin] is more likely to occur on a time-averaged basis. The substrate will flip-flop between these two possible binding modes with different lifetimes for the two orientations, explaining the effect of the C3 halogen substituent on the regioselectivity of the reaction, decreasing possibilities for hydroxylation at C2 further than expected on the basis of chemical reactivity of this site.

Finally, the regioselectivity of the asymmetric phenols with both a hydrogen and a fluorine *ortho* substituent can be compared to the calculated reactivity difference of the two sites. For 2-fluoro-, 2,3-difluoro-, 2,4-difluoro-, 2,3,4-trifluoro-, 2,3,5-trifluoro- and 2-fluoro-4-nitrophenol, the hydrogen substituted *ortho* C6 position becomes preferentially hydroxylated over the fluorine-substituted *ortho* C2. This indicates that the fluorine C2 substituent seems to hamper the hydroxylation at C2. However, the fact that 2,5-difluorophenol becomes preferentially hydroxylated at the fluorinated C2 position and not at the hydrogen-substituted C6, and the fact that the fluorine-substituted phenols fit into the MO-QSAR, indicate that the effect originates more likely from an effect of the fluorine at C2 on the substrate orientation than from an effect of the fluorine on the rate of catalysis at this position. Therefore, as with the halogen at the C3, a halogen at C2 might result in an overall orientation of the substrate with C2 on average further away from the C(4a)-hydroperoxyflavin, resulting in decreased chances for an attack at the fluorinated C2 position. In

asymmetric substrates with two similar *meta* substituents, i.e. 2-fluorophenol, 2,4-difluorophenol, 2,3,5-trifluorophenol and 2-fluoro-4-nitrophenol, C6 is usually hydroxylated 1.2 - 4 times more than C2 (Table 5.4). With 2,3-difluorophenol and 2,3,4-trifluorophenol, where, in addition to the orientating effect of the fluorine at C2, there is an orientating effect of a fluorine at C3, the preference for C6 hydroxylation is more pronounced, C6 being hydroxylated 7 - 99 times more than C2. Finally, with 2,5-difluorophenol the orientating effect of the halogen at the *meta* C5 position seems to dominate over the orientating effect of the fluorine at C2 resulting in preferential hydroxylation at C2 in spite of the fluorine substituent at this position.

Thus, the data of the present study indicate that the regioselectivity of the hydroxylation of asymmetric phenols by phenol hydroxylase is directed by (a) an orientating effect of halogen substituents at the *meta* C3/C5 position and, to a somewhat lesser extent, by (b) an orientating effect of a fluorine at the *ortho* position and (c) differences in the chemical reactivity of the two *ortho* positions for a nucleophilic attack on the C(4a)-hydroperoxyflavin intermediate.

5.5 References

- Besten den, C., Bladeren van, P.J., Duizer, E., Vervoort, J. and Rietjens, I.M.C.M. (1993) *Chem. res. Toxicol.* **6**, 674-680.
- Brown, H.C., McDaniel, D.H. and Häfliger, O. (1955) *Determination of organic structures by physical methods*, Academic Press, New York.
- Cnubben, N.H.P., Peelen, S., Borst, J.-W., Vervoort, J., Veeger, C. and Rietjens, I.M.C.M. (1994) *Chem. Res. Toxicol.* **7**, 590-598.
- Cooper, M.A., H.E., W. and Manatt, S.L. (1971) *J. Am. Chem. Soc.* **93**, 2369-2380.
- Detmer, K. and Massey, V. (1984) *J. Biol. Chem.* **259**, 11265-11272.
- Detmer, K. and Massey, V. (1985) *J. Biol. Chem.* **260**, 5998-6005.
- Entsch, B., Ballou, D.P. and Massey, V. (1976) *J. Biol. Chem.* **251**, 2550-2563.
- Escherich, K., Bolt van der, F.J.T., Kok de, A. and Berkel van, W.J.H. (1993) *Eur. J. Biochem.* **216**, 137-146.
- Fleming, I. (1976) *Frontier orbitals and organic chemical reactions*, John Wiley & Sons, Chichester.
- Fukui, K., Yonezawa, T., Nagata, C. and Shingu, H. (1954) *J. Chem. Phys.* **22**, 1433-1442.

- Husain, M., Entsch, B., Ballou, D.P., Massey, V. and Chapman, P.J. (1980) *J. Biol. Chem.* **255**, 4189-4197.
- Kemal, C. and Bruice, T. (1979) *J. Am. Chem. Soc.* **101**, 1635-1638.
- Lowry, O.H., Rosebrough, N.J., Far, A.L. and Randall, R.J. (1951) *J. Biol. Chem.* **193**, 265-275.
- Maeda-Yorita, K. and Massey, V. (1993) *J. Biol. Chem.* **268**, 4134-4144.
- Mörtberg, M. and Neujahr, H.Y. (1988) *FEBS Lett.* **242**, 75-78.
- Neujahr, H.Y. (1988) *Biochemistry* **27**, 3770-3775.
- Neujahr, H.Y. (1991) in *Chemistry and biochemistry of flavoenzymes* (Müller, F., Ed.) Vol. 2, pp. 65-85, CRC Press, Boca Raton.
- Neujahr, H.Y. and Gaal, A. (1973) *Eur. J. Biochem.* **35**, 386-400.
- Neujahr, H.Y. and Kjellén, K.G. (1978) *J. Biol. Chem.* **253**, 8835-8841.
- Peelen, S., Rietjens, I.M.C.M., Berkel van, W.J.H., Workum van, W.A.T. and Vervoort, J. (1993) *Eur. J. Biochem.* **218**, 345-353.
- Rietjens, I.M.C.M., Soffers, A.E.M.F., Veeger, C. and Vervoort, J. (1993) *Biochemistry* **32**, 4801-4812.
- Sejlitz, T. and Neujahr, H.Y. (1987) *Eur. J. Biochem.* **170**, 343-349.
- Shaka, A.J., Keeler, J. and Freeman, R. (1983) *J. Magn. Reson.* **53**, 313-340.
- Vervoort, J., Rietjens, I.M.C.M., Berkel van, W.J.H. and Veeger, C. (1992) *Eur. J. Biochem.* **206**, 479-484.

6

Summarizing discussion

Flavoproteins play an important role in a variety of catalytic reactions. The chemistry underlying these reactions is quite different from case to case. The basis for this broad reaction spectrum is formed by the flavin. Free flavin is a versatile molecule, capable to undergo many different chemical reactions. The steering of a particular chemical reaction of a flavin in a flavoprotein results from the interaction with the apoprotein. The latter, therefore, determines the specificity of the reaction catalyzed by the flavoprotein. Although flavin is capable to undergo many different reactions, flavoproteins, mainly, can be classified in only four major groups. The flavoproteins studied in this thesis are flavodoxins and phenol hydroxylase. Flavodoxin is an electron transferring protein and therefore belongs to the class of the electron-transferases. Phenol hydroxylase belongs to the class of the mono-oxygenases, as it inserts one oxygen atom of O_2 into the substrate, whereas the other is reduced to water. Firstly, the results on the flavodoxins will be summarized.

6.1 Flavodoxins

In chapter 2 the flavodoxin, in its three redox-states, from *Desulfovibrio vulgaris* (Hildenborough) is investigated by homonuclear two-dimensional NMR techniques. The NMR results are compared to existing X-ray crystallographic data (Watt, et al., 1991). From NOE intensities and the chemical shift values of the flavodoxin spectra in the three redox-states it is concluded that outside the FMN binding site no structural

changes occur upon reduction of the flavodoxin. This is in agreement with the X-ray crystallographic data (Watt, et al., 1991), because the only change in structure upon reduction of the flavodoxin was observed near the FMN: the conformation of Gly⁶¹-Asp⁶² near the FMN N(5) changes upon reduction of the oxidized flavodoxin. The carbonyl oxygen of Gly⁶¹ points away from the N(5) group of the FMN in the oxidized state, whereas it points towards the N(5)H in the reduced states, forming a hydrogen bond with the N(5) proton. Although it is impossible from the current NMR data to determine the exact nature of the conformational change of the Gly⁶¹-Asp⁶² peptide bond in the solution structure, the data are in agreement with the changes observed in the X-ray structures. A similar change is observed for the flavodoxin from *Clostridium MP* (Smith, et al., 1977), therefore, the change near the FMN N(5) seems to be important for the function of flavodoxins. As judged from the high chemical shift values of some resonances near the FMN phosphate group, a hydrogen-bonding scheme towards the phosphate is determined. This scheme very much resembles the hydrogen bonds observed in the X-ray structure, except that the amide proton of Gly¹³ does not seem to be involved in hydrogen bond formation towards the phosphate, whereas the amide proton of Ser¹⁰ does not seem to form a hydrogen bond to the phosphate as determined from the X-ray structures. This may mean that the loop which is responsible for binding the FMN phosphate to the flavodoxin is in a different conformation in solution than in the X-ray structure.

Upon two-electron reduction of the oxidized flavodoxin the FMN N(1)-C(2) region becomes negatively charged. The resonances of the amide protons of Asp⁹⁵ and Cys¹⁰² show a large down field shift upon two electron reduction. This shift is induced by the negative charge on the N(1)-C(2) region, which forms hydrogen bonds with Asp⁹⁵ and Cys¹⁰².

Upon reduction of the flavodoxin the FMN N(5) becomes protonated. Due to this protonation the N(5) nitrogen changes from a sp²-type to a sp³-type nitrogen. This means that the central pyrazine ring is expected to be less aromatic in the reduced state. This is indeed the case, because the ring current effect on the C^α proton of Trp⁶⁰, which is located above the pyrazine ring of the FMN, is less pronounced in the two-electron reduced state. Thus less electron density is expected on the pyrazine moiety of the FMN. Whether this is important for the function of the flavodoxin remains unclear.

In chapter 3 the flavodoxin from *Azotobacter chroococcum* is investigated by heteronuclear multi-dimensional NMR spectroscopy. This flavodoxin is involved in

the electron transfer to the Fe-protein of the nitrogenase enzyme complex (Yates, 1972). In contrast with the flavodoxin from *D. vulgaris* this flavodoxin belongs to the long-chain flavodoxins. The complete backbone assignment of the ^1H , ^{13}C and ^{15}N resonances of the oxidized *A. chroococcum* flavodoxin is given in chapter 3. For this assignment the gradient enhanced versions of the CBCANH (Grzesiek and Bax, 1992b) and the CBCA(CO)NH (Grzesiek and Bax, 1992a) experiments were essential. How the enhancement was incorporated in the original experiments is also explained in chapter 3. From the NMR data the secondary structure elements could be determined. The secondary structure of the *A. chroococcum* flavodoxin consists of a five stranded parallel β -sheet and five α -helices. The outer strands of the β -sheet show some deviation from a regular extended conformation. The outer strand $\beta 4/\beta 6$ is interrupted by a loop region. This extra loop is typical for the long-chain flavodoxins. It is proposed in this chapter that the extra negatively charged amino acid residues in this loop contribute to the very low redox-potential found for this flavodoxin. From a titration with the Fe-protein of the nitrogenase complex, it is concluded that a small loop near the FMN binding site, that is not present in most other flavodoxins, is important for the complexation with the Fe-protein. This loop, Gly⁶⁵-Glu⁷¹, thus may be important for electron transfer to the nitrogenase enzyme complex. In chapter 3 it is shown that electrostatic interactions are important for the complex formation. Also it is found that MgADP influences this complexation, probably caused by a change in conformation of the Fe-protein upon ADP binding. One of the helices from the flavodoxin, helix $\alpha 1$, consists of many positively charged residues. Such a positively charged helix is generally not observed in other flavodoxins. Besides possible stabilisation of the negatively charged FMN phosphate, this helix may be important for the interaction with the electron donor of the flavodoxin. Future studies will have to determine the function of this helix.

6.2 Phenol hydroxylase

For the conversion of phenol to catechol a whole set of successive reactions has to be performed by phenol hydroxylase (Scheme 1.2) (Maeda-Yorita and Massey, 1993). The step in which an oxygen atom actually is inserted in the substrate is the attack of the peroxide function of the C(4a)-hydroperoxyflavin intermediate (intermediate I, Scheme 1.2) on the substrate. This attack is believed to proceed by an

electrophilic attack of this peroxide function on the substrate. It is found by Maeda-Yorita and Massey (1993), at least for resorcinol as a substrate, that this step is one of the slowest in the reaction cycle of phenol hydroxylase. It is therefore that this step is expected to be important in determining the overall reaction rate. Bearing this in mind, the conversion of a series of phenolic substrates was analysed in combination with theoretically calculated parameters, using semi-empirical methods.

Chapter 4 shows that the *ortho*-hydroxylation of 3-fluorophenol by phenol hydroxylase is regioselective. This means that the two *ortho* positions, C2 and C6, of the phenol are not equally hydroxylated. This regioselectivity is observed to be pH dependent; the C6/C2 *ortho*-hydroxylation ratio decreases with increasing pH. At pH values below 5.5 this ratio has a maximum of 6.7, whereas a minimum of 2.2 is reached for pH values above 7.5. A second observation is that the rate of *ortho*-hydroxylation increases with increasing pH. The pH dependency observed for both effects, has a pK_a value of 6.5. In order to get insight in the basis of this pH-dependent regioselectivity and rate of the *ortho*-hydroxylation, binding studies using ^{19}F -NMR and molecular orbital calculations are performed. Binding of 3-fluorophenol to oxidized phenol hydroxylase clearly showed a ^{19}F -NMR resonance for the bound substrate. This broad, inhomogeneous resonance shifted to higher field values upon reducing the enzyme in the absence of molecular oxygen. Whether or not the ^{19}F -NMR resonance in the reduced enzyme also has an inhomogeneous lineshape could not be detected due to partial overlap with the resonance of the substrate free in solution. When the pH is increased a similar shift to higher field is observed for 3-fluorophenol free in solution. Molecular orbital calculations showed that the electron density in the HOMO of the reaction center C6 is about seven times higher than of C2 for 3-fluorophenol, whereas equal HOMO density is calculated for 3-fluorophenolate. In combination with the high field shift of the ^{19}F resonance of the bound substrate upon enzyme reduction, it was assumed that deprotonation of the phenolic substrate causes the observed regioselectivity. The regioselective *ortho*-hydroxylation could be caused by different orientations of 3-fluorophenol in the active site, leading to either C6 or C2 hydroxylation. A change in the relative contribution of discrete orientations with changing pH could then explain the observed decrease in C6/C2 hydroxylation ratio with increasing pH. Due to the broad nature of the ^{19}F resonance of the 3-fluorophenol bound to reduced phenol hydroxylase, it is not possible to exclude this possibility. Binding studies of 4-fluorophenol, however, indicate to deprotonation of the phenolic substrate. At pH

6.2 in the reduced phenol hydroxylase a single broad ^{19}F resonance of the bound 4-fluorophenol is observed. In the oxidized phenol hydroxylase the resonance of the bound 4-fluorophenol resonates at the same frequency. If the pH is increased a second resonance, which is shifted to higher field, is observed for the 4-fluorophenol bound to reduced phenol hydroxylase. A high field shift can be explained by the deprotonation of the substrate bound to the active site. Deprotonation in combination with frontier orbital theory also provides an explanation for the increased hydroxylation rate with increasing pH. Molecular orbital calculations calculate a less negative energy of the electrons in the HOMO of 3-fluorophenolate than of 3-fluorophenol. Transition-state theory in combination with frontier orbital theory (paragraph 1.3) explains that a substrate with a less negative E(HOMO) is expected to have a higher rate of conversion, assuming that the E(LUMO) of the C(4a)-hydroperoxyflavin does not vary for the different substrates. Based on these results a hypothesis is put forward to explain the pH-dependent effects observed. This hypothesis states that an active site amino acid residue, which acts like a base with a pK_a of 6.5, is able to (partial) deprotonate the hydroxyl group of the phenolic substrate. Upon deprotonation of the substrate the rate of conversion is increased.

In chapter 5 it is indeed observed that the energy of the electrons in the HOMO of the substrates plays an important role in determining the overall rate of their conversion. This because the $\ln k_{cat}$ for the conversion of a series of phenolic substrates correlates with their E(HOMO)'s. The presence of such a correlation strengthens the idea that the electrophilic attack of the C(4a)-hydroperoxyflavin of phenol hydroxylase on the substrate is a major factor in determining the overall rate of catalysis. However, since the correlation is 0.85, it is concluded that additional factors contribute to the fine-tuning of the overall rate of conversion. Future research should reveal which factors.

For 3-fluorophenol it is observed that the *ortho* position with the highest electron density of the HOMO electrons is preferentially hydroxylated (chapter 4). For asymmetric phenolic substrates with similar *ortho* substituents, i.e. either two hydrogen or two fluorine substituents, it is also observed that the *ortho* position with the highest density of the HOMO electrons is preferentially hydroxylated. This indicates that chemical reactivity of the two *ortho* positions for an electrophilic attack of the C(4a)-hydroperoxyflavin intermediate is a factor influencing the regioselectivity of the phenol-hydroxylase-catalysed hydroxylation. However, comparison of the regioselectivity observed to the one predicted on the basis of the

calculated chemical reactivity of the two *ortho* sites in a partially deprotonated phenol, demonstrates that the presence of a *meta* halogen substituent adjacent to the *ortho* position decreases the possibilities for hydroxylation of this *ortho* position. Local dipole-dipole interactions of the *meta* halogen substituent of the substrate with the enzyme active site, probably cause one of the two binding modes, i.e. C2 or C6 closer to the reactive hydroperoxide group of the C(4a)-hydroperoxyflavin, to occur more likely on a time averaged base. For most phenols with both a hydrogen and a fluorine *ortho* substituent, the hydrogen substituted *ortho* position becomes preferentially hydroxylated. However, the fact that 2,5-difluorophenol becomes preferentially hydroxylated at the fluorine substituted *ortho* position, indicates that probably also an *ortho* fluorine has an effect on the substrate orientation. Thus besides the difference in chemical reactivity on the *ortho* positions, also dipolar effects, which orientate the substrate in the active site, seem to play a role in the regioselectivity of the hydroxylation by phenol hydroxylase.

6.3 References

- Grzesiek, S. and Bax, A. (1992a) *J. Am. Chem. Soc.* **114**, 6291-6293.
- Grzesiek, S. and Bax, A. (1992b) *J. Magn. Reson.* **99**, 201-207.
- Maeda-Yorita, K. and Massey, V. (1993) *J. Biol. Chem.* **268**, 4134-4144.
- Smith, W.W., Burnett, R.M., Darling, G.D. and Ludwig, M.L. (1977) *J. Mol. Biol.* **117**, 195-225.
- Watt, W., Tulinsky, A., Swenson, R.P. and Watenpaugh, K.D. (1991) *J. Mol. Biol.* **218**, 195-208.
- Yates, M.G. (1972) *FEBS Letters* **27**, 63-67.

Samenvatting

Eiwitten zijn essentieel voor elk levend organisme en zij zijn betrokken bij bijna elk proces dat zich in een organisme afspeelt. Zij transporteren en bewaren een grote verscheidenheid aan deeltjes, variërend van macromoleculen tot electronen; zij kunnen zorgen voor de communicatie tussen cellen en organen; zij beschermen het organisme tegen schadelijke stoffen via het immuunsysteem; zij reguleren de expressie van genen; zij geven structuur en stevigheid aan hogere organismen in de vorm van onder andere botten en nagels; en zij zetten chemische componenten (voedsel) om in energie, zodat het organisme in staat is zijn taak te verrichten.

Levende wezens gebruiken chemische reacties om zichzelf van chemische energie te voorzien. Op zichzelf, echter, verlopen deze chemische reacties te langzaam onder fysiologische omstandigheden (waterig milieu, 37 °C, pH 7 en atmosferische druk) om leven mogelijk te maken. Om leven mogelijk te maken, worden deze reacties in organismen op een zeer efficiënte manier versneld. Dit gebeurt door enzymen. Enzymen zijn eiwitten die werken als een katalysator voor een bepaalde chemische reactie. Dat wil zeggen dat ze de snelheid van een reactie verhogen zonder zelf te zijn veranderd aan het einde van die reactie. Na de betreffende reactie zijn ze weer klaar om een volgende reactie te katalyseren.

Eiwitten en dus enzymen, zijn eigenlijk niets meer dan een lineaire keten van aminozuren. Dit is te vergelijken met een snoer van verschillende en gekleurde kralen, waarbij de kralen de aminozuren en de kleuren het soort aminozuur representeren. Het bijzondere van eiwitten is, dat zij naast een primaire structuur, het aantal en de volgorde van de verschillende aminozuren, een drie-dimensionale structuur (= tertiaire structuur) bezitten. Zo'n drie-dimensionale structuur ontstaat doordat de

aminozuur keten op een specifieke manier gevouwen is. Dit is voor te stellen als het kralen snoer, met een metaaldraad als snoer, dat wordt opgepropt als een vel papier. In de drie-dimensionale structuur van een eiwit kunnen zich regelmatige structuren zoals helices of "sheets" bevinden, deze structuren worden dan secundaire structuur elementen genoemd. De drie-dimensionale structuur is uiterst belangrijk voor de functie van een enzym (eiwit) en zij maakt dat het enzym specifiek een chemische reactie katalyseert. Soms bevat een enzym naast de verschillende aminozuren nog een ander molecuul, dat essentieel is voor de werking van het enzym. Een dergelijk molecuul wordt een prosthetische groep genoemd.

De enzymen die in dit proefschrift bestudeerd zijn, behoren tot de zogenaamde flavine eiwitten, omdat zij allen als prosthetische groep een flavine molecuul (Fig. 1.1) bevatten. Het bekendste flavine is waarschijnlijk riboflavine, dat beter bekend staat als vitamine B₂. Flavine eiwitten zijn doorgaans geel van kleur. Dit komt doordat het flavine in deze eiwitten een geel molecuul is. Een mooi voorbeeld hiervan is de dooier van een ei; deze dankt zijn gele kleur aan de aanwezigheid van flavine eiwitten. Een vrij flavine molecuul is in staat verscheidene chemische reacties te ondergaan. Als nu zo'n flavine molecuul ingepakt zit in een eiwit dan ondergaat het flavine specifiek één bepaalde chemische reactie. Dit betekent dat een bepaald flavine eiwit, door middel van die specifieke chemische reactie, slechts één soort molecuul (= substraat) omzet. Het moge dus duidelijk zijn dat de interacties tussen het flavine en de aminozuren van het enzym bepalend zijn voor de specificiteit van de reactie.

Een zeer krachtige techniek om naar de interacties tussen de individuele atomen in een eiwit molecuul te kijken is "kernspin resonantie" (Nuclear Magnetic Resonance). Deze techniek maakt gebruik van de magnetische eigenschappen van atoomkernen. Deze eigenschappen zijn te bestuderen als de eiwit moleculen in een sterk magneetveld geplaatst worden. Door vervolgens op bepaalde momenten voor een bepaalde duur radio signalen naar de eiwit atomen te zenden en hun reactie te meten (dit is wat een NMR apparaat doet), is het mogelijk informatie over deze kernen te verkrijgen. Deze naam, kernspin resonantie, doet vermoeden dat dit iets met radioactiviteit te maken heeft, het tegendeel is echter het geval. Met de informatie die uit een NMR meting verkregen is, is het mogelijk om de zo belangrijke drie-dimensionale structuur van een eiwit te bepalen. Ook is het met NMR mogelijk om informatie over de dynamische eigenschappen van de atomen in een eiwit molecuul te krijgen. In hoofdstuk 1 wordt in het kort uitgelegd wat NMR nu eigenlijk is. In dit

hoofdstuk wordt ook uitgelegd hoe de drie-dimensionale structuur van een eiwit kan worden bepaald met behulp van NMR.

In hoofdstuk 2 is de interactie tussen het flavine molecuul (FMN) in zijn verschillende redox-toestanden, met zijn eiwit omgeving bestudeerd voor het flavine eiwit flavodoxine van de bacterie *Desulfovibrio vulgaris*. Omdat flavodoxine fungeert als een electron transport eiwit is het mogelijk op dit eiwit, en wel op het flavine molecuul, één of twee extra electronen te plaatsen. De toestanden van het flavodoxine met nul, één of twee extra electronen worden redox-toestanden genoemd. Verschillen in de drie-dimensionale eiwit structuur tussen de drie redox-toestanden buiten het FMN bindingsgebied werden niet gezien. Daarentegen werden wel enkele verschillen in het FMN bindingsgebied gezien. Met name de electronen verdeling binnen het flavine veranderde wanneer er extra electronen op het flavine geplaatst worden. Een functionele betekenis voor de werking van het flavodoxine op grond van deze waarnemingen kan echter niet worden gegeven.

In hoofdstuk 3 is de eerste stap gemaakt in de structuur bepaling, met behulp van NMR, van het flavodoxine van de bacterie *Azotobacter chroococcum*. Dit flavodoxine geeft electronen door aan het zogenaamde nitrogenase enzymcomplex, dat in staat is stikstof uit de lucht (N_2) om te zetten in ammoniak (NH_3). Deze omzetting is essentieel voor de in stand houding van de stikstofkringloop hier op aarde. Alvorens tot een drie-dimensionale eiwitstructuur te komen, moeten eerst alle NMR signalen van het flavodoxine molecuul toegekend worden aan de betreffende atomen van dit flavodoxine. Deze toekenning van de zogenaamde "backbone" atomen (Fig. 1.6) van de aminozuren van het flavodoxine is gegeven in dit hoofdstuk. Verder is met behulp van NMR bepaald wat de secundaire structuur elementen zijn in dit flavodoxine. Om de exacte werking van dit flavodoxine te leren begrijpen is het essentieel te weten te komen welke aminozuren van het flavodoxine van belang zijn voor de interactie met de electronen-acceptor van het nitrogenase enzymcomplex. In dit hoofdstuk is bepaald welke aminozuren dit zijn. Deze aminozuren blijken zich te vinden op een stukje in de primaire structuur dat ontbreekt bij de meeste andere flavodoxines. Dit extra stukje is daarom waarschijnlijk van belang voor de electronen overdracht van het flavodoxine naar het nitrogenase enzymcomplex.

De snelheid van omzetting van een substraat door een enzym wordt niet alleen bepaald door de eigenschappen van het enzym, maar ook door de eigenschappen van het substraat: niet alle substraten worden even snel omgezet. In hoofdstuk 5 zijn

een aantal eigenschappen van verschillende substraten onderzocht met betrekking tot de omzettingssnelheden. In dit hoofdstuk is een verband gevonden tussen bepaalde eigenschappen van deze substraten (fenolen) en de omzettingssnelheden van de verschillende substraten door het enzym "fenol hydroxylase". De eigenschappen van het substraat die bestudeerd zijn, zijn de energie van de reactieve electronen (de electronen die betrokken zijn bij de reactie met het enzym) en de dichtheid van die electronen op de potentiële reactie centra (daar waar het enzym met het fenol kan reageren) van het fenol. Deze twee eigenschappen kunnen met een bepaald computerprogramma berekend worden. Fenolen (zie schema 1.1) zijn stoffen die onder andere vrijkomen bij de afbraak van lignine. Lignine is het materiaal wat een plant of boom zijn stevigheid geeft. Wanneer planten of bomen afsterven komen deze fenolen dus vrij in het milieu. De omzetting van deze milieu schadelijke fenolen in stoffen, die weer gebruikt kunnen worden door andere organismen, wordt onder andere door het gist *Trichosporon cutaneum* uitgevoerd. Dit microorganisme bevat namelijk het bovengenoemde fenol hydroxylase. Dit fenol hydroxylase is ook een flavine eiwit. Het moge duidelijk zijn dat het flavine in fenol hydroxylase een geheel andere reactie katalyseert dan in flavodoxine. Dit geeft nogmaals aan dat de eiwitomgeving bepalend is voor de manier waarop een flavine een bepaalde reactie ondergaat. Als de veronderstelling gerechtvaardigd is dat de aanval van het C(4a)-hydroperoxyflavine van het fenol hydroxylase (de stap van intermediair I naar II, schema 1.2) op het fenol snelheidsbepalend is voor de enzymreactie van fenol hydroxylase, dan wordt er een correlatie verwacht tussen de energie van de reactieve electronen van de verschillende substraten en hun omzettingssnelheden. Voor fenol hydroxylase is inderdaad een dergelijke correlatie gevonden. Het blijkt dus dat bovenstaande aanname gerechtvaardigd is, wat betekent dat de aanval van het C(4a)-hydroperoxyflavine op het substraat inderdaad belangrijk is voor snelheid waarmee het fenol hydroxylase zijn substraat omzet. Een dergelijke correlatie geeft meer inzicht hoe de enzymreactie van fenol hydroxylase verloopt. Het is namelijk belangrijk om te begrijpen hoe enzymen een bepaalde reactie katalyseren, om zo gebruik te maken, bv. voor een bepaalde toepassing, van de efficiënte manier waarop enzymen dit doen.

Om de exacte werking van een enzym te achterhalen is één studie meestal onvoldoende. Voor het bovengenoemde enzym, fenol hydroxylase, is daarom nog een andere studie uitgevoerd. In deze studie (hoofdstuk 4) is het effect van de zuurgraad (pH) op de omzetting van het substraat 3-fluorfenol onderzocht. Dit

substraat kan door fenol hydroxylase omgezet worden in twee verschillende produkten. De hoeveelheid en verhouding van de gevormde produkten blijkt te variëren met de pH. Uit hoofdstuk 4 blijkt nu dat er een verband gelegd kan worden tussen deze verhouding en de dichtheid van de reactieve electronen op de reactie centra van het substraat. Deze electronendichtheid blijkt beïnvloed te worden door de mate waarin het proton (H^+) van de OH-groep van het fenol (zie schema 1.1) verwijderd kan worden. Verwijdering van dit proton, waarschijnlijk door een aminozuur van het fenol hydroxylase, blijkt zowel invloed te hebben op de *verhouding* van de gevormde producten, als op de *omzettingssnelheid*. Tevens bleek naast de pH ook de redox-toestand waarin het enzym verkeert van belang te zijn voor de toestand waarin het substraat aan het enzym bindt. Aan de hand van deze uitkomsten is er in hoofdstuk 4 een mechanisme opgesteld voor de werking van de enzymreactie van fenol hydroxylase.

Ondanks dat deze studie ons meer inzicht heeft gegeven in de werking en structuur van een tweetal flavine eiwitten, blijven er nog veel vragen onbeantwoord. Het blijft echter intrigerend hoe één soort molecuul, namelijk een flavine, door de subtiële werking van een mooi gevouwen eiwitketen in staat is onder fysiologische omstandigheden, zeer efficiënt en specifiek een bepaalde chemische reactie uit te voeren, en op deze manier bijdraagt aan de zo belangrijke energie voorziening van een organisme.

Curriculum vitae

Jacobus Carolina Johannes Peelen (Sjaak) werd geboren op 1 januari 1967 te Meerlo. In 1985 behaalde hij het Gymnasium β diploma aan het Boschveld College te Venray. In datzelfde jaar werd de studie Moleculaire Wetenschappen aangevangen aan de Landbouwniversiteit (toen nog Landbouwhogeschool) te Wageningen. In maart 1991 studeerde hij af als Moleculaire Wetenschapper in de fysisch-chemische en chemische oriëntaties. Tijdens de doctoraalfase werden afstudeervakken gevolgd bij de vakgroepen Moleculaire Fysica (Prof. T. Schaafsma: Eiwit-lipide interacties in gereconstitueerde M13-bacteriofaag manteleiwit-lipide bilaag systemen) en Biochemie (Prof. C. Veeger: Mechanisme van omzetting en bio-activering van monogehalogeneerde anilines door cytochroom P450). De stageperiode is doorgebracht aan het Max Planck Institut für Biophysikalische Chemie te Göttingen (dr. D. Marsh: Eiwit-lipide interacties in cholaat-geïsoleerde M13-bacteriofaag manteleiwit-fosfolipide bilaag systemen).

Van mei 1991 tot december 1995 is hij als OIO verbonden geweest aan de vakgroep Biochemie van de Landbouwniversiteit te Wageningen, waar het in dit proefschrift beschreven onderzoek werd uitgevoerd onder supervisie van dr. ir. J. Vervoort en Prof. dr. C. Veeger. Zijn onderzoek werd gesubsidieerd door Scheikundig Onderzoek Nederland (NWO).

Vanaf februari 1996 is hij als postdoc werkzaam aan het Unilever Research Laboratorium te Vlaardingen.

List of publications

J.C.J. Peelen, J.C. Sanders, M.A. Hemminga and D. Marsh (1992), Stoichiometry, selectivity, and exchange dynamics of lipid-protein interaction with bacteriophage M13 coat protein studied by spin label electron spin resonance. Effects of protein secondary structure, *Biochemistry* **31**, 2670-2677.

S. Peelen, I.M.C.M. Rietjens, W.J.H. van Berkel, W.A.T. van Workum and J. Vervoort (1993), ^{19}F -NMR study on the pH-dependent regioselectivity and rate of the *ortho*-hydroxylation of 3-fluorophenol by phenol hydroxylase from *Trichosporon cutaneum*. Implications for the reaction mechanism, *European Journal of Biochemistry* **218**, 345-353.

N.H.P. Cnubben, J.W. Borst, S. Peelen, J. Vervoort and I. Rietjens (1994), Molecular orbital-based quantitative structure activity relationship for the cytochrome P450-catalyzed 4-hydroxylation of halogenated anilines, *Chemical Research in Toxicology* **7**, 590-598.

S. Peelen and J. Vervoort (1994), Two-dimensional NMR studies of the flavin binding site of *Desulfovibrio vulgaris* flavodoxin in its three redox states, *Archives of Biochemistry and Biophysics* **314**, 291-300.

S. Peelen, I.M.C.M. Rietjens, M.G. Boersma and J. Vervoort (1995), Conversion of phenol derivatives to hydroxylated products by phenol hydroxylase from *Trichosporon cutaneum*. A comparison of regioselectivity and rate of conversion with calculated molecular orbital substrate characteristics, *European Journal of Biochemistry* **227**, 284-291.

J. Vervoort, D. Heering, S. Peelen and W. van Berkel (1994) Flavodoxins, in *Methods in Enzymology* **243**, 188-203.

I.M.C.M. Rietjens, M.G. Boersma, A.E.M.F. Soffers, N.H.P. Cnubben, J. Koerts, S. Peelen, W.J.H. van Berkel and J. Vervoort (1994) Use of molecular orbital calculations in studies on mechanism of enzyme catalysis, in *Flavins and flavoproteins* (K. Yagi ed.), pp. 3-12, Walter de Gruyter & Co, Berlin.

S. Peelen, S.S. Wijmenga, P.J.A. Erbel, R.L. Robson, R.R. Eady and J. Vervoort (1996), Short extra loop of the long-chain flavodoxin from *Azotobacter chroococcum* may be important for electron transfer to nitrogenase. ^1H , ^{15}N and ^{13}C backbone assignments and secondary solution structure of the flavodoxin, *Journal of Biomolecular NMR*.